DETERMINATION OF ALLELIC EXPRESSION OF H19 IN PRE- AND PERI-IMPLANTATION MOUSE EMBRYOS

A Thesis

Presented to the Faculty of the Graduate School

At the University of Missouri

In Partial Fulfillment

Of the Requirement for the Degree

Master of Science

By

VERÓNICA M. NEGRÓN PÉREZ

Dr. Rocío Melissa Rivera, Thesis Supervisor

July 2013

The undersigned, appointed by the dean of the Graduate School, have examined the thesis entitled

DETERMINATION OF ALLELIC EXPRESSION OF H19 IN PRE- AND PERI-IMPLANTATION MOUSE EMBRYOS

Presented by Verónica M. Negrón Pérez

A candidate for the degree of Master of Science

And hereby certify that, in their opinion, it is worthy of acceptance.

_____

Rocío M. Rivera, Ph.D.

_____

Randall S. Prather, Ph.D.

_____

Laura Schulz, Ph.D.

ACKNOWLEDGEMENTS

There are many people I would like to thank for their contribution. I would not have been able to finish my Master of Science degree without their generous and much appreciated help. First, I want to thank my major professor, Dr. Rocío Rivera for giving me the opportunity of pursuing my degree in her laboratory, for her time and patience throughout the past two years and for believing in me. I had little knowledge in epigenetics, working with molecular biology and working with embryos before coming to Mizzou, and with your help, time and encouragement I was able to finish my project and gain more knowledge in the field. Thank you very much for sharing your passion for science, teaching me how to work with embryos and for always reminding me to "hang in there" and to "go for the gold". Next, I would like to thank my degree committee members Dr. Randall S. Prather and Dr. Laura Schulz for their time, advice and guidance throughout this endeavor.

I want to thank Dr. Prather for allowing me to use the micromanipulator used for my research project and Jennifer Hamm and Lee Spate from the Prather Laboratory for their training and assistance with the micromanipulator. Also, I would like to thank Dr. Peter Sutovsky and Young-Joo Yi of Dr. Sutovsky's laboratory for helping me with the immunofluorescence procedure and fluorescent microscope, and Dr. R. Mike Roberts for kindly donating the mouse anti-Oct4 antibody used in the same procedure. Dr. Paula McSteen and Dr. Amanda Durbak, thank you also for kindly providing us with the *in vitro* transcribed *ZmNIP3* RNA used in the appendix. And Mamun, thank you for

stopping by the lab again to give me some advice and teach me how to do the immunohistochemistry.

I would like to acknowledge my lab-mates, Matthew Sepúlveda, Angela Schenewerk, Zhiyuan Chen (a.k.a. Chen), Laura Moon and Jasmine Randle for their friendship and support these past two years. Matt, Angie and Chen, thank you for being awesome, for making the lab experience even more fun, and for always making sure I had a way back home and my groceries in place. Laura and Jasmine, it was a lot of fun having you around and sharing some of the knowledge I gained. I also want to thank other graduate students in Animal Sciences and other departments for making my Missouri experience a lot better than expected. Liz (and Mark), Holly, Dane and Katy, thank you very much for your friendship and all the extracurricular activities, specifically painting, bingo and volleyball nights! Marvyn, Sarah, Daniel, Ray and all my other Latino people, thank you for the salsa nights and many potlucks that kept me close to my roots. Jessica, Latina in heart, for dancing with us, being fun, keeping Joseline and I company the late nights and crashing at our place. And most definitely, thank you Joseline for being an awesome roommate, friend, and almost family; I will miss the Sunday morning breakfast catch-up talks.

Also, thank you Dr. Matt Lucy, from across the hall for welcoming me to the department, for your graduate school stories, planning the trips outside Missouri and encouraging me to keep going. Thank you Cinda for always helping with our documents and with any administrative-related question I had. Thank you Tyler, from Dr. Lucy's lab, for teaching me how to ski and for being so nice and friendly. And Dan for making

sure the real-time machine was always working, and for the occasional conversation in the lab.

Finally, I would like to thank my two undergrad professors, family and friends back home for all their support and for being my number one fans. Drs. Esbal Jiménez and Melvin Pagán, thank you for being wonderful mentors, for your guidance and encouragement, and for believing in me. Mom and Dad, Efra and Yayi, Marianito, Martín, Cecy and Eve, I would not have been able to make it this far without you on the other side to push me and cheer for me. Papito, Mamita, Abuelo Puca and Abuela Carmen, thank you for being examples and putting me on your prayers so that everything would go ok. Carmen, Camila, Adriana, Victoria, Gaby and Daniel, thank you for your long-lasting friendship, the memories at home and for reminding me that I could handle this.

To all, I would not have made it this far without your cheers, love and encouragement. Best wishes, it really has been a pleasure, and remember that wherever I go, you have a place to visit.

PREFACE

The mammalian embryo undergoes a series of cleavage divisions to form a blastocyst. The blastocyst-stage embryo contains two cell types, the inner cell mass (ICM) and the trophectoderm (TE) which will give rise to the fetus and placenta, respectively. During peri-implantation, primary trophoblast giant cells (PTGC) will terminally differentiate from the trophectoderm to control uterine implantation. PTGCs have been characterized as having tumor-like behavior.

Epigenetics may be defined as heritable changes in gene expression caused by mechanisms that modify the genome but do not involve a change in the nucleotide sequence. In this thesis I will focus on genomic imprinting, an epigenetic mechanism that controls parental-allele specific expression. I will also describe DNA methylation and histone post-translational modifications as they control imprinted gene expression. Imprinted genes play an important role in fetal growth, placental development and normal brain function. Misregulation of imprinted gene expression may lead to epigenetic disorders.

The use of assisted reproductive technologies (ART) as therapy to circumvent infertility has increased over the past decade. While the majority of children conceived with these technologies are healthy, retrospective studies cautions of an increased incidence of imprinting syndromes.

One of the techniques used as part of the ART procedures is embryo culture where the embryo is grown outside the uterus until it reaches a specific stage and later on

is transferred back into the uterus. Several studies have demonstrated that the expression of imprinted genes can be affected by this process. One of the imprinted genes that has been shown to be misregulated by embryo culture is *H19*. Preliminary data from our laboratory questions the validity of that finding. We hypothesize that biallelic expression of *H19* is a normal physiologic event during peri-implantation in the mouse and that it is specific to the PTGCs. We speculate that this phenomenon exists to control implantation. The work of this thesis was designed to test this hypothesis.

TABLE OF CONTENTS

LIST OF FIGURES

LIST OF TABLES

NOMENCLATURE

ART	Assisted Reproductive Technologies
AS	Angelman syndrome
Ascl2	achaete-scute complex homolog 2 (Drosophila)
BWS	Beckwith-Wiedemann syndrome
bHLH	basic helix-loop-helix
Cd81	CD81 antigen
CDC	Centers for Disease Control and Prevention
CDK1	cyclin-dependent kinase 1
Cdkn1c	cyclin-dependent kinase inhibitor 1C (P57)
CDX1	caudal type homeobox 1
Cdx2	caudal type homeobox 2
CGIs	CpG islands
CTCF	CCCTC-binding factor
Ctsq	cathepsin-q
Dek	DEK oncogene (DNA binding)
DNMT	DNA methyltransferase
DMR	Differentially methylated region
Dppa3	developmental pluripotency-associated 3; also known as Stella or Pgc7
eCG	equine chorionic gonadotropin (also referred to as PMSG; pregnant mare's serum gonadotropin)
Eomes	eomesodermin homolog (Xenopuslaevis)
EPC	Ectoplacental cone

Esrrb	estrogen related receptor, beta
ExE	Extraembryonic ectoderm
Fgfr2	fibroblast growth factor receptor, 2
FRET	Fluoresence resonance electron transfer
FSH	Follicule-stimulating hormone
Gata2	GATA binding protein 2
Gcm1	glial cells missing homologue 1 (Drosophila)
H19	H19 fetal liver mRNA
H3/4	Histone 3/ 4
H3K4/9/27/36	Histone 3 lysine 4/9/27/36
Hand1	heart and neural crest derivatives expressed transcript 1
hCG	human chorionic gonadotropin
5hmC	5-hydroxymethylcytosine
Iap	intracisternal A particles
ICF	Immunodeficiency-Centromeric Instability-Facial Anomalies syndrome
ICM	Inner cell mass
ICR	Imprinted control region
ICSI	Intra-cytoplasmic sperm injection
Id 1/2	inhibitor of DNA binding 1/2
IGF1R	insulin-like growth factor I receptor
Igf2	insulin-like growth factor 2
IGF2R	insulin-like growth factor II receptor

IGFBP	insulin-like growth factor binding proteins
IR	insulin receptor
IR-B	insulin receptor, isoform B (also known as INSR)
Itga7	integrin alpha 7
IU	International units
IVF	*in vitro* fertilization
Kcnq1	potassium voltage-gated channel, subfamily Q, member 1
Kcnq1ot1	KCNQ1 overlapping transcript 1 (also known as *Lit1*)
LH	Luteinizing hormone
lncRNA	Long non-coding RNA
LOI	Loss of imprinting
MBD	Methyl-CpG binding domain
5meC	5-methyl-cytosine
Mdfi	MyoD family inhibitor; also known as I-mfa
MEM	Minimum Essential Media
Mlv1	murine leukemia virus 1
Nanog	Nanog homeobox
ncRNA	Non-coding RNA
Osbpl5	oxysterol binding protein-like 5
PBS	Phosphate buffered saline
PcG	Polycomb group protein complexes
PCNA	proliferating cell nuclear antigen
PGC	Primordial germ cell

Phlda2	pleckstrin homology-like domain, family A, member 2
Plgal1	pleiomorphic adenoma gene-like 1 (also known as *Zac1*)
Pou5f1	POU domain, class 5, transcription factor 1 (also known as *Oct4*)
PRC	Polycomb repressive complexes
Prl2c2	prolactin family 2, subfamily c, member 2 (also known as *Plf*)
Prl3b1	prolactin family 2, subfamily b, member 2 (also known as *Pl2*)
Prl3d1	prolactin family 2, subfamily d, member 1 (also known as *Pl1*)
PTGC	Primary trophoblast giant cells
PVP	Polyvinylpyrrolidone
PWS	Prader-Willi syndrome
RFLP	Restriction fragment length polymorphism
SAM	S-adenosyl-methionine
SART	Society for Assisted Reproductive Technology
Slc22a18	solute carrier family 22 (organic cation transporter), member 18
Sox2	SRY-box containing gene 2
TE	Trophectoderm
Tet1/2/3	tet methylcytosine dioxygenase 1/2/3
TGC	Trophoblast giant cells
Tpbpa	trophoblast specific protein alpha
Tme	T-associated maternal effects
TRC	Transcription-required complex
Tssc4	tumor-suppressing subchromosomal transferable fragment 4
ZGA	Zygotic genome activation

CHAPTER I

Literature Review

General introduction

Regulation of the mammalian genome changes during embryonic development and has the ability to induce cell differentiation and to regulate and maintain cell fate. In the mouse, at approximately day 3.5, the embryo acquires a fluid filled cavity leading to the formation of a blastocyst. The blastocyst-stage embryo is composed of two types of tissues; the inner cell mass (ICM) and the trophectoderm (TE). Each of these cell types differentiate to give rise to the fetus and placenta, respectively. In mouse embryos and mammals with invasive placentas, trophoblast giant cells (TGC) are derived from the trophectoderm to assist in the process of attachment into the uterus. TGCs have tumor-like behavior and go through endoreduplication, the replication of the genome without cell division.

Epigenetics can be defined as the study of heritable changes in gene expression and cellular phenotype caused by mechanisms that control the genome but do not involve a change in the nucleotide sequence. Epigenetic regulation includes modifications such as DNA methylation and post-translational modifications of histone proteins as well as mechanisms like genomic imprinting and X-chromosome inactivation. For this thesis, I specifically studied genomic imprinting. The outcome of this type of epigenetic regulation is parental allele-specific regulation of gene expression. Expression of these genes is regulated by a neighboring discreet region of differential DNA methylation which is known as the imprinted control region (ICR).

H19 is a maternally-expressed ncRNA which is associated with tumor suppressor activity. *H19* is expressed in the TE of blastocyst-stage embryos and is downregulated after birth except in cardiovascular and skeletal muscle. Expression of *H19* is regulated by DNA methylation of the ICR on the paternal chromosome. The *H19* ICR is shared with insulin-like growth factor type 2 (*Igf2*), another imprinted gene that is paternally-expressed and has been linked to tumor enhancing activity throughout embryo development.

According to the United States' Centers for Disease Control and Prevention (CDC), about 10 percent of women between the ages of 15–44 suffer from infertility or are unable to conceive a child. These women seek help from assisted reproductive technologies (ART) which allows them to bypass the cause of infertility and have children. As a consequence, approximately one percent of all the children born in the United States are conceived with the use of ART. While in most cases the use of ART results in a positive outcome, ART procedures are also associated with birth defects some of which are epigenetic disorders.

Studies from several laboratories including ours have shown that the use of ART can affect gene expression that may lead to abnormal mammalian embryo development. Among the genes that are misregulated as a result of ART are the imprinted genes. For this thesis, I studied the effects of ART on the expression of the imprinted gene *H19*.

The following review of the literature will introduce various concepts necessary for the full understanding of the research chapter (Chapter II). The topics that will be discussed are; early embryonic development, epigenetic regulation of the genome with emphasis on genomic imprinting, and assisted reproductive technologies.

EMBRYO DEVELOPMENT

Pre-implantation embryo development

After fertilization, the mammalian embryo undergoes several cell divisions key to the formation of a blastocyst. On approximate day 1.0 of mouse embryo development, the fertilized egg goes through the first cleavage division to develop into a 2-cell stage embryo [1]. It has been suggested that either the polarity of the oocyte or the sperm entry position and the expression of *Ped* (preimplantation embryo development) in combination, pre-determine the site of first cleavage [2-4], although these views are highly debated [3-7]. By embryonic day 2.5 (2.5E), the embryo has undergone the second and third cleavage divisions, to form an 8-cell stage embryo (or morula). At the 8-cell stage, the embryo will begin the process of compaction [1, 8, 9]. This process involves E-cadherins, a component of adherens junctions found in cell to cell contact sites.

Two types of junctions, namely tight junctions and gap junctions form during compaction. Tight junctions form to maintain polarity and create a permeability seal between the outer cells while gap junctions form to support intercellular communication between all the cells [10-12]. Approximately at 3.5E, the outer cells pump sodium into the intercellular space in the morula which drives osmotic water accumulation and the formation of the blastocoel (a fluid-filled cavity) finally forming the blastocyst. Water movement can occur as a result of the sodium-potassium ATPase on the outer cells [13] and/or can be facilitated by aquaporins that are present in the outer cells [14]. At this point, the outer cells are flattened and the gap junctions between the inner cells allow

them to polarize. As a result, the first two embryonic cell types, the inner cell mass (ICM) and the trophectoderm (TE) are formed [15].

Two models have been proposed to describe how the ICM and TE acquire their identity: the polarized model, based on cell polarity [16, 17], and the inside-out (positional) model, based on cell location [18]. The polarized model states that cells located towards the animal pole (related to the location of the second polar body) are more likely to become ICM cells while the ones located towards the vegetal pole (opposite to animal pole) are more likely to become TE cells [16]. Furthermore, *Cdx2* (caudal type homeobox 2) mRNA appears to play an important role in maintaining the identity of the TE cells located towards the outside of the embryo, or apical domain [17]. The cells located on the apical domain block the Hippo signaling cascade allowing Yap1 (yes-associated protein 1; also known as Yap) to activate *Tead4* (TEA domain family member 4). This activates *Cdx2* which suppresses *Pou5f1* (POU domain, class 5, transcription factor 1; also known as *Oct4*), a pluripotency regulating gene. Hippo signaling is associated with tumor suppressor activity, was described in *Drosophila* and appeared to be conserved in mammals [19, 20]. Hippo is linked to the salvador-warts signaling pathway (*i.e.* Sav1-Lats1 in mice) also related to growth control and apoptosis. It appears that in the non-apical domain (*i.e.* inside of the embryo) direct cell-to-cell contact activates Hippo signaling and large tumor suppressor 1/2 (Lats1/2) (reviewed by [21]). Hippo and Lats1/2 can then phosphorylate Yap1 preventing it from entering the nucleus [22, 23]. By consequence, *Tead4* and *Cdx2* are not expressed [22, 24], allowing *Pou5f1* to be upregulated in ICM cells.

On the other hand, the positional model states that the inside or outside cells are exposed to different microenvironments (*i.e.* uterine or embryonic environment) causing the inside cells to become part of the ICM and the outside cells to become TE cells [18]. Regardless of how TE specification occurs, the same genes are needed to maintain cell pluripotency in ICM (*i.e. Pou5f1*, *Nanog* and *Sox2* [25-28]) or lineage specification in TE (*i.e.Cdx2*, *Eomes*, and *Gata2* [29-32]). Around embryonic day 4.5E, the embryo will have reached the late blastocyst stage and will start preparing for implantation.

Trophoblast giant cell (TGC) differentiation

Once the embryo has reached the late blastocyst stage at approximately day 4.5E, primary trophoblast giant cells (PTGC) begin differentiating from the mural TE located opposite to the ICM (**Figure 1.1** [33-36]) to assist in the uterine invasion process. However, a second round of TGC differentiation is necessary for implantation to occur at approximately day 6.5E. These secondary TGC are derived from the polar TE adjacent to the ICM and are composed of five subtypes namely, maternal canal-, ectoplacental cone [EPC]-, parietal-, sinusoidal-, and spiral artery-associated-TGC; [37]. Nonetheless, in mice, most placental tissues originate from the ExE or from the EPC also derived from the polar TE [37, 38].

The PTGC are the first terminally differentiated cells during embryonic development. Both primary and secondary TGC are polyploid cells that undergo endoreduplication [39], mediate uterine invasion, and combine to form the yolk sac placenta for nutrient exchange [40]. Endoreduplication is the replication of the genome without subsequent cell division. In other words, the cell goes through multiple S-phases

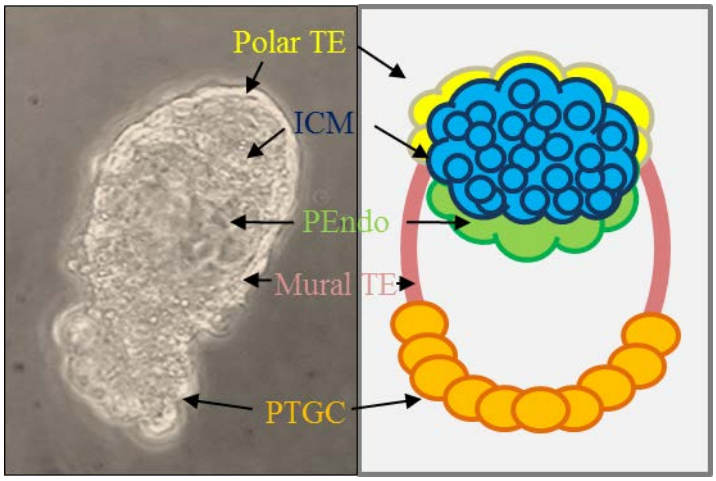

Figure 1.1. Embryonic cell population at day 5.5E. After several rounds of cleavage, compaction and blastocoel formation, at day 5.5 of embryo development (E), the embryo contains five embryonic subpopulation of cells: inner cell mass (ICM; blue), primitive endoderm (PEndo; green), polar trophectoderm (polar TE; yellow), mural trophectoderm (mural TE; pink), and primary trophoblast giant cells (PTGC; orange). ICM cells are pluripotent cells that will give rise to the fetus, the primitive endoderm will form extraembryonic endoderm layers and TE cells will give rise to the majority of placental tissues throughout development. At this stage specifically, from the mural TE, PTGCs will differentiate to mediate attachment. At day 6.5E, a second round of trophoblast giant cells will differentiate from the polar TE. PEndo and TE cells are the first to differentiate from pluripotent cells and PTGC are the first terminally differentiated group of embryonic cells.

without entering mitosis or completing cytokinesis [41]. Mitotic arrest is coordinated in the TGC by the expression of the cell cycle regulator Cdkn1c (p57Kip2) which inhibits the Cyclin B/Cdk1 complex [40-42].

After endoreduplication, mouse TGC remain mononucleate cells, but are bigger in size compared to other embryonic cells. TGC differentiation has been observed to be primarily regulated by the basic helix-loop-helix (bHLH) family of transcription factors and its interaction with other transcription factors such as Hand1 (heart and neural crest derivatives expressed transcript 1), Ascl2 [achaete-scute complex homolog 2 (Drosophila); also known as Mash2], Id1/2 (inhibitor of DNA binding 1/2), and Mdfi (MyoD family inhibitor; also known as I-mfa) [37, 40, 43-48]. Hand1 enhances TGC differentiation [46], whereas Ascl2 is required to maintain ectoplacental cone and spongiotrophoblast differentiation while simultaneously minimizing TGC differentiation [49]. In addition, Mdfi promotes TGC development by decreasing Ascl2 activity [45]. Expression of Id1/2 minimizes TGC differentiation and enhances chorion extra-embryonic ectoderm development [43, 44]. Simultaneously, *Esrrb* (estrogen related receptor, beta), *Eomes* [eomesodermin homolog (Xenopuslaevis)], *Cdx2*, *Fgfr2* (fibroblast growth factor receptor 2), *Gcm1* [glial cells missing homolog 1 (Drosophila)], and *Tpbpa* (trophoblast specific protein alpha) have been suggested to be responsible for TGC maintenance by interfering with the transcription of pluripotency [30, 50-55].

Trophoblast giant cell function

Peri-implantation

The entire peri-implantation mouse embryo contains approximately 120 cells [35], with approximately 50 belonging to the mural TE [37]. Concurrently, the polar TE number increases moderately [36] due to polarized migration of the polar TE cells to the mural TE [56]. During implantation around day 4.5E, the PTGC become adhesive and acquires invasive characteristics to attach to the uterus [57], but the secondary TGC are the ones responsible for invasion into the decidua and connection with the maternal vasculature [40].

Post-implantation development

From day 7.5E to 10.5E, each TGC subtype has distinct functions regulated by the expression of prolactin superfamily members such as, *Prl2c2* (prolactin family 2, subfamily c, member 2; also known as *Plf*), *Prl3b1* (prolactin family 3, subfamily b, member 1; also known as *Pl2*), *Prl3d1* (prolactin family 3, subfamily d, member 1; also known as *Pl1*), and cathepsin-q (*Ctsq*). Initially, the parietal-TGC, located at the implantation site and in the outer layer of parietal yolk sac, facilitate implantation, make initial maternal vascular connections and regulate differentiation of decidual cells [58, 59]. The three types of TGC associated with the maternal blood flow are; 1) Spiral-associated-TGCs, 2) maternal canal-TGCs, and 3) sinusoidal-TGCs. The spiral-associated-TGCs are located in spiral arteries that bring blood to the placenta. The maternal canal-TGCs are found in the canals that bring maternal blood into the base of the labyrinth. And finally, the sinusoidal-TGCs located within the maternal blood

sinusoids of the labyrinth layer, are responsible for regulating the maternal spiral artery remodeling and blood flow into the placenta, and for modulating hormone and growth factor activities before they enter the fetal and/or maternal circulation [59]. The maternal canal-TGCs and the sinusoidal-TGCs also regulate maternal physiology by exchanging cell signaling hormones [40].

TGC are also known to produce many paracrine factors important for implantation, uterine decidualization, vasculature remodeling and immune evasion. At day 9.5E secondary TGCs produce Prl3b1 and Prl3b2, two factors involved in maternal recognition of pregnancy [60]. In addition, secondary TGCs have lysosomes which phagocytize uterine epithelial cells [34]. Other endocrine factors including progesterone, and prolactin-like proteins Prl7a1, Prl7a2, Prl7b1, Prl8a6 (prolactin family 7/8, subfamily a/b, member 1/2/6), are also produced by TGC to control maternal adaptive behavior, mammary epithelial cell proliferation and differentiation, maintenance of the corpus luteum, insulin synthesis and secretion, adaptive functions of the liver and maternal immunological adaptation after implantation [40, 61, 62].

Trophoblast giant cells in other mammals

Embryos of different mammalian species infiltrate the uterus using various species-specific mechanisms that result in three primary placenta types, hemochorial (maternal blood in direct contact with fetus), epitheliochorial (uterine epithelium and chorion are in contact), and endotheliochorial placenta (endometrium vessels bared into the endothelium are in contact with the chorion). Regardless of the placental type,

trophoblast cell markers (*e.g. Cdx2*, Hand1, and *Ascl2*) are very similar to those detected in mouse trophoblast cells [55].

Implantation in the human, mouse and other species with hemochorial placenta is controlled by enzyme activity from the TGC (also referred to as extravillous trophoblasts in human). The TGC phagocytize uterine endothelial cells, resulting in maternal blood being in direct contact with two layers of syncytiotrophoblasts derived from EPC [55, 63]. In the mouse, the embryo first aligns itself with the ICM towards the mesometrial side of the uterus to later on adhere and invade the uterus. Then, PTGCs are responsible for that first adhesion, but the invasion and decidualization are controlled by the secondary TGC. Throughout implantation, the TGC express integrins, growth factors and prostaglandins on their surface that will communicate with the endometrium [59]. By day 9.5E, in mouse, the decidua has regressed and the placenta is established [59]. Human implantation is similar to mouse, but is more invasive, and the ICM is oriented towards the epithelium (reviewed by [64]). In addition, the trophoblast cells adhere together to form one single layer with mono-nucleated cells, generating the only barrier separating maternal blood from the fetus [65].

In pigs, horses, and cows, the polar TE disappears before gastrulation. The ICM flattens to form an epiblast, and implantation is regulated by trophoblast cells differentiated into binucleate cells [66]. These are less invasive, and adhere with the uterine epithelial cells to form an epitheliochorial placenta [55, 67]. Dogs and cats placentas are examples of species with placentas classified as endotheliochorial placentas [68, 69] composed of five layers between uterus and fetus (*i.e.* maternal endothelium, interstitial lamina, trophoblast, basal laminas, and fetal endothelium; reviewed by [70]).

It is apparent that although all TGC are in charge of the embryo-uterine molecular dialogue, there are differences in TGC functions that are species specific in mammals, and dependent on the placental type. It is currently not understood what advantages the various types of placentae have given to the different mammalian species throughout evolution.

Timed events post fertilization

Events occurring at a specific time post-fertilization which are independent of cellular circumstances or the environment in which the embryo develops are referred to as molecular clocks. To date, four such events have been studied and described during mouse early embryonic development. These are; zygotic genome activation (ZGA; reviewed by [71]), Dnmt1o (DNA methyltransferase oocyte specific isoform) nuclear translocation [72], compaction [8], and blastocoel formation [9, 73]. The next paragraphs will describe each one of these events in detail.

Zygotic genome activation **–** The developmental programming when maternally inherited transcripts are replaced by newly synthesized transcripts of embryonic origin is known as zygotic genome activation (ZGA; also referred to as maternal to zygotic transition; reviewed by [71, 74]). Transcription-requiring complex (TRC) is first detected in mouse embryos within a few hours of cleavage to the 2-cell stage [75] thus TRC detection is used as hallmark of ZGA (reviewed by [71]). Zygotic genome activation was shown to be a timed event post-fertilization during a series of studies in which zygotes were treated with cytochalasin D (cytokinesis inhibitor [76]), aphidicolin

(replicative DNA polymerase inhibitor [76, 77]), or alpha-amanitin (RNA pol II inhibitor [78]). In those studies, cleavage-arrested embryos showed similar levels of TRC as control 2-cell stage embryos. Researchers were also able to detect functional RNA polymerase I, II and III at the 1-cell stage [79, 80]. Authors concluded that a minor ZGA occurs at the 1-cell stage prior to the major ZGA at the 2-cell stage and described ZGA as a zygotic clock (reviewed by [71]).

Dnmt1o nuclear translocation **–** Dnmt1o, the predominant DNA methyltransferase 1 isoform (refer to DNA methylation section) during preimplantation development is sequestered in the cytoplasm of the oocyte and preimplantation stage embryos until the 8-cell stage when it mobilizes to the nucleus [72]. Dnmts are enzymes required for maintaining DNA methylation. A study suggested that Dnmt1o may be playing an important role at the 8-cell stage that requires movement to the nucleus. In an attempt to understand if cell division, DNA replication, RNA pol II or protein synthesis were involved in this phenomenon, 2- to 4-cell stage embryos were treated with cytochalasin D, nocodazole, alpha-amanitin or cycloheximide, respectively. Treated embryos showed Dnmt1o was translocated into the nucleus regardless of the treatment when the developmental timing of the treated embryos was equivalent to the 8-cell stage in the control embryos. Doherty *et al.* [72] concluded that movement of Dnmt1o to the nucleus occurs at a specific time post-fertilization and it is governed by a molecular clock.

Compaction - When the mouse embryo has reached the 8-cell stage, the cells begin to flatten, reorganize and to form cell-to-cell junctions necessary for cell communication and permeability [8, 10-12]. In order to determine the events leading to compaction, Levy and coworkers cultured 4-cell stage embryos with anisomycin, puromycin or E-cadherin ECCD-1. Anisomycin and puromycin are protein synthesis inhibitors while E-cadherin ECCD-1 prevents junction formation and cell flattening. Treated embryos showed advanced polarization suggesting that compaction and cell reorganization are independent of protein synthesis and junctions formation. Thus most embryos possess elements (*i.e.* proteins) required for compaction from earlier stages that allow them to complete the process at a specific time post-fertilization [8].

Blastocoel formation – With the objective of describing events that control the cellular differentiation during blastocyst formation, two groups of researchers inhibited cytokinesis and DNA replication of mouse 8-cell stage embryos. Pratt *et al.* [9] and Dean *et al.* [73] demonstrated that treated embryos with either aphidicolin or cytochalasin D exhibited no delay in blastocoel cavity formation. Also, the number of cycles of DNA replication remained unaffected but due to inhibited cell division, blastomeres become binucleate. Cellular polarization was not affected even in disaggregated blastomeres. The authors concluded that blastocoel formation is not guided by the number of cells in the embryo, the number of cytokinetic cycles or DNA replication but by a given time post-fertilization.

EPIGENETICS

Epigenetics may be defined as heritable changes in gene expression caused by mechanisms that modify the genome but do not involve a change in the nucleotide sequence [81]. Epigenetic mechanisms for gene expression control include DNA methylation, histone post-translational modifications, and regulation by interactions with non-protein coding RNAs (ncRNA).

Histone modifications

Note: Although I did not study histone modifications as part of my thesis project, these proteins are associated with other epigenetic modification mechanisms including genomic imprinting. Therefore, a short overview of this epigenetic modification will be presented for better understanding of their mention in other sections.

Histones are basic proteins of small molecular weight (10-22 kilodaltons) that compact DNA and organize chromatin in eukaryotic cells nuclei (reviewed by [82]). The primary unit of chromatin is the nucleosome, an octamer formed by two molecules of histones H2A, H2B, H3, and H4 around which 146 base pairs (bp) of DNA are wrapped twice[83]. Furthermore, H1, a linker histone, interacts with the octamer's entry and exit point and stabilizes compacted DNA [84]. The amino-terminus of the histone proteins protrude the nucleosome and are sites where post-translational modifications may occur.

Post-translational modifications can alter the charge of the histone protein and change the interaction with the DNA [85]. These include methylation (me) on lysine (K)

[86, 87] or arginine (R) residues [88], acetylation (ac) [89, 90] or ubiquitylation (ub) on K residues [91], or phosphorylation (ph) on serine (S) residues [92]. In addition, histone methylation may include binding of up to two methyl groups (me or me2) on R residues or up to three (me3) on K residues. However, the number of methyl groups can be placed and recognized by different enzymes to execute different functions (reviewed by [93]).

Histone modifications mostly occur to histone 3 (H3) and histone 4 (H4) of the nucleosome and are associated with neighboring gene silencing or activation depending on the specific modification [86-92]. Modifications often associated with transcriptional activation are acetylation of histone 3 on lysine nine (H3K9ac), H3K4me, and H3K36me. These modifications are associated with euchromatin, RNA polymerase and other transcription factors (reviewed by [94]). Conversely, some modifications often associated with transcriptional repression are H3K9me3 and H3K27me3. In this case, these modifications are associated with heterochromatin, a dense (packaged) form of chromatin (reviewed by [95]).

DNA methylation

DNA methylation is an epigenetic modification in which a methyl group is added to the 5^{th} position of a cytosine primarily in a CpG context [96]; it can also occur in a CpA context in embryos and ES cells [97]. A study by Bird showed that only half of the CpGs were methylated during DNA replication and they needed to be methylated for maintenance of DNA methylation indicating that this is a post-replication modification [98]. It was first described as the fifth base and was studied as a product of hydrolysis from the digestion of the nucleic acid in the *Tubercle bacillus* with sulfuric acid [99].

The 5-methyl-cytosine (5meC) was isolated in the picrate (crystalline salt) form and matched to the chemically synthesized base created by Wheeler and Johnson in 1904 [99].

In 1975, Holliday and Pugh hypothesized DNA methylation to be the mechanism to control gene activity during development and indicated that other base modifications could lead to heritable changes in bases controlling the activity of adjacent structural genes. Authors explained that the modification would have to occur in the promoter sequence of the gene and suggested that this event is guided by two enzymes: one to methylate the strand within a group of palindromic DNA while the other enzyme methylates the daughter molecules of the new DNA strand after DNA replication [100]. Now it is recognized that there are two types of DNA methyltransferases (Dnmt), one family for *de novo* methylation and another for maintenance.Dnmt3 isoforms place new methyl marks [101] and Dnmt1 maintains methylation in daughter DNA strands [102, 103].

DNA methyltransferases

Dnmts are responsible for methylating the carbon 5 of a cytosine by recognizing the CpG dinucleotide and catalyzing a methyl group transfer to that position. The methyl group is donated by S-adenosyl-methionine or SAM [104-106]. Dnmt1 catalyses methylation reactions after DNA replication by interacting with PCNA (proliferating cell nuclear antigen) and UHRF1 (also known as NP95) which recognize hemimethylated DNA at replication forks [107]. Hemimethylated DNA is a state of DNA methylation

when one strand is methylated (*e.g*. parent strand) and the other strand is unmethylated (*e.g*. daughter strand) [103].

Dnmt1 isoforms - Dnmt1s (somatic) is found to be ubiquitously expressed although, its level changes during the cell cycle division with accumulation at the beginning of the S-phase and reduction after cell division similar to other replication associated proteins [108]. DNMT1b, in human cells, is ubiquitously expressed and functions as a splice variant mRNA but encodes only for a DNA methyltransferase protein with minor activity compared to DNMT1s [109]. Dnmt1p and Dnmt1o are gamete specific expressed only in the pachytene spermatocyte and in the oocyte, respectively [110]. Dnmt1p is a non-functional isoform of Dnmt1 in the spermatocyte pachytene stage. Dnmt1p exon 1 is pachytene-specific and although *Dnmt1p* mRNA levels are detected in the pachytene spermatocyte, no protein is detected thus exon 1 appears to be interfering with translation [110]. Dnmt1o has specific functions in development and is found in the cytoplasm of the early embryo except at the 8-cell stage where it gets transported to the nucleus indicating a specific role at this point [72].

Dnmt3 isoforms - Dnmt3a and Dnmt3b, are expressed in fetal tissue after day 10.5E and adult tissues [101]. A short isoform, Dnmt3a2, is predominant in embryonic stem cells, embryonic carcinoma, testis, ovary and spleen, and functions as transcriptional repressors [111]. DNMT3b is expressed in multiple tissues and when mutated, in humans, can cause Immunodeficiency-Centromeric Instability-Facial Anomalies syndrome (ICF; OMIM 242860; reviewed in [101]). Dnmt3l, contrary to the

previously mentioned Dnmt3 enzymes, has no methyltransferase activity and is not essential for zygotic development; however, it is necessary for the establishment of parental-specific imprints and it increases the binding of SAM and the methyltransferase activity of Dnmt3a by physically associating with it temporarily and targeting Dnmt3a to the appropriate genomic sequence to be methylated [112-116].

Methyl-CpG binding domain (Mbd) proteins

Methyl-CpG binding domain (Mbd) proteins recognize methylated DNA. These proteins can bind repressors and histone deacetylases that lead to an inactive chromatin structure [117-120]. The three mammalian Mbds known to bind to methylated DNA are Mbd1, Mbd2, and Mecp2 [120]. Mbd1 interacts with the chromatin repressors H3K9 methylase, Suv39h1 (enzyme required for trimethylation of H3K9 [121]) and HP1 (binds to H3K9 methylated residues [122]) to stabilize heterochromatic state [120]. Mbd2 binds to methylated DNA and brings the NuRD (Nucleosome Remodeling and Deacetylase) complex in contact with methylated CpGs. The NuRD complex utilizes histone deacetylases 1 and 2, histone binding proteins and ATPase-dependent nucleosome remodeling proteins to maintain a repressive state [123-125]. Mecp2 (methyl CpG binding protein 2) binds to methylated DNA and recruits histone deacetylases to repress transcription [126]. A fourth mammalian Mbd was also identified as Mbd3 but this one does not localize to methylated DNA due to a mutation in the Mbd domain [127]. However, deletion of Mbd3 leads to embryonic death demonstrating it interacts with proteins involved in chromatin remodeling [128]. In addition, Mbd3 is required to

maintain genomic imprinting at least at the *H19* locus (refer to genomic imprinting section) [129].

Functions of DNA methylation

DNA methylation is a highly stable modification and inherited through cellular divisions. Originally, DNA methylation was associated with gene silencing [96]. However, more recent data shows that it can also be involved in increasing gene expression, alternative splicing and intragenic alternative promoters silencing [130-132]. The current understanding of DNA methylation function is as follows: gene silencing occurs when the promoter, the transcription start site and the first exon of a gene are methylated, while gene body methylation through the transcription termination site does not affect DNA polymerase activity and is associated with active gene expression [130]. Intragenic differential methylation studies in the bees' epigenome showed a link between methylation and alternative gene splicing [131]. Finally, DNA methylation targets transposons [133], and other repetitive elements (*e.g.* Iap; intracisternal A particle [134]) for their downregulation.

DNA demethylation

Two rounds of genome-wide DNA demethylation have been observed; one during preimplantation development [135-138] and one during primordial germ cell migration [139-142].

During preimplantation development, the parental genomes go through a round of global demethylation which does not affect the primary imprint (refer to section on

genomic imprinting below). The paternal genome is actively hydroxymethylated [135, 143] by 6 hours post-fertilization [135] (see section on TET proteins), while the maternal genome is passively demethylated during DNA replication as a result of the exclusion of Dnmt1o from the nucleus [136-138]. Dnmt1o reenters the nucleus only during the 8-cell stage when it is thought to be involved in the maintenance of the methylation imprints deposited during gametogenesis [72, 144].

In mice, the second reprogramming (*i.e.* round of demethylation) occurs in the primordial germ cells (PGC). PGC demethylation is observed during their migration to the genital ridge starting around day 7.25E [139-141] and completed by day 13.5E [142]. Demethylation was observed at imprinted and non-imprinted regions and occurred at similar rates in male and female embryos. In that study, Dnmts were localized using immunohistochemical staining and results showed that Dnmt1 is highly present in PGCs throughout days 10.5-13.5E. As a result of this observation, the Surani group proposed that the second round of DNA demethylation occurred in an active manner and that it was independent of Dnmt1 [142]. Interestingly, both male and female germ cells maintain methylation in repetitive elements, including Iap, during the rounds of demethylation [142, 145].

Active demethylation can occur by various mechanisms including deamination of the 5-methyl-cytosine (5meC) to form a thymine (T) followed by base excision repair (BER) and substitution with an unmethylated cytosine (C; [146, 147]) or by hydroxymethylation [148]. The first mechanism can be directed by cytidine deaminases followed by DNA repair systems including a type of T glycosylase (Tdg; thymine DNA glycosylase) and Mbd4 (methyl-CpG binding domain protein 4; it can function as T

glycosylase for DNA repair). In zebra-fish and mouse, activation-induced deaminase (Aid) and apolipoprotein B mRNA editing enzyme, catalytic peptide 1 (Apobec1) are possible candidates to deaminate 5meC resulting in a mismatched T:G dinucleotide that could be repaired by Tdg in cooperation with Mbd4 [146, 149]. Both Aid and Apobec1 are present in mouse oocytes and PGC supporting their possible role in mammal DNA demethylation [147].

Hydroxymethylation involves Tet (tet methylcytosine dioxygenase) proteins, Tet1, Tet2 and Tet3, with their ability of oxydizing 5meC to 5-hydroxymethyl-cytosine (5hmC). Tet1 is capable of binding to both fully- and hemi-methylated DNA and converting 5meC to 5hmC [148]. This other form of methylation is not able to be recognized by Mecp2, Mbd1, Mbd2, Mbd4 or Dnmt1 affecting methylation status by consequence [150-152]. Another mechanism whereas 5hmC can cause demethylation is that it can be recognized by BER and 5hmC-specific DNA glycosylase causing a deamination to form 5hmU; this is then recognized by a DNA repair system that will fix the mismatch [153].

Enrichment of Tet1 decreases along with 5hmC during embryonic stem (ES) cell differentiation indicating that Tet1 plays a role in maintaining ES cell identity [148]. Tet1 has the ability to bind to the Nanog promoter protecting it from DNA methylation to maintain pluripotency [154]. TET2 has not been linked to ES cell differentiation, but when mutated it may result in leukemic disease development along with altered DNA methylation patterns in humans [155-157]. In mice, Tet3 deficiency results in developmental failure; embryos with the absence of Tet3 are not capable of following active demethylation on the paternal pronuclei [143]. In that study, Gu *et al.* [143]

observed the effect of Tet3-deficiency in embryos from Tet3-deficient oocytes fertilized by wild-type sperm. Authors discussed that homozygous mutation resulted in neonatal lethality while conditional deletion in PGC and fertilization with wild-type sperm produced live heterozygous offspring. Investigators then studied the effect of Tet3-deficiency in the paternal genome of developing zygotes and found that the active demethylation is affected. More specifically, in the male zygotic pronucleus, 5hmC was decreased in Line1 transposon and in two other paternally methylated regions showing that Tet3is necessary oxidation of 5meC. Finally, authors showed a requirement of Tet3 for proper embryonic development as absence of Tet3 results in abnormal development and embryonic death.

DNA re-methylation

The rounds of *de novo* methylation in gametes occur at specific times depending on the sex of the germ cell [158-160]. In the male, *de novo* methylation occurs during prospermatogonia formation before birth (day ~16.5E [161]) while in females, re-methylation occurs after birth during oocyte growth [162].

Dnmt3a and Dnmt3b are both required for *de novo* methylation to occur [101]. Dnmt3a and Dnmt3b are both highly expressed in undifferentiated ES cells and less expressed in differentiated cells with diminished levels in adult somatic cells [111]. Inactivation of Dnmt3a and Dnmt3b affects *de novo* methylation in ES cells and early embryos. Dnmt3b is more likely to be necessary during early embryo development [101] while Dnmt3a appears to be more specific for somatic cells [163], late embryo development and after birth [101].

More specific to germ cell *de novo* methylation, Dnmt3a and Dnmt3l were found to be required for the establishment of parental-specific methylation [113, 163]. Embryos from Dnmt3a conditional knockout females mated to wild-type males are smaller than control embryos and fail to survive after day 9.5E. This was associated with disruption of maternal methylation during oogenesis. Furthermore, reciprocal mating produced no pregnancies and showed that males with disrupted Dnmt3a presented azoospermia during adulthood showing that Dnmt3a is also required during spermatogenesis [163].

Disruption of Dnmt3l affects maternal methylation during oogenesis [113] and paternal methylation during non-dividing prospermatogonia [164]. Bourch'is *et al.* showed heterozygous mice with substitution of the *Dnmt3l* gene with the *β-geo* (β-galactosidase–neomycin phosphotransferase) gene presented a normal phenotype and high levels of the *β-geo* in growing oocytes and prospermatogonia [113]. Interestingly, homozygous mice were normal, but their fertility was affected. Homozygous males had normal germ cell formation but testes function was affected during adulthood [113, 164]. Similarly, the females showed normal oogenesis but were not able to maintain pregnancy after day 9.5E. Further analysis of the offspring at mid-gestation revealed that they exhibited abnormalities including neural tube defects and overgrowth in the embryo proper and extra-embryonic tissues respectively [113]. Based on these results, the authors concluded Dnmt3l was necessary for setting parental methylation imprints during gametogenesis.

Genomic Imprinting

The mammalian genome in somatic cells includes one chromosome inherited from the maternal oocyte and another from the paternal sperm. Somatic cells are then diploid cells with most of the genes expressed from both parental chromosomes. Genomic imprinting is an epigenetic mechanism where several epigenetic modifications are combined in a series of steps that lead to parental allele-specific gene expression (reviewed by [81]). Consequently, imprinted genes are functionally haploid. When a gene is maternally-expressed then it is paternally imprinted and vice-versa. The repressed chromosome is referred to as the imprinted allele. Currently, there are approximately 150 imprinted genes identified in mice [165] and approximately 70 out of 156 possible candidates identified in humans [166, 167].

Early studies

Studies in the 1980s with parthenogenetic, gynogenetic and androgenetic embryos showed the requirement of both parental chromosomes for fetal growth control and placental development [168-170]. Embryos generated with two maternal genomes (parthenotes and gynogenotes), although smaller in size when compared to controls, had relatively normal fetal development but significantly reduced extra-embryonic tissues [169] indicating an important role of the paternally imprinted genes in placental formation and development. Conversely, in androgenotes, the fetus was severely underdeveloped when compared to controls but the extra-embryonic tissues appeared relatively normal [168-170] demonstrating the importance of maternally imprinted genes in fetal growth.

The different potential between mammalian parental genomes was also shown in a study were mouse offspring from paternal/maternal chromosomal duplication or deficiencies were abnormally developed [171]. In that study, Cattanach and collaborators [171] discussed that based on previous studies not all the genome is involved in parental-specific effects. For example, normal offspring were obtained from parthenogenetic and gynogenetic zygotes with maternal or paternal disomy for chromosomes 1, 4, 5, 9, 13, 14 and 15 [172]. However, paternal duplication/maternal deficiency or reciprocal of regions of chromosomes 2, 8 and 17 have been recognized for being lethal or for producing abnormal offspring [173-175]. Moreover, Cattanach and collaborators [171] produced mice with maternal or paternal disomy for chromosomes 11 and 13. While no developmental abnormalities were observed when chromosome 13 was duplicated, offspring with maternal disomy on chromosome 11 were smaller and those with paternal disomy of the same chromosome were larger. They also analyzed intercrosses between heterozygous mice and translocation of chromosomes 2 and 11 and provided evidence that only a region of chromosome 11 was related to the effect on size. Offspring which inherited a maternal duplication (*i.e.* paternal deficiency) of the proximal region of chromosome 11 were smaller in size while both maternal and paternal duplications of the distal region of the same chromosome were lethal. Finally, because they had previously produced viable mice with paternal or maternal chromosome 11 disomy, authors attributed lethality to chromosome 2 and reported abnormal development in newborns that inherited distal chromosome 2 duplications from either parent [171].

Characterization of first imprinted genes

Among other strategies to identify imprinted genes, earlier attempts included the study of parental-effect mutations (*i.e. Igf2r* and *Igf2*; [176, 177]) and the study of a transcript located in a chromosomal region known to be parentally imprinted [178] (*i.e. H19* and *Igf2*; [179, 180]). The four studies were published in 1991.

Insulin-like growth factor type 2 receptor- T-associated maternal effects (*Tme*) had been identified as being absent in "Hairpin-tail" mutant mice with deletion of chromosome 17. In that study, *Igf2r* gene was found to be expressed in *Tme* region in wild-type mice and mutant mice that inherited the *Tme* deletion from the paternal chromosome. Contrary to this, *Igf2r* gene was absent in mice that inherited the maternal *Tme* deletion. *Igf2r* expression was compared to *Plg* and*Sod-2*, another two genes localized and near the *Igf2r* in chromosome 17, and non-imprinted pattern of expression was observed. The Barlow group then concluded that *Igf2r* was maternally-expressed and imprinted in the paternal allele [176].

Insulin-like growth factor type 2 - The second imprinted gene to be studied was *Igf2* which is located on chromosome 7 [181]. Two groups of researchers analyzed the effect of *Igf2* expression and phenotype of the offspring during early embryo development [177] or late gestation [180] by targeted deletion or biparental duplication (maternal duplication/paternal deficiency or reciprocal), respectively. The first group observed that newborns with maternal deletion were similar in phenotype to the wild-type while those with paternal deletion showed growth deficiencies, and deduced that *Igf2* was

imprinted on the maternal allele [177]. In accordance with these findings, the second group observed that on day 16E the fetuses with maternal duplication/paternal deficiency showed retarded growth. Those with reciprocal *Igf2* expression died early in gestation [180]. Both groups then concluded that *Igf2* is a paternally-expressed/maternally-imprinted gene important in embryo development [177, 180].

Igf2 was discovered in the 1960's. This gene was originally named NSILA for having non-suppressible insulin-like activity (NSILA) in human serum [182], and designated an IGF in the 1980's [183]. In addition, *Igf2* was described as a mitogenic protein expressed in multiple tissues with a role in paracrine-autocrine regulatory signaling [184, 185]. Later studies indicated that *Igf2* regulates growth and cell proliferation, mitogenesis, steroid hormone activity [186-188], stimulates insulin-like metabolic activity responses [189], and plays a role in muscle and bone development [190-192].

During embryonic and neonatal development, *Igf2* uses at least three promoters and expresses multiple transcripts in many tissues [193-195]. For transport and function in the cell, *Igf2* is dependent on binding to insulin-like growth factor binding proteins (Igfbp; reviewed by [196, 197]). For mRNA cytoplasmic stability, *Igf2* depends on Igf2bp1 (insulin-like growth factor 2 mRNA binding protein 1, also known as Imp1) [198, 199]. For growth regulation, *Igf2* binds to membrane receptors in many mammalian cells [188]. Moreover, *Igf2* receptors seem to be evolutionary conserved [200].

Regulatory signaling of Igfs primarily occurs by binding to the type 1 Igf receptor (Igf1r), but there is significant crosstalk between Igfs and the insulin receptor (Ir) as well

([201]; reviewed by [202]). Additionally, Igf2 can stimulate insulin-like metabolic activity by binding to the isoform B of the Ir (Ir-b). On the contrary, if Igf2 binds to Igf2r it is targeted for degradation (reviewed by [197]). The mannose 6-phosphate/Igf2r (in human known as M6P/IGF2R), mainly located intracellularly (5-10% is located on the cell surface), has the ability to sequester Igf2 and transport it to the cell lysosome for degradation [203].

Mouse *Igf2* is composed of 5 exons and 4 introns [204] and is located on chromosome 7 [181] while the human *IGF2* is composed of 9 exons and 8 introns and is found on chromosome 11 [205]. Target experiments using RT-PCR have found *Igf2* to be expressed during peri-implantation embryo (day 4-6E) while *in situ* hybridization studies have localized it by day 5.5E in the extra-embryonic ectoderm and the ectoplacental cone. From that point on, *Igf2* is found to be in extra-embryonic mesoderm, but not in the primitive streak, and columnar mesoderm (day 7E), embryonic mesoderm, lateral endoderm, developing heart, foregut and somites (day 7.5-8.5E; [206]). *In situ* hybridization of 10-16E rat fetuses show *Igf2* expression in head mesenchyme, mesoderm, cephalic portion of neural crest, tissues of mesodermal origin predominantly those from lateral mesoderm, muscle cells, in endoderm origin tissues: liver and bronchial epithelium, and ectoderm-derived choroid plexus of the brain [207].

Allelic expression of *Igf2* – Although less expression is found at the 8-cell stage when compared to the 2-cell stage and blastocyst stage, analyses of parthenogenetic and gynogenetic embryos suggests *Igf2* is expressed in a biallelic manner until implantation. Latham and collaborators explained that high expression of *Igf2* in parthenogenetic

embryos, containing only maternal chromosomes, indicates no effect of maternal imprinting at this stage [208]. After implantation, transcription is regulated by genomic imprinting and is mainly monoallelically expressed on the paternal allele except in fetal liver, leptomeninges and choroid plexus where it is expressed from both parental alleles [177, 205]. After birth *Igf2* is downregulated and the expression is limited to the liver, leptomeninges and choroid plexus in adult rat and mice where it remains expressed in a biallelic manner [177, 204]. Mutations at the *Igf2* locus result in mice with only 50-60% of the normal size when compared to wild-type littermates, however, viability and fertility are not affected [209].

H19- Previous research had shown that transgenic mice deficient in *H19* died before birth. This suggested that *H19* was produced and regulated during embryo development [210]. In that study, Brunkow *et al.* [210], mentioned that *H19* was present in a region in chromosome 7 that had been described as a genomic imprinted region [179]. They generated F1 hybrid embryos from several strains of mice and used an RNAse protection assay to identify the origin of the parental allele. They observed maternal *H19* expression in the F1 hybrid embryos. In addition, Bartolomei *et al*. [179] referenced the discovery of *Igf2* as an imprinted gene and stated that maternally-expressed *H19* and paternally-expressed *Igf2* are linked but expressed in opposite directions.

H19 was first described and cloned in the 1980's from fetal liver [211] and identified as one of the first imprinted genes in 1991 [179]. *H19* was simultaneously identified in other laboratories as a member of myogenic factors, then named *MyoH*

[212, 213], as a gene regulated along with the *alpha-foetoprotein* gene by the *Raf* gene [211], and as a differentially expressed gene upon screening of non-differentiated embryonic stem cells and differentiated embryoid bodies [214]. Furthermore, it was described as an untranslated RNA (ncRNA) [215] associated with *cis*-acting epigenetic silencing and tumor suppressor activity [216, 217]. Sequencing of this ncRNA in mouse and human revealed it was 2.5 kb long, composed of 5 exons and 4 introns [211], and located in chromosome 7 in the mouse [218, 219] and chromosome 11 in the human [220]. *H19* was classified as a ncRNA until 2002 when Okazaki and collaborators analyzed the mouse transcriptome and gave origin to the classification long ncRNA (lncRNA) in which *H19* and many other ncRNA were included [221].

Initial studies using *in situ* hybridization showed that *H19* was detected in extraembryonic tissues as early as day 5.5E but not in the embryo proper until day 8.5E [214]. Similar results using RT-PCR were seen in the pre-implantation embryo (day ~4.0E) when Poirier *et al.* [214], immunolyzed mouse blastocysts and found *H19* present only in the complete embryo as opposed to the ICM suggesting it to be TE specific at this stage. In that same study, using pools of oocytes and embryos, *H19* was expressed from the oocyte through the blastocyst stage showing maximum expression in the blastocyst [222]. Finally, *H19* becomes one of the most abundantly expressed genes in the developing embryo and placental tissues [212] but it is slowly downregulated after birth except in cardiovascular and skeletal muscle [214].

Regulation of genomic imprinting

Imprinted genes are generally found in clusters including at least one ncRNA and both maternally- and paternally-expressed genes [223]. Regulation of genomic imprinting is dependent on epigenetic modifications on a region of DNA which is neighboring to the genes that form part of the cluster. This region can be up to several kb long, have a high CpG dinucleotide content and has been denominated as the imprinted control region or ICR [218, 224].

Imprinting Control Regions

Earlier studies suggested that the modification in charge of controlling genomic imprinting had to fit four criteria including 1) the capability of affecting transcription, 2) heritable and maintained throughout cell division, 3) set on paternal and maternal chromosome individually and finally, 4) resettable in order for a chromosome to establish new marks in new germline formation [225]. Bartolomei, *et al*. [225], suggested DNA methylation was the modification most suitable for these conditions (reviewed by [81]). ICRs become differentially methylated regions (DMR) during gametogenesis and direct parental-specific gene expression of clustered imprinted genes [218, 226]. In addition to differential DNA methylation, ICRs are marked by differential histone modifications [227]. It is important to note that not all DMR act as ICR. Imprinting control regions can have different functions, and loss-of-imprinting (LOI) in these regions results in misregulation of gene expression (reviewed by [81]). The two mechanisms that allow an ICR to control imprinting include control by insulator activity (*e.g. H19/Igf2* cluster) and by regulation of expression of a long ncRNA (*e.g. Kcnq1ot1* region).

Regulation by insulator activity

Located 90kb upstream of *H19* is the paternally–expressed fetal growth factor *Igf2* [177]. *H19* and *Igf2* are reciprocally imprinted and share enhancers downstream of *H19* (**Figure 1.2**). Tissues of endodermal origin (*i.e.* liver, gut, choroid plexus and yolk sac) use the first set of enhancers located 8kb from *H19* [210, 228, 229] while those of mesodermal origin (*i.e.* skeletal and cardiac muscle) use the second set found 25kb from *H19* [230].

The locus' ICR is located 2-4 kb upstream of *H19*. This ICR is hypermethylated on the paternal allele in sperm and somatic tissues [231-233]. The methylation spreads 2kb to the *H19* promoter in somatic cells [218, 234]. Nonetheless, this methylation is not stable and becomes hypomethylated after the genome-wide demethylation in the blastocyst and becomes re-methylated after implantation [235].

The *H19/Igf2* ICR contains four 21bp repeats that are highly conserved between different species. These four short sequences are binding sites for the eleven zinc finger DNA binding nuclear protein, CCCTC-binding factor or CTCF [236]. This protein has various functions including transcriptional activation and repression, insulation, imprinting and X-chromosome inactivation. Insulator proteins separate a gene from their enhancers, thus inhibiting the enhancer induced expression of that specific gene [237]. The binding of CTCF is prevented by methylation. When bound, CTCF protects the CpG sites from acquiring DNA methylation, and based on this it can suggest a role in epigenetic regulation [238, 239].

In the *H19/Igf2* imprinted gene cluster, CTCF functions as an enhancer-blocking insulator on the unmethylated maternal allele preventing *Igf2* from interacting with the shared enhancers. When methylated (*i.e.* on the paternal allele), CTCF protein cannot

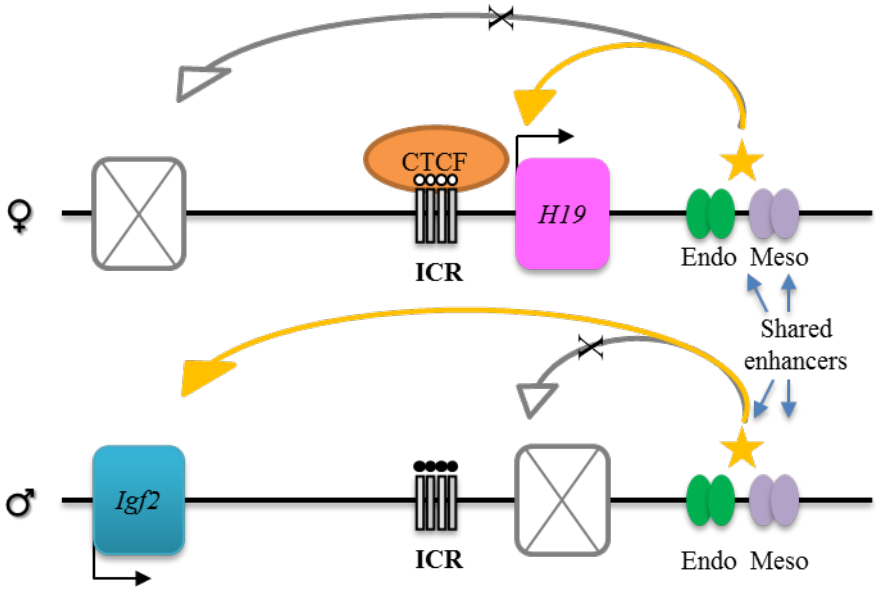

Figure 1.2. *H19/Igf2* imprinted gene cluster. The cluster is found in chromosome 7 and 11 in mouse and human, respectively. The ICR is located 2-4kb upstream of *H19* in the mouse. Two sets of shared enhancers located 8kb and 25kb downstream of *H19* interact with *H19* or *Igf2* for expression in tissues of endodermal (endo) or mesodermal (meso) origin. On the maternal allele (top line) the unmethylated ICR allows binding of the insulator protein CTCF to this region causing a chromatin conformation where the shared enhancers interact with *H19* but prevent the interaction with the *Igf2* promoter resulting in *H19* expression and *Igf2* gene repression. On the paternal allele (bottom line), reciprocal expression occurs when the hypermethylated state of the ICR prevents CTCF binding and enhancer interaction with *H19*; as a result *H19* gene is silenced and *Igf2* is paternally expressed. ♀ = female (maternal allele); ♂ = male (paternal allele). *H19* = maternally expressed non-coding RNA (pink). *Igf2* = paternally expressed fetal growth factor (blue). Black arrows indicate gene expression direction. White boxes with crossed gray lines represent the imprinted gene. Gray squared bars = imprinting control region (ICR). Open circles = unmethylated CpGs, closed black circles = methylated CpGs. Horizontal orange oval = insulator protein CTCF. Yellow star and arrows = activation and enhancer-gene interaction. Vertical green ovals = shared endodermal enhancers. Vertical purple ovals = shared mesodermal enhancers. Gray arrows with an "X" indicate no enhancer-gene interaction. The figure is not drawn to scale and not all imprinted and non-imprinted genes in the cluster are shown.

bind to the ICR allowing *Igf2* to be expressed [240, 241]. This was confirmed using a chromosome conformation capture analysis and observing the formation of a tight loop around the maternal *Igf2* that silenced it, and interactions of the shared enhancers with paternal *Igf2* [241, 242]. Perturbations in this region may affect CTCF function on the maternal allele allowing *Igf2* to be expressed in a biallelic manner [241]. It is important to mention that, although *Igf2*'s transcription is epigenetically regulated by imprinting, is not dependent on the presence of the ICR or the *H19* ncRNA for expression. Studies where the two aforementioned regions were deleted produced offspring with biallelic expression of *Igf2* and bigger in size than wild-type mice but viable and fertile [243]. An intergenic region upstream of *Igf2* contains a silencing element that can assist in repressing the maternal *Igf2* [181, 244]. This element has been shown to also regulate *Igf2* after implantation by DNA methylation [245] and to be specific for mesodermal tissues. Although it is suggested that a similar silencing element specific for endodermal tissues exists, to date it has not been identified [181, 244]. The *Igf2* gene itself also includes three DMRs but it is not known if their function is dependent on the *H19*/*Igf2* ICR. Additionally, *Igf2* promoters are unmethylated on the maternal allele which suggests another mechanism may account for repression on the maternal chromosome [246].

Regulation by long non-coding RNA

Non-protein coding RNAs (ncRNA) are sequences of functional RNA that are not translated into protein. Originally, only 1% of the genome was described as functional (*i.e.* protein coding). However, ongoing research in humans demonstrates that

approximately 98% of the transcriptional output is of non-coding RNA origin [247]. Moreover, ncRNAs play a role in gene expression control mechanisms such as genomic imprinting [248], X-chromosome inactivation [249] and transcriptional silencing [250]. Non-coding RNAs are classified in a number of subclasses based on their length and biogenesis mechanism. These subclasses include but are not limited to: ribosomal RNA (rRNA), transfer RNA (tRNA; 75-95 base-pairs [bp]), short-interfering RNA (siRNA; 21bp[251-253]), microRNA (miRNA; ~22nt[254, 255]), piwi-interacting RNA (piRNA; 26-31bp [256, 257]), small nucleolar RNA (snoRNA; 60-300bp), and long ncRNA (lncRNA; >1,000bp) [258], and a more recently identified class the large-intergenic RNA (lincRNA).

At least two imprinted domains have been shown to be regulated in *cis* by the transcription of a lncRNA (*i.e. Airn* and *Kcnq1ot1*) by attracting chromatin remodelers to the locus. In the following section I will discuss in detail the regulation of the KvDMR1 locus by *Kcnq1ot1*.

Kcnq1ot1 expression and imprinted regulation - The *Kcnq1* cluster is found in chromosomes 7 and 11 in mouse and human respectively, and is one of the largest clusters of imprinted genes covering ~1Mb. This cluster contains one paternally-expressed gene (*Kcnq1ot1* [*Kcnq1* overlapping transcript 1]) and at least 6 (depending on species) maternally-expressed genes. The maternally expressed-genes in the mouse are: *Osbpl5*, *Phlda2*, *Slc22a18*, *Cdkn1c*, *Kcnq1*, *Tssc4*, *Cd81*, and *Ascl2*.

The promoter of the *Kcnq1ot1* gene, KvDMR1, is found in an antisense orientation in the 10th intron of the maternally-expressed gene *Kcnq1*. KvDMR1 serves also as the locus'

ICR (**Figure 1.3**). In this locus, the KvDMR1 is unmethylated on the paternal chromosome allowing expression of the ~90 kb intronless lncRNA *Kcnq1ot1* which represses flanking imprinted genes in *cis* (explained below). Conversely, on the maternal allele, the KvDMR1 is hypermethylated resulting in repression of *Kcnq1ot1* and bidirectional activation of the other genes [259, 260]. Acquisition of DNA methylation in the KvDMR1 occurs during oogenesis and is maintained in the maternal chromosome of diploid cells [258]. Previous studies show that deletion of the KvDMR1 in mice results in smaller offspring when compared to the wild-type litter [248]. Loss of methylation at the KvDMR1on the maternal allele results in biallelic expression of *Kcnq1ot1* and misregulation of flanking imprinted mRNAs [261].

Other epigenetic regulation at the Kcnq1 locus - In addition to DNA methylation, histone modifications have been shown to assist in the silencing of the genes at this locus in the paternal chromosome. Terranova *et al.*[262] and Pandey *et al*. [263], proposed an association between *Kcnq1ot1* and the Polycombgroup proteins (PcG). Polycomb group proteins complexes are histone tail modifiers found to act as chromatin remodelers and to control genomic programming and differentiation [264, 265]. There are two types of Polycomb repressive complexes; PRC1 and PRC2 [266]. PRC2 is composed of several members including Suz12, RdAp46/48, Eed and the histone methyltransferase Ezh2. Cbx2, a member of the PRC1 complex recognizes the PRC2 repressive mark H3K27me3 through its chromodomain, and promotes monoubiquitylation of H2AK119 by Ring1. In addition, these complexes can

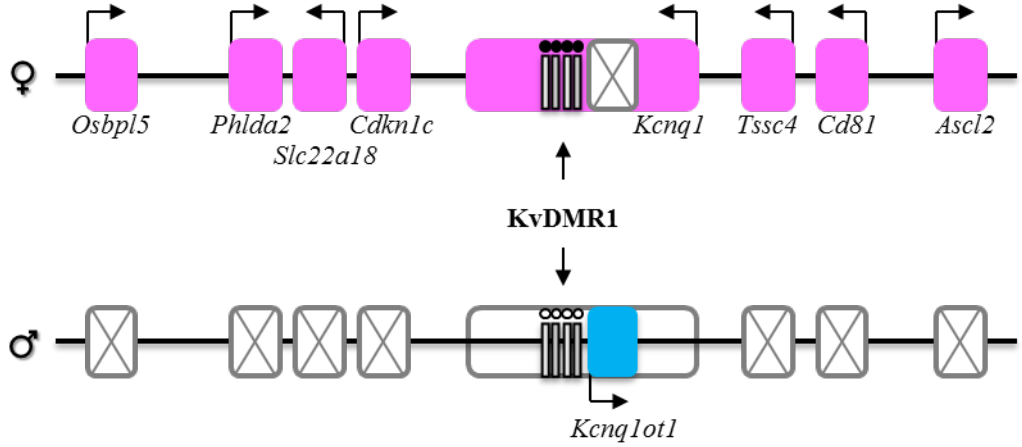

Figure 1.3. *Kcnq1* imprinted gene cluster. The cluster is found in chromosome 7 and 11 in mouse and human, respectively. The ICR involved in genomic imprinting in this cluster is the KvDMR1 (~2kb in length) found within the 10th intron of the *Kcnq1* gene. Hypermethylation of the KvDMR1 on the maternal allele (top line) represses expression of the antisense long non-coding RNA (lncRNA), *Kcnq1ot1*; silencing of this gene allows expression of the other genes located upstream and downstream of *Kcnq1*. On the paternal allele (bottom line), the KvDMR1 is unmethylated allowing expression of the *Kcnq1ot1* gene; expression of this lncRNA forms a chromatin loop involved in the silencing of the other imprinted genes. ♀ = female (maternal allele); ♂ = male (paternal allele). Pink boxes = maternally expressed genes (labels below correspond to the other genes present in the cluster). Blue box = paternally expressed *Kcnq1ot1* lncRNA. Black arrows indicate gene expression direction. White boxes with crossed gray lines represent the imprinted gene. Gray squared bars = KvDMR1. Open circles = unmethylated CpGs, closed black circles = methylated CpGs. The figure is not drawn to scale and non-imprinted genes are not shown.

interact with histone deacetylaces to assist in chromatin silencing [266, 267].

G9a methyltransferase is also found to be involved in promoting chromatin repression by dimethylating H3K9 [263, 268]. In undifferentiated ES cells, embryo and placenta, H3K27me3 and H3K9me2 repressive marks are found on the methylated KvDMR1, while active marks, H3K4me and acetylated H3/H4, are present on the unmethylated region [268-271]. Finally, embryos lacking Ezh2 and G9a show loss-of-imprinting (LOI) for placental specific imprinted genes in the paternal allele [262].

In summary, repressive histone modifications, together with the PcGs bring silencing to the paternal locus by bidirectional contraction of the chromatin which creates a region devoid of RNA polymerase [262, 266].

Previous work has found *Kcnq1ot1* expression from the zygote to the blastocyst stage [262, 268]. Additionally, in mice, at day 14.5E *Kcnq1ot1* was expressed in lung, gut, heart and kidney. Then, in adult mice, *Kcnq1ot1* was also found in brain, skeletal muscle, spleen, liver and placenta [272] with higher expression in the placenta than in the liver [263]. Likewise, in human tissues, paternal allelic expression of *KCNQ1OT1* was observed in fetal liver, heart, spleen, cerebrum, muscle, lung and thymus [260].

Establishment of gametic (primary) and somatic imprints

Gametic (primary) imprints – Most of the imprinted domains acquire DNA methylation on the maternal genome during oocyte growth [273, 274] and only four DMRs have been characterized to acquire DNA methylation on the paternal allele before

birth (*i.e.* during spermatogenesis). In mice, the maternal methylation imprints are *Airn*/*Igf2r*, *Diras3*, *Gnas*, *Impact*, *Inpp5fv2*, *Kcnq1ot1'*s KvDMR1, *L3mbtl1*, *Mcts2*, *Mest* , *Nnat*, *Peg10*, *Peg3*, *Plagl1*(also known as *Zac1*), *Ptpn4* (also known as *Grb10*), *Rb1*, *Snrpn* DMR1, *Zrsr1* [258, 275-278], while the paternal imprints are *H19/Igf2*, *Dlk1*, *Rasgrf1* and *Zdbf2* [275, 279].

New methyl marks within both parental germ cells are placed by Dnmt3a and Dnmt3l [113, 163, 164, 274, 280]. A study on the structure of Dnmt3a suggested a recognition site for the *de novo* methylation at imprinted loci [115]. There is a periodic pattern of CpG sites every 8-10 bp in imprinted genes which was recognized by Dmnt3a [115]. Dnmt3b, on the other hand, is not essential for the establishment of gametic imprints, but it was suggested to have an important role in maintaining DNA methylation at pericentromeric heterochromatin [281].

Other factors such as Kdm1b (lysine (K)-specific demethylase 1B) and Hells (helicase, lymphoid specific) were found to be necessary for *de novo* methylation of various gametic DMRs. The Kdm1b encodes for a H3K4 demethylase, and Dnmt3l can interact with H3 to recognize unmethylated H3K4 for *de novo* methylation suggesting that the Kdmb1 factor and unmethylated H3K4 are required to place new methyl marks [282, 283]. The Hells factor is related to chromatin-remodeling ATPase family and has been associated with *de novo* methylation specific to the *H19/Igf2* ICR but not KvDMR1 [284, 285]. In addition, Eed (a PRC2 component), mediates trimethylation of H3K27 for transcription repression in the embryo [286, 287]. Also, the histone methyltransferase G9a is essential for the establishment or maintenance of the *Snrpn* ICR and transmitting

the imprinting signal to targeted genes but is not linked to the *H19/Igf2* ICR or KvDMR1 [288].

Maintenance of the primary imprints during preimplantation development

Gametic imprint marks escape the DNA demethylation event that occurs during preimplantation development [289]. It has been demonstrated that Dppa3 (developmental pluripotency-associated 3; also known as Stella or Pgc7) is required for protection of DNA methylation of the maternal genome during early embryogenesis [290]. In that study, Dppa3 plays a protective role against 5meC oxidation of the DNA in the maternal pronucleus [290]. In another study, the same group showed that Dppa3 can recognize and bind to chromatin rich in H3K9me2 [291]). Also, in zygotes, the maternal pronucleus showed more Dppa3 than the paternal pronucleus suggesting that Dppa3 prevents active demethylation of the maternal genome. Furthermore, chromatin-immunoprecipitation analysis in mature sperm showed enrichment of H3K9me2 in the *H19* and *Rasgrf1* DMRs. Dppa3 and H3K9me2 then confer protection of the two paternal primary imprints during the zygotic Tet3-driven active demethylation. Finally, demethylation of H3K9me2 by the histone demethylase *Jhdm2a* and inhibition of Dppa3's function by RanBP5-meR resulted in high levels of 5hmC [291]. In summary, these studies demonstrate that Dppa3 protects the maternal genome and various paternal methylation imprints by recognizing dimethylated H3K9 and inhibiting Tet3 oxidizing activity.

However, the question regarding how the gametic imprints are maintained during the passive demethylation which occurs during preimplantation development remains

unclear. It was proposed that Dnmt1 played a role in maintaining these methyl marks during early embryo development [292]. In addition, other factors such as Zfp57 (zinc finger protein 57), Suv39h and Dppa3 were found to be necessary for maintaining DNA methylation of several ICRs [290, 291, 293, 294]. Zfp57 and Dppa3 assist Dnmt1 by recruiting Setdb1 complex which brings the H3K9me3 repressive mark [293, 294] while Suv39h can directly recruit Dnmt1 during preimplantation development [295]. More specifically, the Dnmt1 isoform Dnmt1o (Dnmt1of maternal origin) was suggested to maintain imprinted marks during the pre-implantation stage until the embryo is able to transcribe Dnmt1s [110, 296]. Dmnt1s was shown to be required for the methylation of regions related to monoallelic expression of imprinted genes post-implantation [269, 297, 298].

Somatic (secondary) imprints **–** Methylation imprints are established after implantation in somatic cells. To date, somatic imprints have been identified at a subset of imprinted loci including *H19* [218, 234, 299], *Igf2* [300, 301] and *Cdkn1c* [302, 303]. However, these methyl marks are placed after imprinted expression has been established showing *de novo* methylation of secondary imprints is related to other epigenetic marks already present in the specific parental allele.

The *H19* locus contains two DMRs, one gametic imprint that regulates monoallelic expression of *H19* and *Igf2* (*i.e.* the *H19/Igf2* ICR) and another overlapping the promoter region of *H19*. The second DMR is unmethylated in sperm and blastocysts, and methylated during mid-gestation [218, 226, 234, 235, 301]. For the *Igf2* gene, three DMRs have been identified [300, 304, 305], one overlying the placental-specific

promoter and exhibiting hypermethylation in placenta (*Igf2*-DMR0; reviewed by[306], and two surrounding the*Igf2* promoter regions (*Igf2*-DMR1 and *Igf2* DMR2). These are methylated in the sperm, demethylated after fertilization and methylated by day 9.0E (*Igf2*-DMR1) and day 15.0E (*Igf2*-DMR2) on the paternal allele [301, 307]. The *Igf2*-DMR2 methylation is tissue-specific and methylated only in the tissues where *Igf2* is expressed [305]. Also, the methylation established after cell differentiation is dependent on the *de novo* DNA methyltransferases [101]. Finally, similar to the establishment of gametic imprints, Eed and Hells factors are also involved in assisting with maintenance of methyl marks in somatic imprints associated with the *Cdkn1c* imprinted gene [285, 286].

Although not included as part of this thesis, it should be noted that imprinted genes have been shown to regulate normal brain function, metabolic regulation and maternal behavior [308-310].

Genomic imprinting – a barrier to parthenogenesis in mammals

The existence of genomic imprinting prevents the experimental production of uniparental mouse embryos as these embryos lack the proper parental-specific expression of these genes and as a result fail to survive past mid-gestation [168, 169, 311, 312]. Bimaternal embryos generated by the combination of a 1n genome from a non-growing oocyte and a 1n genome from a fully-grown oocyte results in embryonic lethality by 13.5E [313]. The Kono group concluded that biallelic expression of *H19* as well as lack of *Igf2* expression was the cause for this result.

In 2004, the same group generated bimaternal mice by balancing the expression of the *H19*/*Igf2* imprinted cluster [314]. They used the DNA from oocytes from mutant new-born female mice containing a 3 kilobase (kb; *H19*Δ3) or13 kb (*H19*Δ13) deletion of the maternally-expressed gene, *H19*. The nuclei from these non-growing oocytes ($ng^{H19\Delta3}$and $ng^{H19\Delta13}$) were transferred into full-grown oocytes from adult wild-type females (fg^{wt}) to create bimaternal embryos. It should be noted that oocytes in newborn mice are hypomethylated. The lack of DNA methylation will allow expression of *Igf2* from the non-growing oocyte's genome while *H19* will only be expressed from the allele donated by the fully grown oocyte. After *in vitro* maturation and artificial activation of these oocytes, bimaternal embryos were then transferred into pseudopregnant females for further analysis. The fetuses from $ng^{H19\Delta3}/fg^{wt}$ parthenogenetic embryos only survived up to day 17.5 of gestation while those from $ng^{H19\Delta13}/fg^{wt}$ parthenogenotes produced two normal live offspring with similar phenotype compared to control pups, 8 live but abnormally developed and 18 dead pups. The live but abnormally developed pups died soon after birth. Of the two live offspring, one proved to be fertile and normal all through adulthood and the other was used for gene expression analyses. Microarray analysis was used to study and compare genes expression in the different groups at day 12.5 of gestation. Most imprinted genes expression was normalized in $ng^{H19\Delta13}/fg^{wt}$ parthenogenotes indicating that the gene dosage normalization allowed them to develop past mid-gestation. Then to analyze which genes played an important role to increase the competence of bimaternal embryos to survive throughout gestation, the authors compared expression levels of four imprinted genes (*H19, Igf2, Dlk1* and *Glt2*) at day 19.5 of gestation. Equal expression of *H19* and *Igf2* in $ng^{H19\Delta13}/fg^{wt}$ parthenogenotes was found

and the expression of *H19* was from the fg^{wt} oocyte while expression of *Igf2* was from the $ng^{H19\Delta 13}$. Levels of *Dlk1* and *Glt2*, another two imprinted genes in chromosome 12 [315, 316], were increased and decreased, respectively, in live but abnormally developed pups. The change in expression levels of *Dlk1* and *Glt2* imprinted genes may be involved in normal development past mid-gestation and genomic imprinting remains a barrier for development of parthenogenetic embryos [314].

Because this group of researchers was successful in producing bimaternal embryos but the number of live pups obtained was low, they proceeded to repeat the experiment after adding a second deletion to the mutant group of females that would donate the ng oocyte ($ng^{\Delta double}$ [317]). The second deletion belonged to another paternally-methylated region that is part of chromosome 12, the *Dlk-Dio3* DMR [315]. The deletion of the *H19/Igf2* and *Dlk-Dio3* DMRs allowed better development past mid-gestation and more effective production of bimaternal embryos. A total number of 42 live $ng^{\Delta double}$ /fg^{wt} parthenogenetic pups were recovered at day 19.5 of gestation, and of those, all but 4 survived after birth. From the 38 pups that were successfully nursed, 27 had similar body weight to the wild type pups but showed postnatal growth retardation throughout adulthood. The remaining 11 died 3 days after birth also exhibited slight growth retardation and breathing difficulties. Further analysis of the placenta showed similar phenotype to their body weight for all groups analyzed. Then, to understand the effect of both deletions on gene expression and the relation to full-term development, the investigators quantified the levels of expression of genes present in the *H19* and *Igf2* DMR and in the *Dlk1-Dio3* DMR during mid-gestation. *Igf2* was reduced in the group of 11 $ng^{\Delta double}$ /fg^{wt} parthenogenotes that were alive until day 3 after birth. Finally,

microarray analysis of $ng^{\Delta double}$ /fg^{wt} parthenogenotes compared to bimaternal embryos with only one chromosome deleted (*i.e.* $ng^{\Delta ch7}$ /fg^{wt} or $ng^{\Delta ch12}$ /fg^{wt}) showed the misregulation of many genes seen in $ng^{\Delta ch7}$ /fg^{wt} and $ng^{\Delta ch12}$ /fg^{wt}, was normalized in $ng^{\Delta double}$ /fg^{wt}. Thus the removal of these two regions somehow makes the embryos more capable of surviving through adulthood. The protocol for the generation of bi-maternal embryos was then published in 2008 [318].

Loss-of-imprinting (LOI)

Human loss-of-imprinting associated conditions

Several disorders in human have been associated with LOI. Three commonly studied disorders are: Angelman syndrome (AS; OMIM 105830; reviewed in [319]), Prader-Willi syndrome (PWS; OMIM 176270; reviewed in [319]), related to neurobehavioral development, and the overgrowth pediatric syndrome Beckwith-Wiedemann (BWS; OMIM 130650; reviewed in [320]).

Angelman syndrome is a neurogenetic disorder that leads to mental retardation, speech and behavioral delays [321, 322]. In this case, there is loss of methylation on the maternal allele on the *SNRPN* (small nuclear ribonucleoprotein N) locus which results in silencing of the maternally-expressed gene UBE3a in the brain. UBE3a is a ubiquitin ligase involved in protein degradation and LOI results in abnormal protein accumulation (reviewed by [323]). PWS is characterized by behavioral problems in addition to hyperphagia and obesity (reviewed by [324]). The paternal allele on the *SNRPN* locus gains methylation and silences expression of small nucleolar RNAs (reviewed by [319]).

Individuals afflicted with Beckwith-Wiedemann Syndrome show enlarged tongue, gigantism, are overweight and have abdominal wall defects as primary characteristics [325]. These characteristics are linked to epigenetic mutations and LOI in the KVDMR1 domain affecting the expression of various genes located in this region [261, 325-329].

In addition, LOI of the *Igf2* gene has been associated with growth disorders, tumor development and cancer [326]. Previous studies in mice show that deletion of the *H19/Igf2* ICR and *H19* or of a 3kb region of the *H19* gene results in LOI and biallelic expression of *Igf2*. In that study, heterozygous pups from both groups showed higher body and placental weight when compared to the wild-type pups [243] thus providing a link between *Igf2* and growth disorders. Conversely, deletion of *Igf2* results in smaller pups when compared to the wild-type [177, 209]. Moreover, in humans, mutation or loss of expression of the *IGF2R* gene has been correlated with the occurrence of several cancers due to failure to degrade IGF2 [330-332].

ASSISTED REPRODUCTIVE TECHNOLOGIES (ART)

The number of couples that seek the use of assisted reproductive technologies (ART) as a primary option to improve infertility is constantly increasing [333, 334]. A woman is considered to be infertile if she is of reproductive age (15-34) and unable to conceive a child after one year of trying, if she is between the age of 35-44 and cannot conceive a child after six months, or if she is not capable of maintaining a pregnancy [333]. Currently, in the United States, 10% of women [333] and 7.5% of men of reproductive age [335] seeking help are infertile. A clinic summary report provided by

the Society for Assisted Reproductive Technology (SART) shows that by the year 2011 in the United States, 6% of the diagnosed infertility cases were caused by absence, blockage or diseases in the fallopian tubes, 7% by disorders in ovulation leading to egg release failure, 16% by decreased number of eggs in the ovary, 4% by endometriosis, and 1% by uterine diseases or abnormalities [336]. Also, 18% of the cases included infertile men with decreased number of sperm, absence of sperm and/or abnormal sperm motility or function [333].

Preliminary data from ART Fertility Clinic Success Rates Report provided by the United States' Centers for Disease Control and Prevention in 2011 indicates that over 1% of all children born in the US yearly are conceived by the use of ART. Approximately 163,000 ART cycles were performed in the United States during 2011, resulting in ~48,000 live births and ~62,000 live born infants [333]. To date, approximately four million children worldwide have been conceived by ART since the birth of the first IVF-conceived baby, Louise Brown, in 1978 [337].

Common ART procedures

Most ART procedures include: ovarian hyperstimulation, *in vitro* fertilization IVF, intra-cytoplasmic sperm injection (ICSI), embryo culture, and embryo transfer. An ART cycle generally includes, ovarian pre-stimulation treatment, ovarian stimulation, transvaginal oocyte retrieval, IVF/ICSI, embryo culture, embryo transfer, progesterone supplementation, and a follow up pregnancy test [333]. Ovarian hyperstimulation is defined as the use of exogenous hormones to suppress early ovulation (*i.e.* prior to retrieval), stimulate follicular growth and development and to increase the number of

oocytes that will be ovulated. This includes hormones with either GnRH agonist or antagonist activity and can also be used to schedule oocyte collection [338]. It should be noted that ovarian hyperstimulation is not considered to be an ART procedure by the CDC, but it is a step preceding the other techniques and a step included in the process of studying ART effects in many animal studies. IVF is defined by the CDC as the exposure of the retrieved oocytes to sperm for fertilization in the laboratory, followed by embryo transfer into the uterus [333]. ICSI is a specific type of IVF where a single sperm is directly injected into the oocyte [333]. Moreover, embryo culture is growing the fertilized oocytes and potential embryos in media with the nutrients required for their development until they reach the desired stage for embryo transfer [333]. Finally, embryo transfer is the selection of the embryos and transfer into the woman's uterus or fallopian tubes.

Adverse outcomes of ART procedures

Although the use of ART procedures is increasing, there are some adverse outcomes leading to epigenetic reprogramming that increase the probability of abnormal development in these children. The previously mentioned procedures can affect embryo development and result in epigenetic disorders [222, 339-341]. In our laboratory, we have recently shown the effects of superovulation (ovarian hyperstimulation) on the methylation state and gene expression of blastocysts collected from naturally ovulated and superovulated female mice (Huffman *et al.*, unpublished results). In this experiment zygotes were used to measure the level of global DNA methylation on the maternal pronucleus, and a 50% decrease of global DNA methylation was observed as a result of

superovulation. Then, acetylation of H3K9 and H3K14 was determined and a 50% increase of this modification was observed in 1-cell stage embryos from superovulated females. Both observations showed that superovulation interfered with epigenetic reprogramming of the maternal genome and may explain the increase in gene expression observed at the blastocyst stage [342].

A follow-up study [343] localized and measured the amount of 5-methyl-cytosine in ovarian sections to analyze global DNA methylation in developing oocytes after equine chorionic gonadotropin (eCG) and human chorionic gonadotropin (hCG) injection. These two hormones have FSH- and LH-like activity, respectively. As a result, they showed that global DNA methylation is interrupted in developing oocytes from superovulated females when compared to oocytes from naturally ovulated females [343]. Other studies also suggest that superovulation may be linked to abnormal embryonic and fetal growth in humans and mice [344-347] and to the LOI disorder, BWS [326, 327]. Further, children born from embryos that were cultured have a higher probability to develop neurogenetic disorders and overgrowth syndromes than their naturally-conceived counterparts. The incidence of BWS is also increased in children conceived by ART [326, 327, 348-350].

Embryo culture has been shown to affect gene expression. In 2004, a study in mouse showed misregulation of gene expression in embryos cultured from the 1-cell stage to the blastocyst stage (96 hour post hCG) when compared to those flushed from the uterus 96 hours (h) post hCG injection [340]. These embryos were from superovulated females and were cultured in KSOM + AA or Whitten's media to follow a previous study that showed LOI after culturing in Whitten's media [222]. A microarray

analysis with oligonucleotides was used to assess the number of expressed genes on pools of 80 embryos. One hundred fourteen genes were misregulated in embryos cultured in Whitten's media, and 29 genes in embryos cultured in KSOM + AA when compared to *in vivo* developed embryos; only 14 of the genes were misregulated in both groups [340]. Placentae of human pregnancies from ART babies can be of abnormal shape and weight [351]. Using a mouse model for IVF, it was suggested in 2010 that the abnormal placental growth after IVF in some cases is an effect of the embryo culture before the embryo transfer and not necessarily the IVF alone [352].

H19 loss of imprinting (LOI) after mouse embryo culture

Although *H19* expression in a monoallelic manner has been documented in *in vivo* developed mouse embryos, biallelic expression of *H19* has been observed in *in vitro* cultured embryos [222, 299, 339]. Sasaki *et al*., [299] showed that blastocysts cultured for an extended period of time exhibited biallelic expression of *H19*. In that same study they discussed that in fact, this region is differentially methylated in normal ES cells and proposed that the prolonged embryo culture altered allele-specific expression of *H19*.

To follow up these studies, Doherty and collaborators [222]analyzed the effect of culture from the 2-cell stage to the blastocyst stage on allele-specific *H19* expression. Using single strand conformation polymorphism analysis of RT-PCR products in a pool of embryos, they found that embryos cultured in Whitten's media had ~40% of paternal *H19* expression. Also, they compared this to KSOM +AA cultured and *in vivo* developed embryos and found no significant biallelic expression of *H19*. Analysis of *Snrpn* expression, another imprinted gene, showed no LOI of this gene in either of the groups

[222]. Later, another study by the same group analyzed LOI in single embryos and the methylation status of the *H19/Igf2* ICR in a pool of embryos. Approximately 65% (24/38) of the Whitten's cultured embryos had biallelic expression of *H19*, and although it wasn't significant, 14% (3/21) of the KSOM + AA cultured embryos had biallelic expression of *H19* when compared to *in vivo* controls (6% [1/17]). Subsequently, the methylation status analysis showed a significant loss of methylation in the *H19*/*Igf2* ICR of Whitten's cultured embryos but no significant hypomethylation in KSOM + AA cultured embryos. They concluded that the LOI resulted as a consequence of embryo culture [339]. Similarly, a recent study from the Mann group showed biallelic expression of *H19* in fast developing embryos when compared to slower growing ones [353]. Contrary to these studies, another study of conceptuses at day 9.5E showed *H19* to be expressed in a biallelic manner in a group of embryos that were *in vivo* developed to the blastocyst stage and transferred to pseudo-pregnant females, thus biallelic expression can occur even in less manipulated embryos (*i.e.* not cultured but transferred) [341].

SYNOPSIS-RATIONALE FOR THESIS

The current knowledge on the effects of ART procedures on the epigenome of developing embryos strictly states that embryo culture affects genomic imprinting and gene allele-specific expression. Previous research shows that *H19*, a maternally expressed ncRNA with tumor suppressor activity, loses allele-specific expression and becomes biallelic after culture in Whitten's medium from the 2-cell stage to the blastocyst stage. In addition, other research shows biallelic expression of *H19* in day 9.5E conceptuses from embryos that had been manipulated during the preimplantation stage. Preliminary results in our laboratory show that *H19* is expressed in a biallelic manner in non-manipulated (*i.e.* control) late blastocyst-stage embryos.

At peri-implantation the blastocyst stage embryo is composed of five cell types, namely the inner cell mass, primitive endoderm, polar trophectoderm (TE), mural TE and primary trophoblast giant cells (PTGC). The PTGC are the first terminally differentiated cells during embryogenesis. These cells are involved in uterine implantation around day 4.5E and are known to undergo endoreduplication. We hypothesize that *H19* becomes biallelically expressed in PTGC as part of a physiological event during peri-implantation. We speculate that *H19* becomes biallelic to control the expression of the tumor enhancer gene, *Igf2*, to control TE invasion at this stage.

The research conducted for this thesis (Chapter II) determined allele-specific expression of *H19* in control and cultured pre- and peri-implantation mouse embryos. This work has been recently published in Biology of Reproduction [354].

CHAPTER II

Determination of allelic expression of *H19* in pre- and peri-implantation mouse embryos

ABSTRACT

H19 is a maternally-expressed imprinted non-coding RNA with tumor suppressor activity. During mouse preimplantation development, *H19* is primarily expressed in the trophectoderm cells. The purpose of this project was to determine allelic expression of *H19* in pre- and peri-implantation mouse embryos. We were further interested in determining if loss of imprinted *H19* expression during blastocyst development occurred as a result of superovulation and/or culture. Our last goal was to ascertain if differential *H19* allelic expression occurred between the inner cell mass (ICM)-containing half and the primary trophoblast giant cell (PTGC)-containing half of the embryo. C57BL/6J$^{(Cast\text{-}7)}$xC57BL/6J F1 embryos were collected from the uterus at 84, 96, and 108 hours following natural ovulation or superovulation. In vitro-cultured F1 embryos were harvested from the oviduct at the 2-cell stage and cultured in KSOM + aa supplemented with amino acids or Whitten's media and collected at the above-mentioned times. Allele-specific *H19* expression in single embryos was determined by qRT-PCR followed by fluorescence resonance electron transfer or RT-PCR followed by restriction fragment length polymorphism and polyacrylamide gel electrophoresis (RFLP-PAGE). Peri-implantation embryos were microdissected into two sections, one containing the ICM and the other containing the PTGC. TaqMan probes for *Dek*, *Pou5f1*, *Itga7*, *H19* and *Igf2* were used to ascertain gene expression enrichment in each section. Allele-specific *H19*

expression in embryo sections was determined by RFLP-PAGE. We found that as embryos advance through preimplantation development they start expressing *H19* in a biallelic manner and this phenomenon was observed in the cultured and the in vivo developed embryos. The PTGC-containing half of the embryo had greater expression of *H19* when compared to the ICM containing half of the embryo, as determined by qRT-PCR. In conclusion, loss of imprinting of *H19* occurs in the PTGC containing section of peri-implantation mouse embryos. We speculate that this is part of a physiologic event at the time of implantation in the mouse.

INTRODUCTION

Genomic imprinting is an epigenetic mechanism where gene expression is limited to a single parental allele. Imprinted genes are dependent on the epigenetic machinery for maintenance of their parent-of-origin specific gene expression [81]. In mammals, about 100 imprinted genes have been described [81]. They play important roles in fetal growth control, placental development and normal brain function. A change in expression of imprinted genes may result in developmental disorders [81]. These genes are usually found in clusters and their expression is controlled by a discrete region of DNA known as the imprinted control region (ICR) [223]. The ICRs show differential methylation between the parental alleles. DNA methylation is a heritable chemical modification that occurs principally in the fifth carbon of a cytosine when followed by a guanine (*i.e.* CpG).

Imprinted gene clusters have been found to typically contain a noncoding RNA (ncRNA) and both maternally and paternally expressed genes. The regulation of allelic

specific expression is not the same for all clusters of genes. Some clusters are regulated by the resident long ncRNA [81, 248] while others are regulated by an insulator protein [81, 248, 258].

The *H19/Igf2* cluster of genes is an example of reciprocally imprinted genes regulated by binding of the zinc-finger insulator protein, CCCTC-binding factor (CTCF) [81, 236]. *H19* (*H19* fetal liver mRNA) is a maternally-expressed imprinted long ncRNA associated with tumor suppressor activity [217]. It is expressed in mouse embryos during pre-implantation development and slowly downregulated after birth except in cardiac and skeletal muscles [211, 214]. *H19* is located ~90 kb downstream of *Igf2* (insulin-like growth factor type 2) and 2-4 kb downstream of the ICR [226, 231, 235, 355]. *Igf2* encodes a paternally-expressed fetal growth factor after implantation, associated with tumor enhancer activity. It is expressed during embryogenesis and downregulated after birth except in chroroid plexus and leptomeninges where it maintains biallelic expression [177, 197, 204]. *Igf2* plays a role in embryonic growth; it has been noticed to be present in the region of the mural trophectoderm of peri-implantation embryos [206]. This cluster's ICR is differentially marked by methylation in the gametes. The maternal allele is unmethylated while the paternal allele is methylated. The *H19/IGF2* ICR orchestrates the accessibility of each gene to shared enhancers [241] through the binding of CTCF to the unmethylated maternal allele [223, 238]. This cluster of imprinted genes is located on mouse chromosome 7 and human chromosome 11 [223].

It has become a concern that assisted reproductive technologies (ART) such as superovulation, embryo culture or embryo transfer, may be involved in loss of imprinting (LOI) [222, 236, 339, 341, 353, 356]. LOI refers to misregulation of imprinted genes

expression. Children conceived by the use of ART have been reported to have an increased incidence of the overgrowth LOI syndrome Beckwith-Wiedemann [323, 326, 341]. Beckwith-Wiedemann syndrome patients show LOI of the *Kcnq1ot1*imprinted gene. *Kcnq1ot1* (*KCNQ1* overlapping transcript 1) or *Lit 1* is a paternally-expressed long ncRNA, located within KvDMR1 cluster in the mouse chromosome 7 [248] and human chromosome 11, and is located telomeric of the *H19/Igf2* cluster in the mouse [248, 261]. In embryonic and placental tissues, expression of *Kcnq1ot1* results in the repression of several flanking protein-coding maternally-expressed genes on the paternal chromosome [258, 357].

Previous research showed that embryo culture from the 2-cell stage to blastocyst stage results in LOI leading to biallelic expression of *H19*. After immunolyzing mouse blastocysts, and analyzing *H19* expression in pooled blastocysts by the use of single-stranded conformation polymorphism gel electrophoresis, it was suggested that *H19* was trophectoderm specific and expressed in a biallelic manner in blastocysts cultured in Whitten's culture medium [222]. A follow up study by the same group analyzed individual allele-specific expression of blastocyst stage and found ~65% blastocysts from the Whitten's media culture group showed biallelic expression when compared to controls [339].

Preliminary studies in our laboratory revealed biallelic expression of *H19* in in vivo-produced (not cultured) peri-implantation mouse embryos. Therefore, the current work was designed to study this phenomenon and to test the hypothesis that the late mouse blastocyst expresses *H19* in a biallelic manner as part of a necessary physiologic event during peri-implantation. The goals of the present study were to ascertain allelic

expression of *H19* through blastocyst development and to determine which section of the embryos show biallelic expression of this gene using in vivo- and in vitro-cultured mouse embryos.

MATERIALS AND METHODS

Animals

In order to do this allelic-specific expression study, C57BL/6J$^{(Cast\text{-}7)}$ (C7) females containing *Mus musculus castaneus* (Cast) chromosome 7 on a C57BL/6J (B6) background were mated to B6 males (The Jackson Laboratory). Mice were exposed to a 12 hour (h) light/dark cycle with lights on at 7am Central Standard Time (CST); presumed ovulation occurred at the middle of the dark cycle [358]. Hybrid C7xB6 F1 preimplantation embryos were collected and analyzed at 84, 96 and 108 h post presumed ovulation. The genomic polymorphisms between the strains allowed us to determine *H19* parent-specific expression in the F1 progeny. Mice had *ad libitum* access to food and water with a laboratory standard diet. All animal procedures were approved by the Animal Care and Use Committee of the University of Missouri.

Type of ovulation

***Natural Ovulation*:** Naturally cycling females (NO) were cohoused with B6 males. Ovulation was expected to occur at 1:00 am CST (midpoint between the dark and light cycles; [358]), and was determined by the presence of copulatory plug the morning after cohousing (**Figure 2.1**).

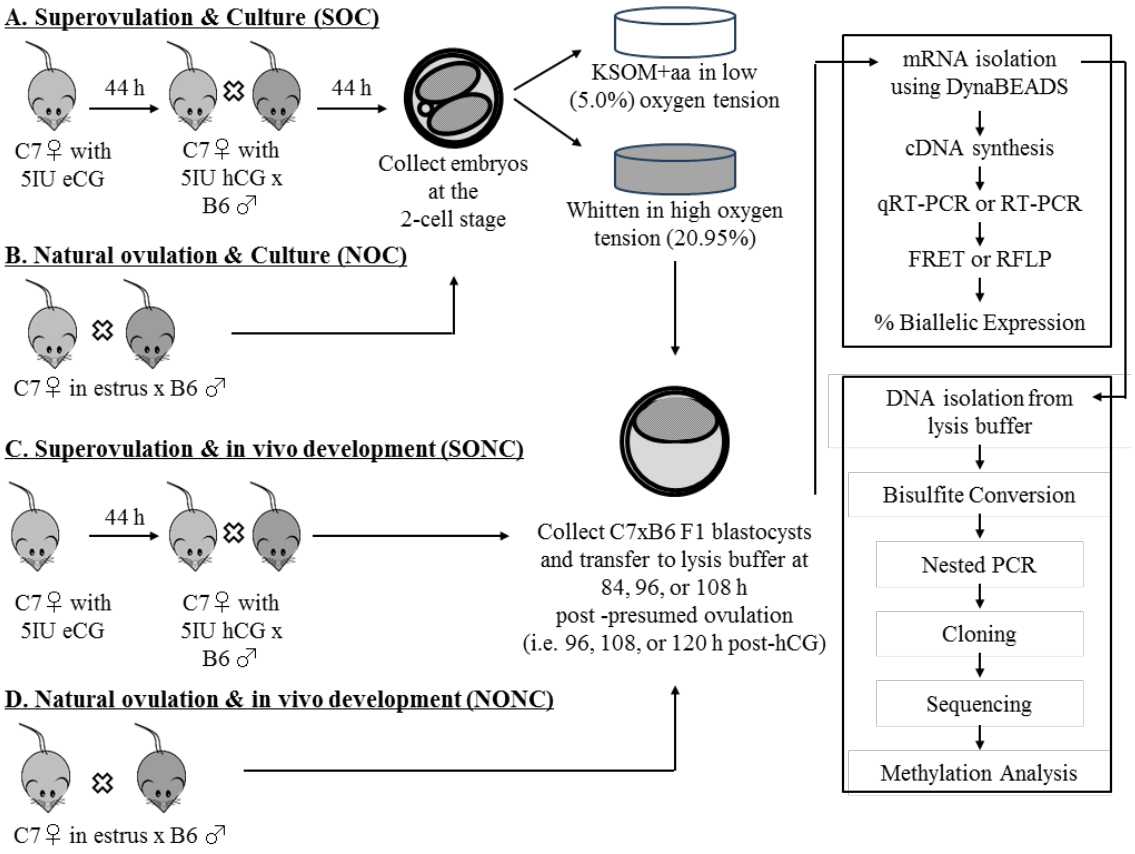

Figure 2.1. Experimental Design. Four experimental groups were used in this study. **(A)** SOC embryos collected at the 2-cell stage and cultured. These embryos were collected from females that had undergone a superovulation scheme; **(B)** NOC embryos collected at the 2-cell stage and cultured. These embryos were collected from females that had undergone natural ovulation; **(C)** SONC embryos collected from the uterus at 84, 96, or 108h post presumed ovulation which was induced from a superovulation scheme; **(D)** NONC embryos collected from the uterus at 84, 96, or 108h post natural ovulation. Females were C57BL/6J$^{(Cast\text{-}7)}$ (C7) and studs were C57BL/6J (B6); F1 embryos were C7xB6. In vitro culture was done in KSOM + aa medium in low (5.0%) oxygen tension or Whitten's media in high (20.95%) oxygen tension. Incubator was set at 37°C and 5.0% CO_2. Embryos were collected at 84 h, 96 h, and 108 h post presumed ovulation and developmental stage recorded. Individual embryos were transferred to lysis buffer for allele-specific expression analysis. DNA from individual embryos was isolated by ethanol precipitation from the lysis buffer after mRNA isolation. DNA was bisulfite-converted, used for PCR to amplify the first CTCF site of the *H19*/*Igf2* ICR, cloned and sequenced to allow us to differentiate allelic-specific methylation status. eCG = equine chorionic gonadotropin. hCG = human chorionic gonadotropin. FRET = fluorescence resonance electron transfer. RFLP = restriction fragment length polymorphism. IU = international units.

***Superovulation*:** C7 females of 6-10 weeks of age were superovulated (SO) by intraperitoneal (IP) injection with 5 I.U. of equine chorionic gonadotropin (eCG, Calbiochem) followed by 5 I.U. of human chorionic gonadotropin (hCG; Sigma) 44 h later and cohoused with B6 males. Ovulation was expected to occur ~12 h after hCG injection (*i.e.* 1am) [358].

Embryo collection and embryo culture

SO in vitro group: Embryos at the 2-cell stage (44 h post-hCG) were flushed from the oviduct using 0.5 cc of 37 °C bicarbonate free Minimun Essential Media supplemented with 3mg/ml Polyvinylpyrrolidone and 25mM Hepes (MEM + PVP, pH 7.3; Sigma). F1 hybrid embryos were then collected, rinsed in fresh MEM + PVP, washed in either equilibrated potassium simplex optimized medium supplemented with amino acids (KSOM + aa, Specialty Media) or Whitten's media [109.51 mM NaCl, 4.78 mM KCl, 1.19 mM KH_2PO_4, 1.19 mM $MgSO_4$•7 H_2O, 5.55 mM Glucose, 22.62 mM $NaHCO_3$, 2.43 mM, 227.19 µM Na Pyruvate, 6 mM Pen-Strep solution (10 K units/ml Pen and 10 mg/ml strep), and 29.23 µM Phenol red]. Embryos were finally transferred to 70 µl drops of either KSOM + aa or Whitten's media, both at a density of 1 embryo per 3.5 µl of medium. Embryos were then cultured at 37°C in an environment containing 5% CO_2, 5% O_2, and 90% N_2 if in KSOM + aa or in an environment containing 5% CO_2 in airif in Whitten's media (**Figure 2.1A**). At 84, 96, 108 h post-presumed ovulation (*i.e.* 96, 108, 120 h post-hCG) all embryos were collected and briefly washed in MEM + PVP and placed individually in a 1.7ml eppendorf tube containing 100 µl of lysis buffer [100 mM Tris-HCl, pH 7.5, 10mM EDTA, pH 8, 1% LiDS, 5 mM dithiothreitol; [359]] and

immediately stored at -80 °C. A total of 227 embryos were collected and analyzed for KSOM + aa (N = 21, 57, 62 for 84, 96, 108 h respectively) and Whitten's media (N = 17, 36, 34 for 84, 96, 108 h respectively).

NO in vitro group: Embryos at the 2-cell stage (48 h post ovulation) were flushed from the oviduct using 0.5 cc of 37°C bicarbonate free MEM + PVP. C7xB6F1 hybrid embryos were then collected, rinsed in fresh MEM + PVP, washed in either equilibrated KSOM + aa or Whitten's media and finally transferred to 70 µl drops of either KSOM + aa or Whitten's media, both at a density of 1 embryo per 3.5 µl of medium. Embryos were then cultured under the same conditions as the SO in vitro group (**Figure 2.1B**). At 84, 96, 108 h post-presumed ovulation all embryos were briefly washed in MEM + PVP and placed individually in a 1.7 ml Eppendorf tube containing 100 µl of lysis buffer and immediately stored at -80°C. A total of 126 embryos were collected and analyzed for KSOM + aa (N = 17, 27, 25 for 84, 96, 108 h respectively) and Whitten's media (N = 11, 23, 23 for 84, 96, 108 h respectively).

SO in vivo group: At 96, 108, 120 h post-hCG injections, C7xB6 F1 hybrid embryos were flushed from the uterine horns using 1.0 cc of MEM+PVP (**Figure 2.1C**). Collected embryos were individually placed in 100 µl of lysis buffer and immediately stored at -80 °C. A total of 149 embryos were collected and analyzed; N = 40, 49, 60; 84, 96, 108 h respectively.

NO in vivo group: At 84, 96, 108 h post presumed ovulation, C7xB6 F1 hybrid embryos were flushed from the uterine horns using 1.0 cc of MEM+PVP (**Figure 2.1D**). Collected embryos were individually placed in 100 µl of lysis buffer and immediately stored at -80 °C. A total of 76 embryos were collected and analyzed; N = 26, 26, 24 for 84, 96, 108 h respectively.

RNA isolation and cDNA library construction from single F1 hybrid blastocysts

A reusable cDNA library was constructed for each blastocyst obtained using the DynaBEADS mRNA DIRECT KIT (Invitrogen). The equilibration of the Dynabead Oligo $(dT)_{25}$ beads was done according to manufacturer's instructions. RNA isolation, cDNA libraries and second-strand synthesis were prepared as described [356, 359].

RT-PCR primers

H19 intron-spanning primers were constructed using sequence published in the National Center for Biotechnology Information (NCBI Reference Sequence: AF049091). They include forward primer 5'TTGAGAGACTCAAAGCACCCGTGA3' (position 7781-7804) and reverse primer 5'GGCAAAGGATGAAGTAGGGCATGT3' (position 8051-8074). The paternally-expressed imprinted gene *Kcnq1ot1*, was also analyzed to test for loss of imprinting. Gene primers were designed using NCBI reference sequence: NR_001461 and they include forward primer 5'TATACAACCTGGGTGAGCCTCAGA3' (position 17,174-17,197), and reverse primer 5'AGAAGTCGCTGTTCCCAATGCTCA3' (position 17,783-17,806). The housekeeping gene glyceraldehyde-3-phosphate dehydrogenase (*Gapdh*) primers were constructed using NCBI reference sequence:

NM_008084.2 to test the successful mRNA isolation from single embryos. They include forward primer 5'TCACGGCAAATTCAACGGCACA3' (position 200-221) and reverse primer 5'AGATGCCTGCTTCACCACCTTCTT3' (position 819-842).

RT-PCR &*Gapdh* expression

Following 2nd strand synthesis, PCR amplification of *Gapdh* was conducted in an Eppendorf Master Cycler. The final concentration of the primers was 0.3 µM and the PCR conditions were as follows: an initial denaturation step at 94°C for 2 min 15 sec, followed by 35 cycles of denaturation step at 94°C for 15 sec, annealing at 58°C for 30 sec and extension at 72°C for 45 sec. The reaction concluded with a final elongation at 72 °C for 5 min yielding a 643 bp PCR product. *Gapdh* expression was determined through the use of 7% polyacrylamide gel washed in a 4 µg/ml Ethidium Bromide solution for 5 min, exposed to UV trans-illuminator and photographed. Samples that expressed the 643 bp *Gapdh* PCR product were then subjected to *Kcnq1ot1* and *H19* allelic determination.

***H19* Allelic determination**

Allele specific *H19* expression was determined using two methods targeting two different single nucleotide polymorphisms (SNP) between Cast and B6 mouse strains.

Quantitative real-time PCR andfluorescence resonance electron transfer. The *H19* Light Cycler Real Time PCR system (Roche Molecular Biochemicals) quantitative real-time (qRT-PCR) assay was conducted as previously described (**Figure 2.2A**)

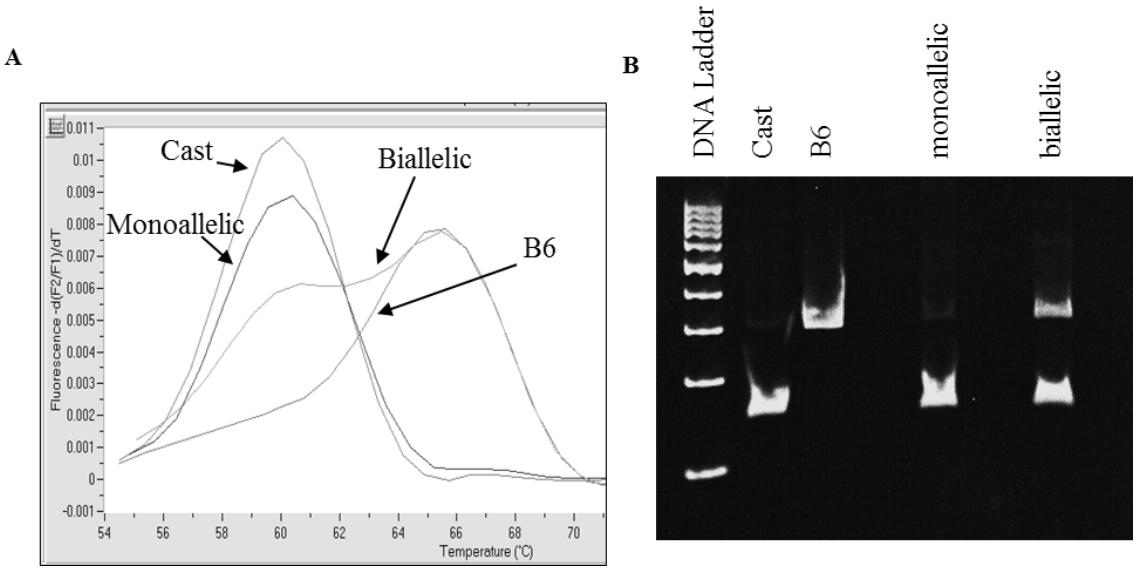

Figure 2.2. *H19*allele-specific expression assays. (A) Resulting graph from qRT-PCR followed by FRET. Fluorescent hybridization probes were used for allelic discrimination assays. *Mus musculus casteneus* and B6 cDNA from neonatal liver were used as control to determine the dissociation temperature of the fluorescent probe and the PCR product; dissociation temperature and area under the curve were used to determine allele-specific expression. Figure shows one embryo with monoallelic expression and one with biallelic expression. **(B)** RT-PCR followed by RFLP. The PCR amplicon was digested with the restriction enzyme BgLI. The restricted product was resolved by 7% polyacrylamide gel electrophoresis in order to determine parental contribution of *H19*. Differences in DNA sequence (*i.e.* SNP) between B6 and Cast were used to ascertain allelic expression in C7xB6 F1 single embryos. The restriction enzyme BgLI cuts the maternal (Cast) allele leaving two fragments of 138 bp and 156 bp size (indistinguishable in this 7% polyacrylamide gel). Embryos with biallelic expression show two bands: one of 294 bp size from paternal allele, and one of 138 bp and 156 bp from maternal allele. Digestion controls (pure B6 and Cast) show the mobility of each amplicon and are used to determine allelic expression in F1 embryos. Controls = B6 and Cast neonatal muscle. Monoallelic = monoallelic expression, biallelic = biallelic expression.

[236, 341, 356]. Fluorescence resonance electron transfer (FRET) hybridization probes (labeled with fluorescein at the 3' end) were designed to bind with perfect complementarity to the B6 allele over a SNP at nucleotide 7954 (NCBI AF049091) between B6 (G) and Cast (A), located in exon 5 [236].

RT-PCR & Restriction Fragment Length Polymorphism*:* Following 2nd strand synthesis, PCR amplification of *H19* was conducted in an Eppendorf Master Cycler, followed by restriction fragment length polymorphism (RFLP) analysis. The final concentration of the primers was 0.3 µM and the PCR conditions were as follows: an initial denaturation step at 94 °C for 2 min 10 sec, followed by a touchdown PCR starting with a denaturation step at 94°C for 30 sec, annealing at 64.8°C for 30 sec and extension at 72°C for 1 min (one cycle); this was repeated for another six steps of one cycle each while decreasing the annealing temperature 1°C; the PCR was finalized with 45 cycles at 94°C for 30 sec, 57.8°C for 30 sec, and 72°C for 45 sec. The reaction concluded with a final elongation at 72°C for 5 min yielding a 294 bp PCR product. *H19* expression was determined through the use of 7% polyacrylamide gel washed in a 4 µg/ml Ethidium Bromide solution for 5 min, exposed to UV trans-illuminator and photographed. Samples that expressed the 294 bp*H19* PCR product were then subjected to digestion with the BgLI restriction enzyme (New England Biolabs). BgLI only cuts the 294 bp maternal Cast transcript at nucleotide 7918 (NCBI AF049091) between B6 (A) and Cast (G) leaving a 138 bp and 156 bp product (**Figure 2.2B**). The digestion reaction consisted of a 30 µl reaction [23.5 µl H_2O, 1x NEB #3 Buffer (10x; New England Biolabs), 1.5 µl BgLI restriction enzyme (10,000 U/ml; New England BioLabs) & 2 µl PCR product] and was

digested at 37 °C for 2 h followed by a 20 min incubation at 65°C for inactivation. Allele-specific contribution of the total was determined through the use of 7% polyacrylamide gel washed in a 4 µg/ml Ethidium Bromide solution for 5 min, exposed to UV trans-illuminator and photographed. TIFF images of the gels containing samples that expressed the imprinted paternal *H19* allele were downloaded and analyzed using the Java-based image processing program ImageJ [360]. Only samples that had at least 10% expression from the paternal allele were considered biallelic.

Kcnq1ot1 Allelic determination

Allele specific *Kcnq1ot1* expression was determined using RT-PCR and RFLP targeting a SNP between Cast and B6 mouse strains. *Kcnq1ot1* PCR amplification was conducted in an Eppendorf Master Cycler following 2nd strand synthesis. The final concentration of the primers was 0.3 µM and the PCR conditions were as follows: an initial denaturation step at 94°C for 2 min 15 sec, followed 35 cycles of one denaturation step at 94°C for 15 sec, an annealing step at 60.5°C for 30 sec and an extension step at 72°C for 45 sec. The reaction concluded yielding a 633 bp PCR product. *Kcnq1ot1* expression was determined through the use of 7% polyacrylamide gel washed in a 1ml solution of 0.08 mM Ethidium Bromide for 5 min, exposed to UV trans-illuminator and photographed. Samples that expressed the 633 bp *Kcnq1ot1*PCR product were then subjected to digestion with the HincII restriction enzyme (New England Biolabs). HincII only cuts the 633 bp maternal Cast transcript at nucleotide 17,409 (NCBI NR_001461) between B6 (C) and Cast (A) leaving a 176 bp and 457 bp product (**Supplemental**

Figure S2.1). The digestion reaction consisted of a 40 µl reaction [25.1 µl H_2O, 100µg/ml BSA (New England Biolabs), 1x NEB #3 Buffer (10x; New England Biolabs), 1.5 µl HincII restriction enzyme (10,000 U/ml; New England BioLabs) & 9 µl PCR product] and was digested at 37 °C for 2 h followed by a 20 min incubation at 65 °C for inactivation. Allele-specific contribution was determined through the use of 7% polyacrylamide gel washed in a 4 µg/ml Ethidium Bromide solution for 5 min, exposed to UV trans-illuminator and photographed. TIFF images of the gels containing samples that expressed the imprinted maternal *Kcnq1ot1* allele were downloaded and analyzed using the Java-based image processing program ImageJ [360]. Only samples that had at least 10% expression from the maternal allele were considered biallelic.

DNA isolation and *H19*/*Igf2* ICR Methylation analysis

DNA isolation and Bisulfite mutagenesis: DNA saved from single C7xB6 F1 hybrid embryos that presented either monoallelic or biallelic *H19* was subjected to ethanol precipitation as previously described by us [359]. DNA underwent bisulfite mutagenesis following the manufacturer's instructions for the Two Step Bisulfite Modification and Post-Modification Cleanup of Genomic DNA (Sigma Imprint DNA Modification Kit) (**Figure 2.1**) except 21 µl of eluted DNA was added to 1 µl of Carrier RNA and 1 µl of Balance Solution before 10 min incubation at 37°C. Halfway through the 90 min incubation at 65°C, samples were removed from Master Cycler, mixed by inverting tube, and returned to Master Cycler to finish incubation. During post modification DNA clean up, samples were centrifuged for 1 min instead of 20 sec and to

elute post modified genomic DNA, 23 µl of nuclease free water was used instead of Elution Solution; all incubations were done in an Eppendorf Master Cycler PCR Machine.

PCR amplification and gel slice isolation*:* A 427 bp section of the *H19* ICR (Genbank Accession Number U19619.1, position 1304-1730) was amplified as previously described (**Figure 2.1**) [222, 235, 236, 339, 341, 356]. This region contains 15 CpGs, represents the first CTCF binding site [341], and two single nucleotide polymorphisms to differentiate between the paternal (B6) and maternal (Cast) alleles. The first polymorphism is located at nucleotide 1480 (deletion of a G in Cast) and the second, at nucleotide 1566 [B6 (G) and Cast (A)]. Nested PCR primers include outer forward- 5'GAGTATTTAGGAGGTATAAGAATT'3 (position 1278-1301) and outer reverse- 5'ATCAAAAACTAACATAAACCCCT'3 (position 1729-1751) yielding a 474 bp product followed by inner forward- 5'GTAAGGAGATTATGT TTATTTTTGG'3 (position 1304-1328) and inner reverse- 5'CTAACCTCATAAAACCCATAACTAT'3 (position 1706-1730) yielding a 427 bp product. The final concentration of the primers was 0.3 µM and the PCR conditions were as follows: an initial denaturation step at 94 °C for 2 min 15 sec, followed by 40 cycles at 94°C for 30 sec, 55°C for 30 seconds, and 72°C for 1 min; the reaction concluded with a final elongation at 72°C for 5 min. The 427bp band containing the bisulfite converted *H19*ICR PCR product was then excised from a 1% agarose gel, and recovered using the Wizard SV Gel and PCR clean up kit (Promega) according to manufacturer's instructions. The PCR product was eluted in 45 µl of nuclease free H_2O.

Cloning and sequencing*:* Ligation of the 427 bp bisulfite converted *H19/Igf2*ICR PCR product into pGEM-T Easy Vector (Promega) and cloning into NEB 5-alpha F'I^qCompetent *E. coli* (New England Biolabs) was done immediately after the DNA extraction from the agarose gel following the manufacturer's instructions with various alterations. A total of 3.54 ng of DNA from the PCR product was ligated in a 5µl reaction and incubated for 1 h at room temperature. Immediately after incubation, we added 100 ng of plasmid DNA to cell mixture, resuspended in LB Broth Miller (Fisher Scientific, Pittsburg, PA) after heat shock, and incubated at room temperature for 3 h before plating. Finally, 200 µl of a 1/10 dilution, and 150 µl of undiluted samples were plated and incubated at room temperature for 60 – 72 h. Post-cloning PCR was done on NEB 5-alpha F'I^qCompetent *E. coli* positive colonies. All PCR reactions were performed using the inner set of primers used for the *H19*/*Igf2* ICR PCR under the same PCR conditions. The 427 bp region was excised from 1% agarose gel and recovered using the Wizard SV Gel and PCR clean up kit (Promega) according to manufacturer's instructions. Clones were sequenced individually at the University of Missouri DNA sequencing facility using the 96 capillary Applied Biosystems 3730 DNA Analyzer with Big Dye Terminator (**Figure 2.1**). Sequences were analyzed using multiple sequence alignments by MacVector application.

H19 Allelic expression in microdissected F1 hybrid blastocysts

To determine the cell type responsible for the *H19* biallelic expression, C7xB6 F1 hybrid embryos were collected from the uteri of 9 females at 109 h post-presumed ovulation (*i.e.* peri-implantation).

Embryo collection*:* Collected embryos were immediately washed in a 1.5 ml 0.3% Polyvinylpyrrolidone (PVP) (Sigma, St. Louis, MO) in 1x PBS solution for 30 sec at room temperature. Embryos were then fixed by submerging in 1.5ml of 10% Neutral Buffered Formalin (Sigma, St. Louis, MO) for 15 min at room temperature, followed by three separate washes of 1.5 ml 0.3% PVP in 1x PBS solution for 30 sec at room temperature, finally being placed in a fresh volume of 0.3% PVP in 1x PBS solution and stored at 4 °C until microdissection.

Microdissection: Borosillicate glass rods (Sutter Instruments, BR-100-15) were made into micro-dissection needles using a P-87 Flaming/Brown Micropipetter Puller Instrument [Sutter Instruments Rev. 0299c (20081016)]. **Supplemental Table S2.1** shows the program used to make the micro-dissection needles. Microdissection was performed using the needles described above which were attached to a Transferman NK 2 Eppendorf manipulator mounted on either a Nikon Te-2000u or a Nikon Eclipse Ti microscope**.** Individual 109h F1 hybrid in vivo developed embryos were placed in a petri dish submerged in 20 µl droplets of 0.3% PVP in 1x PBS solution and covered with mineral oil. Embryos were microdissected into two parts, one part containing primarily the ICM, primitive endoderm and polar trophectoderm, and the other part containing primarily the mural trophectoderm with adjacent PTGCs. For microdissection, glass needles were placed on each side of the embryo, towards the center of the embryo. Needles were then inserted into the blastocoel cavity of the embryo from each side and moved inwards until the tips of each needle touched the opposite side the embryo. This

was followed by moving the needles towards opposite poles of embryo, with the needle closest to the ICM moved up and the needle closest to the mural trophectoderm moved down. Finally, the needles were moved until the embryo split in the middle and the two poles were separated. After separation, the two portions were placed in separate 1.5ml eppendorf tubes containing 100ul of Proteinase K Buffer from RNease Formalin Fixed Parafin Embedded Kit (Qiagen Cat. No. 73504) and held at 4 °C until RNA isolation.

RNA isolation from ICM and TGC containing sections: RNease Formalin Fixed Paraffin Embedded Kit (Qiagen Cat. No. 73504) was used to isolate RNA from each fixed embryo section. Isolation was done following manufacturer's instructions for purification of total RNA from microdissected FFPE Tissue Sections with minor alterations (*i.e.* no deparaffinization step was required as the samples were not embedded in paraffin. Proteinase K was added (>$6x10^6$mAU) to the entire sample and incubated at 56°C for 15 min followed by another 15 min at 80°C. The sample was immediately transferred to ice for 3 min and centrifuged for 20 min at 17,000 xg. The supernatant was then transferred to a new 1.5 ml micro-centrifuge tube, and DNase Booster Buffer and DNase I stock solution were added (10% of the total volume and 10 µl of 1500 Kunitz units, respectively). Sample was then incubated at room temperature for 15 min, and 320 µl Buffer RBC and 720 µl of 100% EtOH were added. Half of the solution was then transferred to an RNeasy MinElute Spin Column placed in a 2.0 ml collection tube and centrifuged for 15 sec at 8,000 x g; this was repeated until the entire solution had passed through the spin column. To finish washing, 500 µl of Buffer RPE, with previous EtOH added, were added and centrifuged three times for 15 sec at 8,000 x g, 2 min at 8,000 x g,

and 5 min at 17,000 x g. RNA was finally eluted in 28 µl of sterile deionized H_2O; samples were then stored at -80°C until cDNA synthesis.

cDNA library construction*:* To each 28 µl sample of RNA, 20 µl of cDNA synthesis master mix were added and incubated for 1 h at 42°C followed by 10 min at 95°C. The cDNA synthesis master mix consisted of 1x First Strand Buffer (Invitrogen), 10 mM DTT (Invitrogen), 2.5mMdNTP mixture (Promega), 1.1 µg Random Primers (Promega Cat. No. C1181), 44 units Optizyme Ribonuclease Inhibitor, and 200 units SuperScript II Reverse Transcriptase (Invitrogen). After cDNA synthesis, samples were stored at -20°C until RT-PCR and qRT-PCR amplification. All incubations were done in an Eppendorf Master Cycler.

H19 Allelic determination using RFLP*:* PCR amplification and specific allelic expression of *H19* was done using the same primer pair and PCR conditions as described above. RFLP to determine *H19* parent-specific allele expression was conducted as previously described. Samples were then subjected to qRT-PCR using five probes to determine the cellular make up of each half and level of expression of the imprinted genes *H19* and *Igf2*. RT-PCR with *Gapdh* was done as previously described to test the cDNA quality.

Quantitative Real Time PCR (qRT-PCR)

TaqMan gene expression assays (Applied Biosystems; see **Supplemental Table S2.2**) were used to determine if a correlation existed between the total number of cells

present in each section and the total amount of *H19* mRNA. The samples were analyzed for *Dek* (DEK oncogene [DNA binding]), *Pou5f1* (POU domain, class 5, transcription factor 1; previously known as *Oct4*), *Itga7* (integrin alpha 7), *H19*, and *Igf2*, in at least duplicates using a 7500 Real Time PCR Machine (Applied Biosystems); threshold cycle (C_T) was normalized to the proto-oncogene protein, *Dek* [361-363], which has been demonstrated to be equally-expressed throughout the entire embryo [364]. ICM and PTGC cell markers (*Pou5f1* [29, 364], and *Itga7* [365], respectively) were used to determine identity of each embryo section. Both portions of the embryo were analyzed, reactions were run at 50 cycles with 10 µl of 2x TaqMan Universal PCR MasterMix (Applied Biosystems, Part No. 4304437) and 1µl of 20xTaqMan Gene Expression Assays Probe in a 96 well plate. A negative control of each probe used was incorporated.

Normalizing to *Dek* and calculating fold difference in each embryo section

First all values obtained from the duplicates were averaged. Only C_T that showed less than 0.5 cycle standard deviation were used for analyses. To normalize the number of cells in each half, the averaged C_T of the highest value for *Dek* (*i.e.* lowest number of cell) were normalized to the lowest values for *Dek* (*i.e.* largest number of cells) for each embryo. Once the number of cells in each embryo-half was normalized, the ddC_T for *Pou5f1 and Itga7* was determined by comparing the sections. The total amount of *H19* transcript was determined based on the levels of *Dek* for each section. The *Igf2* transcript level in relation to *H19* transcript amount was calculated using corresponding *H19* and *Igf2* dC_T values to calculate a new ddC_T and fold difference.

Statistical analyses

Data were analyzed by Analysis of Variance using SAS 9.3 GLM procedure to obtain least squares means and standard errors.

RESULTS

From here-on-out all times of collection are reported based on the time of presumed ovulation for all groups: 84, 96 and 108 h.

***H19* allele-specific expression in single C7xB6 F1 embryos**

In this study we determined allele-specific expression of the maternally-expressed imprinted gene *H19.* First, we determined that RNA isolation from each embryo (n=578) was successfully accomplished by detecting the levels of *Gapdh* mRNA (data not shown). We then measured the presence of *H19* in those embryos and found that 466 had measurable levels of *H19* transcript. Of the 466 embryos used to establish allele-specific expression of *H19*, 124 were produced after natural ovulation and 342 were produced after superovulation.

We used two methods to determine *H19's* transcripts parental allele of origin, namely qRT-PCR followed by FRET (**Figure 2.2A**) and RT-PCR followed by RFLP and PAGE (**Figure 2.2B**). To determine if *H19*'s allelic expression was perturbed by embryo culture we collected embryos from superovulated females at the 2-cell stage and cultured them until 84, 96, 108 h post presumed ovulation in either KSOM + aa (n = 132 embryos) or Whitten's media (n = 75 embryos). Collected embryos were analyzed based on chronological age rather than developmental stage (*i.e.* only blastocysts). **Figure 2.3**

shows the percent of embryos that expressed *H19* in a biallelic manner (*i.e.* at least 10% from the paternal allele). Overall, the percent of embryos expressing detectable *H19* from both parental alleles was similar between FRET and RFLP (**Figure 2.3Aand 2.3B**; P = 0.45). To determine if *H19*'s LOI was caused by superovulation, we repeated the assay with embryos collected from naturally ovulated females and analyzed using RFLP. No significant effect was found to be caused by the type of ovulation (*i.e.* **Figure 2.3C and 2.3D**; P = 0.12), therefore data were merged for subsequent analyses. **Figure 2.3E** shows the results for all data combined. Statistical differences were observed for age (in hours) of the embryos from time of presumed ovulation (P < 0.0001), and treatment effect of culture (P < 0.004) as a result of fewer embryos in the culture group.

Kcnq1ot1 allelic-specific expression in single C7xB6 F1 embryos

Analysis of another imprinted gene, *Kcnq1ot1*, in single embryos using RT-PCR followed by RFLP and PAGE showed imprinting was maintained in all embryos regardless of treatment and time of collection (**Supplemental Figure S2.1**).

H19/*Igf2* ICR Methylation analysis

DNA methylation of the imprinting control region for *H19* was compared between one monoallelic and three biallelic embryos (**Figure 2.4**). Embryos used for comparison were not cultured. One of the three biallelic embryos showed some hypomethylation of the region analyzed. However, no differences were evident in

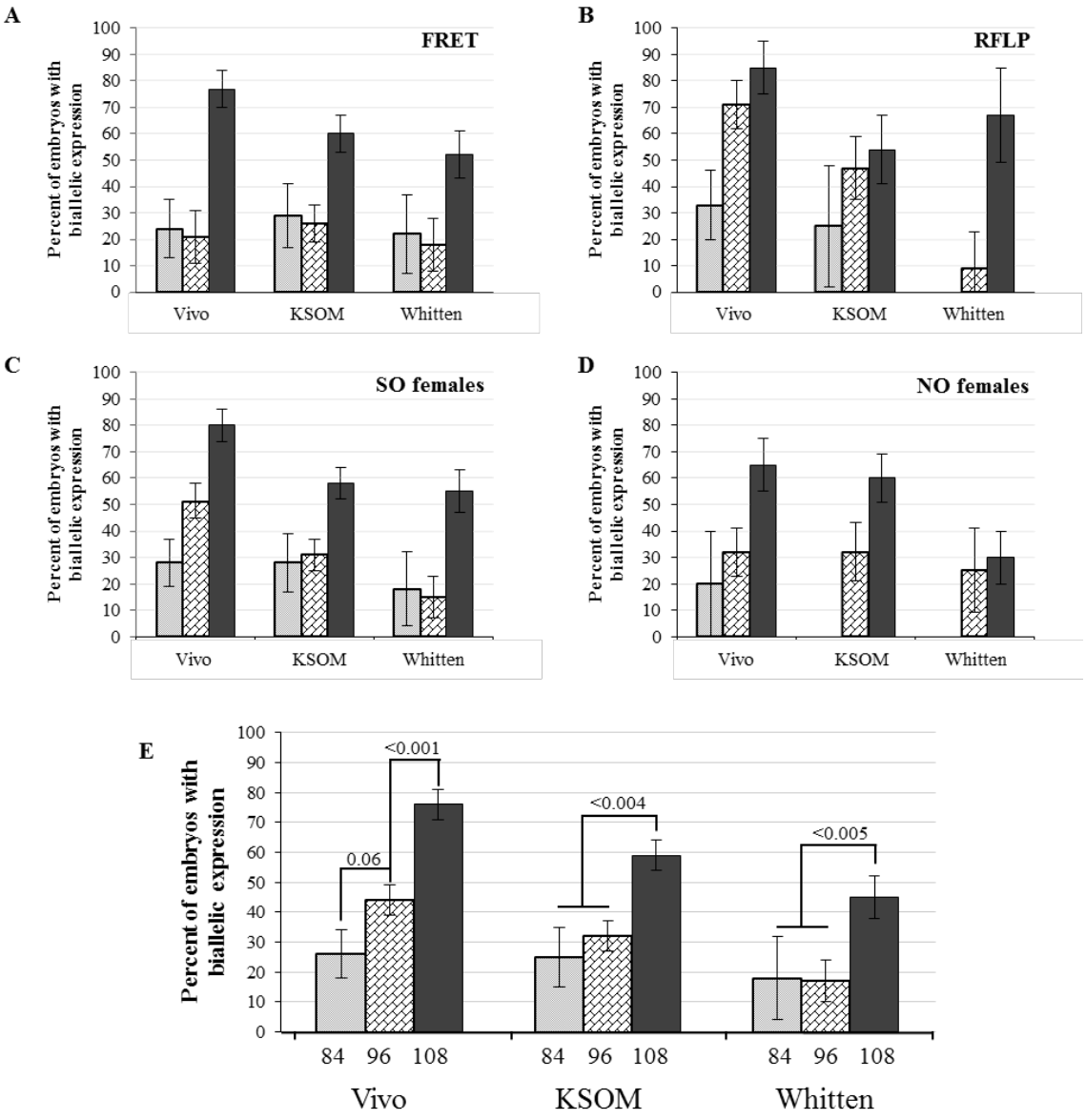

Figure 2.3. Percent of embryos with biallelic expression of *H19*

Figure 2.3. Percent of embryos with biallelic expression of *H19*. Data shown are the percentage of hybrid C7xB6 F1 embryos with biallelic *H19* expression. Allelic expression of *H19* was assessed by two methods. Only blastocysts that expressed *H19* in a detectable manner were included in the figure. **(A and B)** Method of analysis; qRT-PCR and FRET **(A)** (vivo n = 17, 19, 39; KSOM + aa n = 14, 39, 47; Whitten's media n = 9, 22, 25; 84, 96, 108 h respectively), or RT-PCR and RFLP **(B)** (vivo n = 12, 28, 20; KSOM + aa n = 4, 15, 13; Whitten's media n = 2, 11, 6; 84, 96, 108 h, respectively). **(C and D)** Method of ovulation. Superovulation (SO; **C**) (vivo n = 29, 47, 59; KSOM n = 18, 54, 60; Whitten's n = 11, 33, 31; 84, 96, 108 h, respectively) compared to natural ovulation (NO; **D**) (vivo n = 5, 25, 20; KSOM + aa n = 2, 19, 25; Whitten's media n = 0, 8, 20; 84, 96, 108 h, respectively). **(E)** Overall *H19* biallelic expression (vivo n = 34, 72, 79; KSOM + aa n = 20, 73, 85; Whitten's media n = 11, 41, 51; 84, 96, 108 h, respectively). Only samples that had at least 10% expression from the repressed allele were considered biallelic. For each set of bars = leftmost bar (light grey) = 84 h, middle bar (cross hatched) = 96 h and rightmost bars (dark grey) = 108 h. Time points refer to the time of embryo collection after the time of presumed ovulation at 1 AM (12 h after the hCG injection in the SO group and at the midpoint of the light dark cycle in the naturally ovulated NO group). n = number of embryos with *H19* expression. *Statistical significance ($P<0.0001$) noted when comparing the number of embryos with biallelic expression of *H19* and age of embryos (*i.e.*, 84, 96, 108 h), and when analyzing treatment effect of culture ($P<0.004$). Numbers within combined graph (E) are the p-values corresponding to the statistical significance within treatments. Data are expressed as means ± SEM. FRET = fluorescence resonance electron transfer. RFLP = restriction fragment length polymorphism.

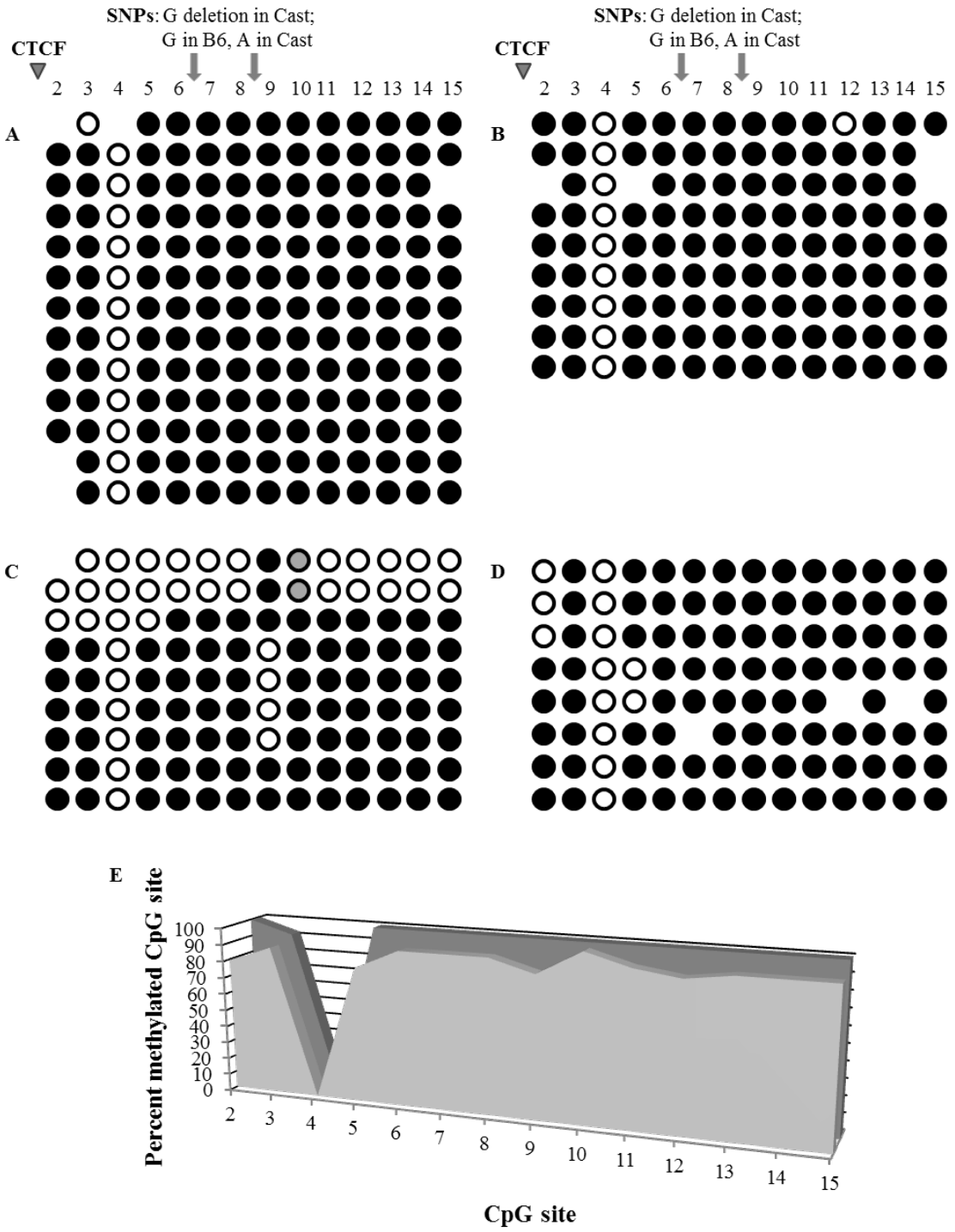

Figure 2.4. Methylation analysis of the paternal allele at the *H19/Igf2* ICR

Figure 2.4. Methylation analysis of the paternal allele at the *H19*/*Igf2* ICR. (A-D) Analysis of the *H19*/*Igf2* ICR **(A)** of one 108 h embryo with monoallelic*H19* expression and **(B-D)** three 108 h embryos that expressed *H19* from both parental alleles. Each sequenced clone was identified as paternally- or maternally-inherited based on DNA sequence polymorphisms. Only the paternal alleles of four embryos are shown. The maternal alleles for these embryos were hypomethylated. DNA was bisulfite converted prior to cloning and sequencing. This region contains 15 CpG's (circles). The CpG corresponding to the first CTCF binding site in the mouse (*i.e.* CpG #1; gray triangle) returned poor sequencing results in most of the clones; this was excluded from the figure. Open circles = unmethylated CpG. Closed circles = methylated CpG. Gray circles = SNP (deletion of a cytosine) found in post-cloning sequences. Missing circles indicate bad sequencing for the corresponding CpG site. **(E)** Average percentage of methylated CpGs on the paternal B6 allele is shown. The sequence of the first CpG site could not be retrieved due to bad sequencing. Solid red area (back) = percentage of methylated CpGs in the monoallelic embryo, shaded blue area (front) = average percentage of methylated CpGs in three biallelic embryos.

the level of methylation of the paternal allele between monoallelic and biallelic embryos with the region showing hypermethylation in both types of embryos. It should be mentioned that, as expected, the maternal alleles were hypomethylated (data not shown). Interestingly, we noted that one of the CpGs was always unmethylated in the paternal allele (**Figure 2.4**). We used the publically available software "TFSEARCH: Searching Transcription Factor Binding Sites (ver 1.3)" which predicted this be a CDX1 (caudal type homeobox 1) binding site.

H19 allelic determination in F1 hybrid embryo ICM and PTGC containing sections

Peri-implantation stage embryos were harvested from unstimulated females at 109 h post ovulation and immediately fixed in 10% Neutral Buffered Formalin to preserve RNA integrity. Embryos (n = 8) were subsequently bisected into ICM-containing and PTGC- containing sections (**Figure 2.5 A and 2.5B**). *H19* allelic expression in ICM and PTGC containing sections was analyzed through the use of RT-PCR followed by RFLP as described above. All ICM and PTGC sections expressed *H19* in a biallelic manner. **Supplemental Table S2.3** shows the percentage of parental-specific *H19* expression for each embryo section analyzed.

Quantitative Real-time PCR

Since the site of dissection varies between embryos, unequal number of cells is expected in each one of the embryo sections. Therefore, we normalized the section with the lowest amount of *Dek* (*i.e.* higher C_T) to the section with the highest amount of *Dek*

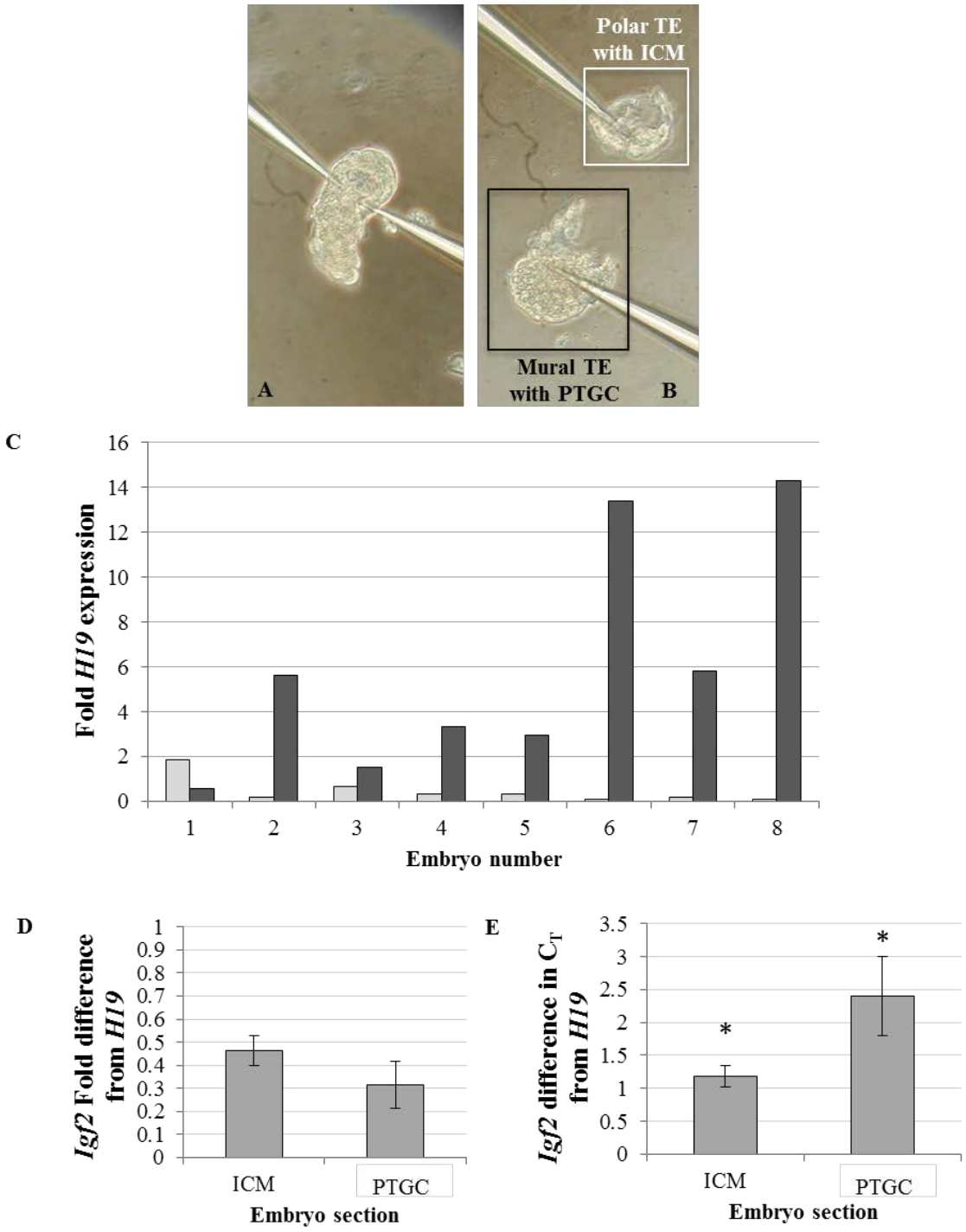

Figure 2.5. Embryo microdissection and section-specific *Igf2* and *H19* expression

Figure 2.5. Embryo microdissection and section-specific *Igf2* and *H19* expression. **(A)** Embryos are collected from the uterus from unstimulated females at 109 h post presumed ovulation. C7xB6F1 embryos were fixed upon collection in 10% neutral buffered formalin. **(A)** Whole blastocyst before dissection: polar TE with ICM above the needles; mural TE with PTGC below the needles. **(B)** Embryo halves: the white square demarcates the ICM, primitive endoderm cells and/or adjacent polar TE; the black square demarcates the mural TE and PTGC. Original magnification X20. **(C)** *H19* expression relative to *Dek* in each embryo section of the 8 embryos analyzed. Fold of *H19* is statistically significant ($P<0.0001$) between ICM and PTGC containing sections. Light gray bars = ICM containing section, dark gray bars = PTGC containing section. **(D)***Igf2* mean fold difference from *H19* (n = 8). **(E)** *Igf2* mean difference in C_T from *H19* (n = 8). *Statistical significance ($P = 0.07$) noted when comparing levels of *Igf2* to *H19* in ICM and PTGC containing sections. All embryos presented biallelic *H19* expression. qRT-PCR was used to determine the amount of *H19* and *Igf2* mRNA present in each embryo section. The fold-change was calculated using the comparative C_T method after normalizing to proto-oncogene *Dek*. The data shown in D are expressed as ± SEM.

(*i.e.* lower C_T). Once the cycle thresholds were normalized between embryo sections we calculated the dC_T (difference in cycle threshold) for *Pou5f1, Itga7, H19 and Igf2* mRNA using *Dek* as a normalizer. *Pou5f1*, a marker for ICM, and *Itga7*, a marker for PTGC, were used to ensure accuracy of dissection. Analysis of fold difference showed that levels of *Pou5f1* were higher in the ICM-containing section than in the PTGC-containing section ($P < 0.0001$; **Supplemental Figure S2.2**). On the other hand, analysis of fold difference showed that levels of *Itga7* were higher in the PTGC-containing section when compared to the ICM-containing section ($P < 0.0001$; **Supplemental Figure S2.2**). Next we compared the levels of *H19* in each of the embryo sections. **Figure 2.5C** shows the fold difference of *H19* when compared to *Dek* in each section of all embryos analyzed. The expression level of *H19* was greater in the PTGC-containing section than the ICM-containing section ($P < 0.0001$). Because there are several possible ways that *H19* may be regulating *Igf2* during implantation [198, 243, 366-368], it was expected to find lower levels of *Igf2* where *H19* levels were higher. The mean amount of *Igf2* transcript was lower in the PTGC-containing section when compared to the ICM-containing section ($P = 0.07$; **Figure 2.5D**). Alternatively, the mean C_T of *Igf2* relative to *H19* was higher in the PTGC-containing section when compared to the ICM-containing section (**Figure 2.5E**). **Supplemental Figure S2.3** shows the fold difference of *Igf2* when compared to *Dek* in each section of all embryos analyzed.

DISCUSSION

In our study, we show an increase in the percentage of embryos with biallelic *H19* expression related to the hour of collection regardless of superovulation or culture. It should be noted that the biallelic expression of *H19* was not mimicked by another imprinted gene, namely *Kcnq1ot1*, which was always monoallelically-expressed. In addition, we also observed that all peri-implantation embryos used in the dissection experiment had expression of *H19* from both parental alleles. Similar to our findings, a recent publication shows a relation between loss of imprinting and faster developing embryos in culture [353]. Taken together these observations suggest that at the late blastocyst stage, *H19's* biallelic expression may be caused by a developmental cue ("molecular clock") that occurs in the embryo around the time of implantation instead of being a direct result of superovulation or embryo culture. A molecular clock is an event occurring at a given time post-fertilization independent of the environment or cellular circumstances [72]. Several molecular clocks have been described to govern developmental transitions during pre-implantation embryo development, among those are: genome activation [71], Dnmt1o nuclear translocation [72], compaction [8], and blastocoel formation [9, 73].

Blastocyst development begins from the tight junctions and the expansion of the trophectoderm (TE) cells that lead to formation of a cavity known as blastocoel [29, 369]. TE cells will then differentiate into mural trophectoderm (farthest from the inner cell mass [ICM]) cells or into polar trophectoderm cells (closer to the ICM). The mural TE will give rise to the highly invasive cells known as the primary trophoblast giant cells (PTGC [33]) which are necessary for embryo implantation into the uterus. At the time of

peri-implantation, the PTGC are detectable from the abembryonic pole to the edge of the ICM [34]. The mural TE derived PTGC undergo endoreduplication [39], are the first terminally differentiated cell type during embryogenesis, mediate implantation to the uterus around embryonic day 4.5, invade the uterus, and come together to form the yolk sac placenta for early nutrient exchange [40]. Endoreduplication is the replication of the genome without subsequent cell division; one possibility is that PTGC undergo endoreduplication to facilitate invasive extra-embryonic tissue formation and growth to save time and energy expenditure [40, 370].

Previous research shows that embryo culture can cause abnormal allelic expression of *H19* in mouse blastocysts [222] and that this loss-of-imprinting is maintained up to day 9.5 of embryo development [339]. Another study [341], also shows abnormal *H19* expression in the fetal and placental components of the conceptus after embryo culture and embryo transfer. The LOI of *H19* as well as other imprinted genes was also observed in the placenta of less manipulated (*i.e.* only embryo transfer) day 9.5 conceptuses [341]. We did not do further experiments to study the adverse effects of embryo manipulation on *H19*'s allelic expression at midgestation as previous reports already have shown this to be the case [339, 341].

Previous analyses of single embryos collected at the blastocyst stage shows that ~65% of embryos cultured in Whitten's medium present significant LOI of *H19*; only 14% of embryos cultured in KSOM + aa, and 6% of in vivo derived blastocysts have biallelic expression of *H19* [339]. Different methodology, chronological age and number of embryos analyzed may have led to the differences observed between our work and those studies. We observed an effect of culture in our study but it was due to fewer

embryos expressing *H19* in the cultured groups when compared to the in vivo group. This is not surprising since embryos develop slower in culture than in vivo. We have noted in the course of our experiments that, on average, embryos cultured in KSOM + aa are approximately 12 h behind in development as compared to the in vivo embryos and furthermore, that embryos cultured in Whitten's media are approximately 12 h behind in development when compared to the KSOM + aa cultured embryos. We did not analyze the embryos collected based on developmental stage but rather by time from presumed ovulation; therefore, cultured embryos will include slower developing embryos at the final time-point examined when compared to in vivo produced embryos. It is probable that the PTGC formation is delayed in culture thus accounting for the fewer embryos with biallelic expression in those groups.

While an association between biallelic *H19* expression and loss of methylation of the paternal allele has been reported for pools of cultured embryos [339], similar results were not observed by us when using individually analyzed in vivo produced blastocysts. The fact that we did not observe loss of methylation at the ICR of in vivo-produced embryos is not inconsistent with our hypothesis that biallelic expression of *H19* only occurs in a subpopulation of embryonic cells, which we hypothesize to be the PTGC. At peri-implantation, the mouse embryo is composed of approximately 120 total cells [35] with only ~50 belonging to the mural trophectoderm [37] which will begin transforming into PTGC at this time [33-36]. Therefore, if our hypothesis is correct, only a few cells would be hypomethylated at the *H19/Igf2* ICR (**Figure 2.4C**) making it difficult to visualize during DNA methylation analyses.

Interestingly, the methylation analyses of the *H19/Igf2* ICR revealed a CpG site that was unmethylated in the majority of the sequences. Through the use of the publically available software, TFSEARCH, we found that the amplified sequence containing the unmethylated CpG was predicted to be a CDX1 binding site. It has been reported that *Cdx1* may have repressing activity [371-373]. Another study in breast cancer tumors also found CDX1 binds to the site at the *H19/IGF2* ICR locus [372].

We hypothesized that *H19* becomes biallelicaly-expressed around the time of implantation to control the invasion of the PTGC to the uterus. Similar to what we found in our work, a study which analyzed *H19*'s expression using allele-specific in situ hybridization showed paternal *H19* expression during cytotrophoblast development (human TGC) [374]. Cytotrophoblast cells are invasive cells derived from the human trophoblast; they have tumor-like behavior in early pregnancy to invade and attach to the uterine epithelial cells [375, 376]. In an attempt to identify which subpopulation of cells expressed biallelic *H19*, we dissected peri-implantation embryos into two sections. One section contained primarily the ICM, primitive endoderm, and adjacent polar trophectoderm while the other section primarily contained the mural trophectoderm and differentiated PTGC. We used the embryonic cell specific markers *Pou5f1* and *Itga7* to ascertain enrichment of each subpopulation of cells. qRT-PCR analysis showed reciprocal levels of *H19* and *Igf2* mRNA in embryo sections with greater *H19* expression levels in the PTGC containing section.

After the blastocyst stage, growth factors such as IGF2 are necessary for normal embryo development [177]. At this stage, *Igf2* is associated with tumor enhancer activity [177, 197, 204]. Upregulation and biallelic expression of *H19* during peri-implantation

stage may suggest a role of this transcript to control uterine implantation. There are several possible mechanisms by which *H19* may be regulating *Igf2* expression during implantation. Firstly, directly at the ICR: loss of *H19* transcript or deletion of *H19*, including the ICR, is not lethal but is associated with placental and fetal overgrowth, and *Igf2* overexpression [243, 366]. Secondly, at the post-transcriptional level: overexpression of *H19* affects expression of *Igf2*as well as that of other imprinted genes involved in growth [367]. Thirdly, as a regulator of *Igf2*'s stability: *Igf2* transcript stability requires binding to *Igf2* mRNA binding protein 1 (IGF2BP1); *H19* transcripts found in the cytoplasm [377] can also bind to IGF2BP1 [198, 368]. Therefore, competition between *H19* and *Igf2* mRNAs for IGF2BP1 may affect *Igf2* expression.

In summary, results reported here show that as blastocysts advance in development and prepare to implant into the uterus, a subpopulation of cells in the mural trophectoderm lose imprinted gene expression of *H19* and begin expressing this transcript from both parental alleles. We propose that this occurs specifically in the primary trophoblast giant cells. We observed this phenomenon in the absence of embryo culture. Even though it is well established that embryo culture can result in loss-of-imprinting at mid-gestation, our results suggest that previous observations made at the late blastocyst stage could be partially explained by the natural occurrence of biallelic *H19* expression in a subpopulation of embryonic cells. We conclude that biallelic expression of *H19* is a normal physiologic event in peri-implantation stage embryos and that this occurs primarily in the primary trophoblast giant cells derived from the mural trophectoderm.

ACKNOWLEDGEMENTS

We would like to thank Dr. Marisa Bartolomei from the University of Pennsylvania for donating the original pairs of C7 mice from which our colony was developed. We would like to acknowledge the contribution of Matthew Sepúlveda from the Rivera laboratory for developing the allele-specific *Kcnq1ot1* assay used in this study. We would also like to thank Dr. Randall Prather and members of his laboratory for technical assistance involving the use of the micromanipulator used for embryo dissection.

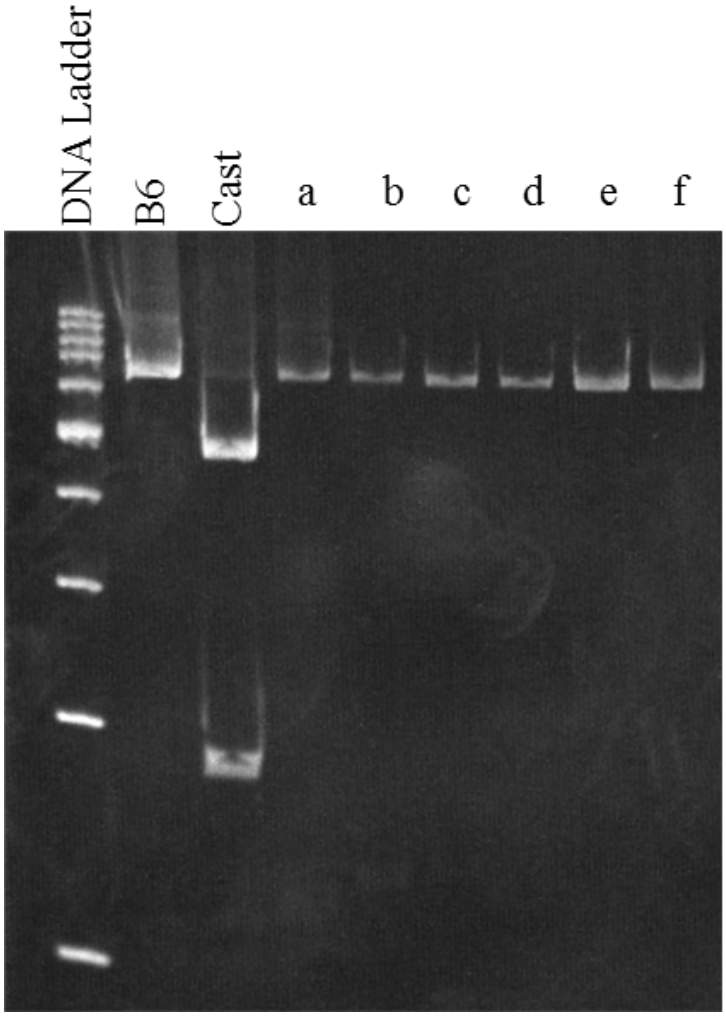

Supplemental Figure S2.1. *Kcnq1ot1* allelic expression assays. Shown is a picture of a 7% polyacrylamide gel containing the restricted product of control tissues and 6 C7xB6 F1 embryos. The PCR product was digested with HincII prior to electrophoresis in order to determine maternal contribution of *Kcnq1ot1*. Differences in DNA sequence (*i.e.* SNP) between B6 and Cast were used to ascertain allelic expression in C7xB6 F1 single embryos. Digestion controls (B6 and Cast) show the mobility of each amplicon and are used to determine allelic expression in F1 embryos. The restriction enzyme HincII cuts the maternal (Cast) allele leaving two fragments of 457bp and 176 bp size. All embryos show monoallelic expression of *Kcnq1ot1*. Controls = B6 and Cast neonatal muscle.

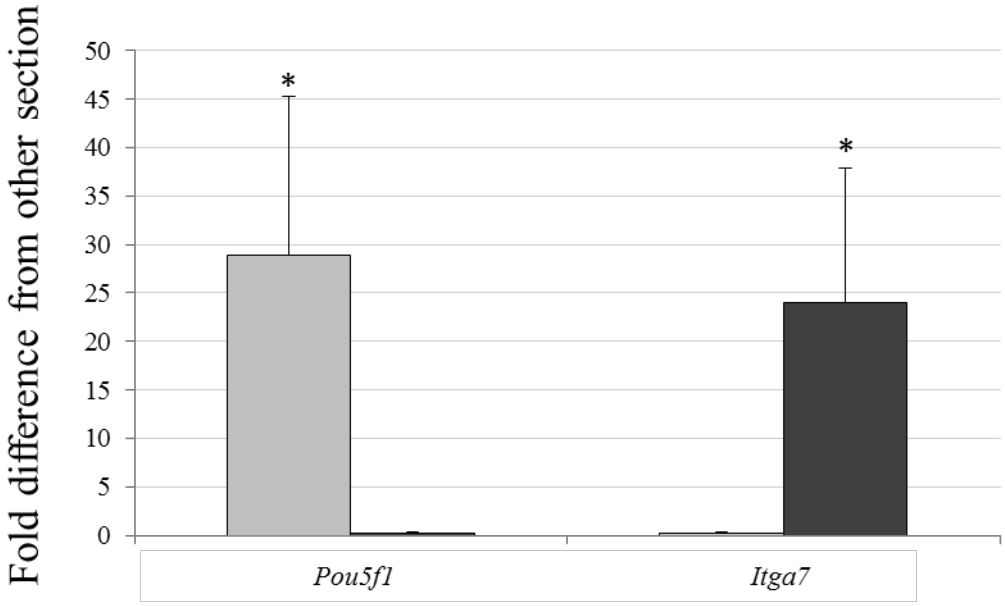

Supplemental Figure S2.2. *Pou5f1* and *Itga7* average fold difference. Fold *Pou5f1* and *Itga7* average fold difference is relative to *Dek* in each embryo section (n = 8). The data are expressed as Mean ± SEM. *Statistical significance noted *Pou5f1* in ICM containing section (P<0.0001) and *Itga7* in PTGC containing section (P < 0.0001) when compared to counter embryo section. Light gray bar = ICM containing section, dark gray bars = PTGC containing section.

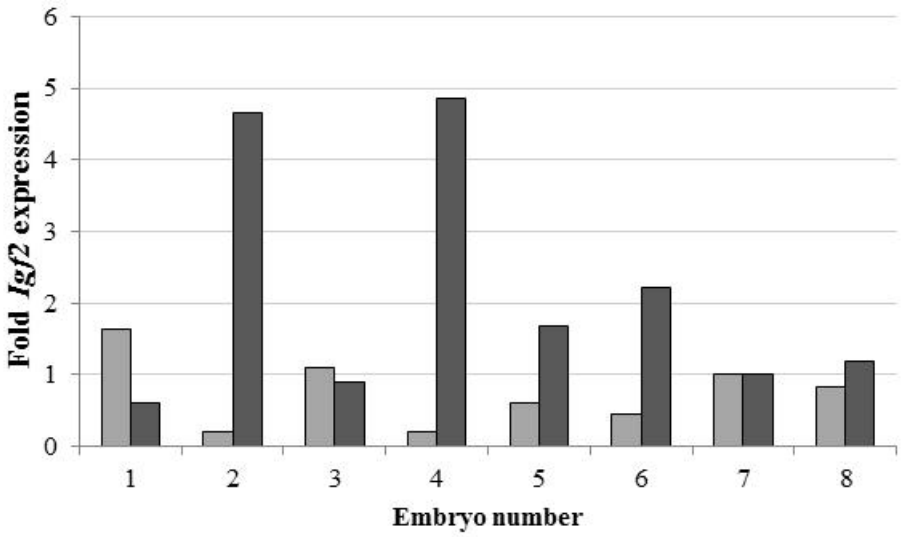

Supplemental Figure S2.3 *.Igf2* fold difference. *Igf2* expression relative to *Dek* in each embryo section of the 8 embryos analyzed. Light gray bars = ICM containing section, dark gray bars = PTGC containing section.

Supplemental Table S2.1. P-87 Flaming/Brown Micropipetter Puller settings used to create microdissection needles.

Heat	Pull	Velocity	Time
550	0	20	250
550	0	20	250
550	0	20	250
550	50	80	220

If VEL>0 then one unit of TIME represents 1/2ms.

Supplemental Table S2.2. Real-time RT-PCR probes used to detect gene expression in microdissected embryo sections.

Real-Time TaqMan Probes (Applied Biosystems)		
Gene	**Assay ID**	**Context Sequence**
Dek	Mm00662582_m1	GTGAAGAGGAGCAACCACCAAAAAA
Pou5f1 (Oct4)	Mm00658129_gH	CTGGGCGTTCTCTTTGGAAAGGTGT
Cdx2	Mm01212280_m1	GCTCTCCGAGAGGCAGGTTAAAATT
Itga7	Mm00434400_m1	CCCAGAGCTGGCTGCTGGTGGGCGC
H19	Mm01156721_g1	TGAACCCTCAAGATGAAAGAAATGG
Igf2	Mm00439564_m1	GCGGCTTCTACTTCAGCAGGCCTTC

Supplemental Table S2.3. Percentage of *H19* allele-specific contribution per embryo section.

ICM Section	% Pat	% Mat	PTGC Section	% Pat	% Mat
1	20.67	79.33	**1**	24.34	75.66
2	19.23	80.77	**2**	20.30	79.70
3	25.60	74.40	**3**	33.57	66.43
4	27.02	72.98	**4**	30.85	69.15
5	28.00	72.00	**5**	31.01	68.99
6	24.22	75.78	**6**	21.30	78.70
7	30.23	69.77	**7**	36.28	63.72
8	30.98	69.02	**8**	20.02	79.98

GENERAL DISCUSSION

Genomic imprinting is an epigenetic mechanism that regulates parental-allele specific gene expression. Imprinted genes are usually found in clusters containing a ncRNA and both maternally and paternally expressed genes. Also, imprinted genes are dependent on epigenetic machinery (*e.g.* DNA methylation) for maintenance of their allele-specific expression and are known to be important during fetal growth and development (reviewed by [81]).

H19 is an imprinted long ncRNA expressed from the maternal allele and is associated with tumor suppressor activity. Expression of *H19* has been detected in oocytes, pre-implantation embryos [222], and throughout gestation. After birth, *H19* expression decreases except in cardiovascular and skeletal muscle [214]. *H19* is part of the *H19*/*Igf2* imprinted gene cluster and shares the imprinting control region (ICR) with the paternally-expressed growth factor, *Igf2*. After implantation, *H19* and *Igf2* genes are reciprocally expressed [179].

Previous experiments have shown biallelic expression of *H19* in mouse blastocysts that were cultured from the 2-cell stage up to the blastocyst stage and loss of methylation in the *H19*/*Igf2* ICR [222, 339]. However, preliminary studies in our laboratory showed biallelic expression of *H19* in non-cultured embryos (*i.e. in vivo* developed) during peri-implantation. Therefore, we hypothesized that *H19* becomes biallelically-expressed as part of a physiological event during peri-implantation.

To test this hypothesis, we collected 2-cell stage embryos and cultured them up to the blastocyst stage in either KSOM + AA or Whitten's media. Embryos were collected

at three different times, 84, 96, and 108 hours (h) post presumed ovulation and immediately transferred to lysis buffer for further analysis. Control embryos were developed *in vivo* and flushed from the uterus at the same time post-presumed ovulation (*i.e.* 84, 96 and 108h). We determined *H19* allele-specific expression in collected embryos and found that there was an increase in, the percentage of embryos showing biallelic expression of *H19* as they increased in age regardless of treatment.

At the late blastocyst stage, the embryo is composed of ICM, primitive endoderm, polar TE, mural TE and PTGC. PTGC are the first terminally-differentiated cells in the embryo and are involved in mediating implantation [39]. Further, PTGC have been characterized as having tumor like behavior. We speculated that *H19* becomes biallelicaly-expressed to control the expression of the tumor enhancer gene, *Igf2* [177, 197, 204], to regulate invasion during initial implantation.

We then compared the methylation status of the *H19*/*Igf2* ICR in *in vivo* developed embryos expressing *H19* from the maternal allele with *in vivo* developed embryos showing biallelic expression of *H19*. We found that embryos expressing biallelic *H19* showed the expected differential DNA methylation on the *H19*/*Igf2* ICR. The PTGC represent a small portion of the total number of cells composing the entire embryo. Thus, if our hypothesis is correct, only a few cells would show hypomethylation on the *H19*/*Igf2* ICR making it difficult to visualize when analyzing an entire embryo.

To analyze expression of *H19* more specifically in the PTGC, we collected and fixed *in vivo* developed embryos at 109 h post-presumed ovulation. Embryo dissections were performed to separate the embryo into two sections: one containing ICM, adjacent polar TE and primitive endoderm, and another containing PTGC and mural TE. Similar

analysis of allele-specific expression of *H19* showed that both sections had *H19* expressed in a biallelic manner. Further, we quantified the expression levels of *H19* and *Igf2* in both sections using cell specific markers for ICM [*Pou5f1* (also known as *Oct4*)] and PTGC (*Itga7*) to account for cell contamination in opposite sections and a normalizer (*Dek*) to control for cell number. There was minimal or no contamination of the opposite cell type in each section, and higher levels of *H19* in the PTGC-containing section when compared to *Dek*. Lower levels of *Igf2* were also detected in the PTGC-containing section when compared to *H19*. Furthermore, biallelic expression of *H19* in the ICM-containing section can be explained by cell contamination of PTGC in ICM-containing sections expressing *H19* in a biallelic manner.

Upregulation and biallelic expression of *H19* during the peri-implantation stage may indicate a role of this transcript to control uterine implantation. There are several possible mechanisms by which *H19* may be regulating *Igf2* expression during implantation. Firstly, directly at the ICR: loss of *H19* transcript or deletion of *H19*, including the ICR, is not lethal but is associated with placental and fetal overgrowth, and *Igf2* overexpression [243, 366]. Secondly, at the post-transcriptional level: overexpression of *H19* affects expression of *Igf2* as well as that of other imprinted genes involved in growth [367]. Thirdly, as a regulator of *Igf2*'s stability: *Igf2* transcript stability requires binding to *Igf2* mRNA binding protein 1 (IGF2BP1); *H19* transcripts found in the cytoplasm [377] can also bind to IGF2BP1 [198, 368]. Therefore, competition between *H19* and *Igf2* mRNAs for IGF2BP1 may affect *Igf2* expression.

Two other possible regulators of *Igf2* and *H19* during peri-implantation are *Plagl1* (pleiomorphic adenoma gene-like 1; previously known as *Zac1*) and *Cdkn1c* [cyclin-

dependent kinase inhibitor 1C (P57)]. *Plagl1* is a paternally-expressed gene encoding a zinc finger transcription factor which induces apoptosis and cell-cycle arrest [378]. Experiments with activation of the normally repressed maternal *Plagl1* allele show that LOI of this gene results in placental overgrowth, bone malformation and neonatal lethality. This study also included a meta-analysis to form an imprinted gene network of the imprinted genes linked to *Plagl1*. Among other genes, they found *H19, Igf2* and *Cdkn1c* to be directly linked to *Plagl1*. Also, significant binding of *Plagl1* to the *H19* enhancer region and *Igf2* promoter was shown [378].

Cdkn1c is a maternally-expressed gene located in the *Kcnq1* imprinted gene cluster. *Cdkn1c* expression is necessary to maintain endoreduplication cycles in PTGC [40-42]. Although we did not observe LOI of the *Kcnq1ot1* imprinted gene, also present in the *Kcnq1* cluster, it is possible that in the PTGCs, there is a change of *Cdkn1c* and *Plagl1* allele-specific expression and/or levels to control *Igf2*. This hypothesis remains to be tested.

Similar to our results from the first experiment, faster developing embryos showed biallelic expression of *H19* when compared to slower developing embryos that were cultured in a different medium [353]. It was concluded that the faster growing embryos that had biallelic *H19* expression were developmentally compromised. Although the observation is similar between theirs and our study, we both show that biallelic expression of *H19* occurs in peri-implantation embryos.

We observed biallelic expression of *H19* in all our groups regardless of the culture or *in vivo* development but we noticed that embryos cultured in Whitten's medium developed slower than those cultured in KSOM + AA. In addition, KSOM +

AA cultured embryos also developed slower that those collected after *in vivo* development. This explains why we observed a lower percentage of embryos with biallelic expression of *H19* after *in vitro* development.

In summary, our data show that as the embryo grows and prepares for implantation, the pre-implantation blastocyst begins to express *H19* in a biallelic manner. The results of this thesis go against the scientific dogma and much cited experiments [222, 339] suggesting that *H19* becomes biallelic as an effect of culture. We believe previous results may have been confounded by the stage of the embryos analyzed. In other experiments, *H19* allele-specific expression was analyzed in fewer embryos and based on developmental stage. In our first experiment we collected embryos based on age post-presumed ovulation and analyzed parental-specific expression of *H19*. In the second experiment of this thesis, we analyzed the section containing the PTGC and showed biallelic expression of *H19* as well as increased level of the transcript. We acknowledge the fact that embryo culture can result in misexpression of genes including imprinted genes. However, our work unequivocally shows that *H19* becomes biallelic as part of a physiological event during peri-implantation and not as an effect of culture as previously published. We speculate that *H19* becomes biallelic in PTGC to control *Igf2* expression during implantation in the mouse. Future research would be necessary to disaggregate the embryo and analyze *H19* allele-specific expression and methylation status of the *H19*/*Igf2* ICR in purified PTGC.

BIBLIOGRAPHY

1. Cockburn K, Rossant J. Making the blastocyst: lessons from the mouse. J Clin Invest 2010; 120:995-1003.

2. Goldbard SB, Warner CM. Genes affect the timing of early mouse embryo development. Biol Reprod 1982; 27:419-424.

3. Piotrowska K, Zernicka-Goetz M. Role for sperm in spatial patterning of the early mouse embryo. Nature 2001; 409:517-521.

4. Gardner RL. Specification of embryonic axes begins before cleavage in normal mouse development. Development 2001; 128:839-847.

5. Bischoff M, Parfitt D-E, Zernicka-Goetz M. Formation of the embryonic-abembryonic axis of the mouse blastocyst: relationships between orientation of early cleavage divisions and pattern of symmetric/asymmetric divisions. Development 2008; 135:953-962.

6. Morris SA, Teo RT, Li H, Robson P, Glover DM, Zernicka-Goetz M. Origin and formation of the first two distinct cell types of the inner cell mass in the mouse embryo. Proc Natl Acad Sci U S A 2010; 107:6364-6369.

7. Gardner RL. Normal bias in the direction of fetal rotation depends on blastomere composition during early cleavage in the mouse. PLoS One 2010; 5:e9610.

8. Levy JB, Johnson MH, Goodall H, Maro B. The timing of compaction: control of a major developmental transition in mouse early embryogenesis. Journal of embryology and experimental morphology 1986; 95:213-237.

9. Pratt HP, Chakraborty J, Surani MA. Molecular and morphological differentiation of the mouse blastocyst after manipulations of compaction with cytochalasin D. Cell 1981; 26:279-292.

10. Ducibella T, Albertini DF, Anderson E, Biggers JD. The preimplantation mammalian embryo: Characterization of intercellular junctions and their appearance during development. Developmental Biology 1975; 45:231-250.

11. Lo CW, Gilula NB. Gap junctional communication in the preimplantation mouse embryo. Cell 1979; 18:399-409.

12. Nikas G, Ao A, Winston RM, Handyside AH. Compaction and surface polarity in the human embryo in vitro. Biol Reprod 1996; 55:32-37.

13. Watson AJ, Barcroft LC. Regulation of blastocyst formation. Front Biosci 2001; 6:D708-730.

14. Barcroft LC, Offenberg H, Thomsen P, Watson AJ. Aquaporin proteins in murine trophectoderm mediate transepithelial water movements during cavitation. Developmental Biology 2003; 256:342-354.

15. Fleming TP. A quantitative analysis of cell allocation to trophectoderm and inner cell mass in the mouse blastocyst. Developmental Biology 1987; 119:520-531.

16. Johnson MH, Ziomek CA. The foundation of two distinct cell lineages within the mouse morula. Cell 1981; 24:71-80.

17. Jedrusik A, Parfitt DE, Guo G, Skamagki M, Grabarek JB, Johnson MH, Robson P, Zernicka-Goetz M. Role of Cdx2 and cell polarity in cell allocation and specification of trophectoderm and inner cell mass in the mouse embryo. Genes Dev 2008; 22:2692-2706.

18. Tarkowski AK, Wroblewska J. Development of blastomeres of mouse eggs isolated at the 4- and 8-cell stage. J Embryol Exp Morphol 1967; 18:155-180.

19. Ota M, Sasaki H. Mammalian Tead proteins regulate cell proliferation and contact inhibition as transcriptional mediators of Hippo signaling. Development 2008; 135:4059-4069.

20. Harvey KF, Pfleger CM, Hariharan IK. The Drosophila Mst Ortholog, hippo, Restricts Growth and Cell Proliferation and Promotes Apoptosis. Cell 2003; 114:457-467.

21. Sasaki H. Mechanisms of trophectoderm fate specification in preimplantation mouse development. Development, Growth & Differentiation 2010; 52:263-273.

22. Nishioka N, Inoue K-i, Adachi K, Kiyonari H, Ota M, Ralston A, Yabuta N, Hirahara S, Stephenson RO, Ogonuki N, Makita R, Kurihara H, et al. The Hippo Signaling Pathway Components Lats and Yap Pattern Tead4 Activity to Distinguish Mouse Trophectoderm from Inner Cell Mass. Developmental Cell 2009; 16:398-410.

23. McPherson JP, Tamblyn L, Elia A, Migon E, Shehabeldin A, Matysiak-Zablocki E, Lemmers B, Salmena L, Hakem A, Fish J, Kassam F, Squire J, et al. Lats2/Kpm is required for embryonic development, proliferation control and genomic integrity. EMBO J 2004; 23:3677-3688.

24. Nishioka N, Yamamoto S, Kiyonari H, Sato H, Sawada A, Ota M, Nakao K, Sasaki H. Tead4 is required for specification of trophectoderm in pre-implantation mouse embryos. Mechanisms of Development 2008; 125:270-283.

25. Avilion AA, Nicolis SK, Pevny LH, Perez L, Vivian N, Lovell-Badge R. Multipotent cell lineages in early mouse development depend on SOX2 function. Genes Dev 2003; 17:126-140.

26. Chambers I, Colby D, Robertson M, Nichols J, Lee S, Tweedie S, Smith A. Functional Expression Cloning of Nanog, a Pluripotency Sustaining Factor in Embryonic Stem Cells. Cell 2003; 113:643-655.

27. Mitsui K, Tokuzawa Y, Itoh H, Segawa K, Murakami M, Takahashi K, Maruyama M, Maeda M, Yamanaka S. The Homeoprotein Nanog Is Required for Maintenance of Pluripotency in Mouse Epiblast and ES Cells. Cell 2003; 113:631-642.

28. Palmieri SL, Peter W, Hess H, Schöler HR. Oct-4 Transcription Factor Is Differentially Expressed in the Mouse Embryo during Establishment of the First Two Extraembryonic Cell Lineages Involved in Implantation. Developmental Biology 1994; 166:259-267.

29. Strumpf D, Mao CA, Yamanaka Y, Ralston A, Chawengsaksophak K, Beck F, Rossant J. Cdx2 is required for correct cell fate specification and differentiation of trophectoderm in the mouse blastocyst. Development 2005; 132:2093-2102.

30. Russ AP, Wattler S, Colledge WH, Aparicio SA, Carlton MB, Pearce JJ, Barton SC, Surani MA, Ryan K, Nehls MC, Wilson V, Evans MJ. Eomesodermin is

required for mouse trophoblast development and mesoderm formation. Nature 2000; 404:95-99.

31. Ma GT, Linzer DI. GATA-2 restricts prolactin-like protein A expression to secondary trophoblast giant cells in the mouse. Biol Reprod 2000; 63:570-574.

32. Ma GT, Roth ME, Groskopf JC, Tsai FY, Orkin SH, Grosveld F, Engel JD, Linzer DI. GATA-2 and GATA-3 regulate trophoblast-specific gene expression in vivo. Development 1997; 124:907-914.

33. Dickson AD. Trophoblastic Giant Cell Transformation of Mouse Blastocyts. J Reprod Fertil 1963; 6:465-466.

34. Dickson AD. Cytoplasmic changes during the trophoblastic giant cell transformation of blastocysts from normal and ovariectomized mice. J Anat 1969; 105:371-380.

35. Handyside AHaH, Susan Cell division and death in the mouse blastocyst before implantation. Roux's Arch Dev Biol 1986; 195:519-526.

36. Copp AJ. Interaction between inner cell mass and trophectoderm of the mouse blastocyst. I. A study of cellular proliferation. J Embryol Exp Morphol 1978; 48:109-125.

37. Simmons DG, Fortier AL, Cross JC. Diverse subtypes and developmental origins of trophoblast giant cells in the mouse placenta. Dev Biol 2007; 304:567-578.

38. Gardner RL, Papaioannou VE, Barton SC. Origin of the ectoplacental cone and secondary giant cells in mouse blastocysts reconstituted from isolated trophoblast and inner cell mass. J Embryol Exp Morphol 1973; 30:561-572.

39. Barlow P, Owen DA, Graham C. DNA synthesis in the preimplantation mouse embryo. J Embryol Exp Morphol 1972; 27:431-445.

40. Hu D, Cross JC. Development and function of trophoblast giant cells in the rodent placenta. Int J Dev Biol 2010; 54:341-354.

41. Ullah Z, Lee CY, Depamphilis ML. Cip/Kip cyclin-dependent protein kinase inhibitors and the road to polyploidy. Cell Div 2009; 4:10.

42. Ullah Z, Kohn MJ, Yagi R, Vassilev LT, DePamphilis ML. Differentiation of trophoblast stem cells into giant cells is triggered by p57/Kip2 inhibition of CDK1 activity. Genes & development 2008; 22:3024-3036.

43. Cross JC, Flannery ML, Blanar MA, Steingrimsson E, Jenkins NA, Copeland NG, Rutter WJ, Werb Z. Hxt encodes a basic helix-loop-helix transcription factor that regulates trophoblast cell development. Development 1995; 121:2513-2523.

44. Jen Y, Manova K, Benezra R. Each member of the Id gene family exhibits a unique expression pattern in mouse gastrulation and neurogenesis. Dev Dyn 1997; 208:92-106.

45. Kraut N, Snider L, Chen CM, Tapscott SJ, Groudine M. Requirement of the mouse I-mfa gene for placental development and skeletal patterning. EMBO J 1998; 17:6276-6288.

46. Riley P, Anson-Cartwright L, Cross JC. The Hand1 bHLH transcription factor is essential for placentation and cardiac morphogenesis. Nat Genet 1998; 18:271-275.

47. Scott IC, Anson-Cartwright L, Riley P, Reda D, Cross JC. The HAND1 basic helix-loop-helix transcription factor regulates trophoblast differentiation via multiple mechanisms. Mol Cell Biol 2000; 20:530-541.

48. Hughes M, Dobric N, Scott IC, Su L, Starovic M, St-Pierre B, Egan SE, Kingdom JC, Cross JC. The Hand1, Stra13 and Gcm1 transcription factors override FGF signaling to promote terminal differentiation of trophoblast stem cells. Dev Biol 2004; 271:26-37.

49. Guillemot F, Nagy A, Auerbach A, Rossant J, Joyner AL. Essential role of Mash-2 in extraembryonic development. Nature 1994; 371:333-336.

50. Arman E, Haffner-Krausz R, Chen Y, Heath JK, Lonai P. Targeted disruption of fibroblast growth factor (FGF) receptor 2 suggests a role for FGF signaling in

pregastrulation mammalian development. Proc Natl Acad Sci U S A 1998; 95:5082-5087.

51. Tanaka S, Kunath T, Hadjantonakis AK, Nagy A, Rossant J. Promotion of trophoblast stem cell proliferation by FGF4. Science 1998; 282:2072-2075.

52. Erlebacher A, Price KA, Glimcher LH. Maintenance of mouse trophoblast stem cell proliferation by TGF-beta/activin. Dev Biol 2004; 275:158-169.

53. Natale DR, Hemberger M, Hughes M, Cross JC. Activin promotes differentiation of cultured mouse trophoblast stem cells towards a labyrinth cell fate. Dev Biol 2009; 335:120-131.

54. Yan J, Tanaka S, Oda M, Makino T, Ohgane J, Shiota K. Retinoic acid promotes differentiation of trophoblast stem cells to a giant cell fate. Dev Biol 2001; 235:422-432.

55. Pfeffer PL, Pearton DJ. Trophoblast development. Reproduction 2012; 143:231-246.

56. Gardner RL. Flow of cells from polar to mural trophectoderm is polarized in the mouse blastocyst. Hum Reprod 2000; 15:694-701.

57. Armant DR. Blastocysts don't go it alone. Extrinsic signals fine-tune the intrinsic developmental program of trophoblast cells. Dev Biol 2005; 280:260-280.

58. Bany BM, Cross JC. Post-implantation mouse conceptuses produce paracrine signals that regulate the uterine endometrium undergoing decidualization. Dev Biol 2006; 294:445-456.

59. Cross JC, Werb Z, Fisher SJ. Implantation and the placenta: key pieces of the development puzzle. Science 1994; 266:1508-1518.

60. Nadra K, Anghel SI, Joye E, Tan NS, Basu-Modak S, Trono D, Wahli W, Desvergne B. Differentiation of trophoblast giant cells and their metabolic functions are dependent on peroxisome proliferator-activated receptor beta/delta. Mol Cell Biol 2006; 26:3266-3281.

61. Wiemers DO, Shao LJ, Ain R, Dai G, Soares MJ. The mouse prolactin gene family locus. Endocrinology 2003; 144:313-325.

62. Simmons DG, Rawn S, Davies A, Hughes M, Cross JC. Spatial and temporal expression of the 23 murine Prolactin/Placental Lactogen-related genes is not associated with their position in the locus. BMC Genomics 2008; 9:352.

63. Wang H, Dey SK. Roadmap to embryo implantation: clues from mouse models. Nat Rev Genet 2006; 7:185-199.

64. Dey SK, Lim H, Das SK, Reese J, Paria BC, Daikoku T, Wang H. Molecular Cues to Implantation. Endocrine Reviews 2004; 25:341-373.

65. Patten BM. Patten's Foundations of embryology. New York: McGraw-Hill; 1981.

66. Smith CS, Berg DK, Berg M, Pfeffer PL. Nuclear transfer-specific defects are not apparent during the second week of embryogenesis in cattle. Cell Reprogram 2010; 12:699-707.

67. Hoffman LH, Wooding FB. Giant and binucleate trophoblast cells of mammals. J Exp Zool 1993; 266:559-577.

68. Concannon PW, Powers ME, Holder W, Hansel W. Pregnancy and parturition in the bitch. Biol Reprod 1977; 16:517-526.

69. Steinetz BG, Goldsmith LT, Harvey HJ, Lust G. Serum relaxin and progesterone concentrations in pregnant, pseudopregnant, and ovariectomized, progestin-treated pregnant bitches: detection of relaxin as a marker of pregnancy. Am J Vet Res 1989; 50:68-71.

70. Enders AC, Carter AM. The evolving placenta: Convergent evolution of variations in the endotheliochorial relationship. Placenta 2012; 33:319-326.

71. Schultz RM. Regulation of zygotic gene activation in the mouse. BioEssays : news and reviews in molecular, cellular and developmental biology 1993; 15:531-538.

72. Doherty AS, Bartolomei MS, Schultz RM. Regulation of Stage-Specific Nuclear Translocation of Dnmt1o during Preimplantation Mouse Development. Developmental Biology 2002; 242:255-266.

73. Dean WL, Rossant J. Effect of delaying DNA replication on blastocyst formation in the mouse. Differentiation 1984; 26:134-137.

74. Schultz RM. The molecular foundations of the maternal to zygotic transition in the preimplantation embryo. Human Reproduction Update 2002; 8:323-331.

75. Poueymirou WT, Schultz RM. Regulation of mouse preimplantation development: Inhibition of synthesis of proteins in the two-cell embryo that require transcription by inhibitors of cAMP-dependent protein kinase. Developmental Biology 1989; 133:588-599.

76. Poueymirou WT, Schultz RM. Differential effects of activators of cAMP-dependent protein kinase and protein kinase C on cleavage of one-cell mouse embryos and protein synthesis and phosphorylation in one- and two-cell embryos. Developmental Biology 1987; 121:489-498.

77. Howlett S. The effect of inhibiting DNA replication in the one-cell mouse embryo. Roux's archives of developmental biology 1986; 195:499-505.

78. Wiekowski M, Miranda M, DePamphilis ML. Regulation of gene expression in preimplantation mouse embryos: Effects of the zygotic clock and the first mitosis on promoter and enhancer activities. Developmental Biology 1991; 147:403-414.

79. Ram PT, Schultz RM. Reporter Gene Expression in G2 of the 1-Cell Mouse Embryo. Developmental Biology 1993; 156:552-556.

80. Nothias JY, Miranda M, DePamphilis ML. Uncoupling of transcription and translation during zygotic gene activation in the mouse. EMBO J 1996; 15:5715-5725.

81. Bartolomei MS, Ferguson-Smith AC. Mammalian genomic imprinting. Cold Spring Harb Perspect Biol 2011; 3.

82. Strahl BD, Allis CD. The language of covalent histone modifications. Nature 2000; 403:41-45.

83. McGhee JD, Felsenfeld G. Nucleosome structure. Annu Rev Biochem 1980; 49:1115-1156.

84. Widom J. Toward a unified model of chromatin folding. Annu Rev Biophys Biophys Chem 1989; 18:365-395.

85. Fenley AT, Adams DA, Onufriev AV. Charge State of the Globular Histone Core Controls Stability of the Nucleosome. Biophysical Journal 2010; 99:1577-1585.

86. Murray K. The occurrence of epsilon-n-methyl lysine in histones. Biochemistry 1964; 3:10-15.

87. Gershey EL, Haslett GW, Vidali G, Allfrey VG. Chemical studies of histone methylation. Evidence for the occurrence of 3-methylhistidine in avian erythrocyte histone fractions. J Biol Chem 1969; 244:4871-4877.

88. Lee DY, Teyssier C, Strahl BD, Stallcup MR. Role of Protein Methylation in Regulation of Transcription. Endocrine Reviews 2005; 26:147-170.

89. Tse C, Sera T, Wolffe AP, Hansen JC. Disruption of higher-order folding by core histone acetylation dramatically enhances transcription of nucleosomal arrays by RNA polymerase III. Mol Cell Biol 1998; 18:4629-4638.

90. Annunziato AT, Frado LL, Seale RL, Woodcock CL. Treatment with sodium butyrate inhibits the complete condensation of interphase chromatin. Chromosoma 1988; 96:132-138.

91. Zhang Y. Transcriptional regulation by histone ubiquitination and deubiquitination. Genes & development 2003; 17:2733-2740.

92. Bradbury EM. Reversible histone modifications and the chromosome cell cycle. BioEssays 1992; 14:9-16.

93. Turner BM. Reading signals on the nucleosome with a new nomenclature for modified histones. Nat Struct Mol Biol 2005; 12:110-112.

94. Campos EI, Reinberg D. Histones: annotating chromatin. Annu Rev Genet 2009; 43:559-599.

95. Peterson CL, Laniel M-A. Histones and histone modifications. Current Biology 2004; 14:R546-R551.

96. Razin A, Riggs AD. DNA methylation and gene function. Science 1980; 210:604-610.

97. Lister R, Pelizzola M, Dowen RH, Hawkins RD, Hon G, Tonti-Filippini J, Nery JR, Lee L, Ye Z, Ngo QM, Edsall L, Antosiewicz-Bourget J, et al. Human DNA methylomes at base resolution show widespread epigenomic differences. Nature 2009; 462:315-322.

98. Bird AP. Use of restriction enzymes to study eukaryotic DNA methylation: II. The symmetry of methylated sites supports semi-conservative copying of the methylation pattern. J Mol Biol 1978; 118:49-60.

99. Johnson TB, Coghill RD. Researches in pyrimidines. C111. The discovery of 5-methyl-cytosine in tuberculinic acid, the nucleic acid if the tubercle bacillus1. Journal of the American Chemical Society 1925; 47:2838-2844.

100. Holliday R, Pugh JE. DNA Modification Mechanisms and Gene Activity during Development. Science 1975; 187:226-232.

101. Okano M, Bell DW, Haber DA, Li E. DNA Methyltransferases Dnmt3a and Dnmt3b Are Essential for De Novo Methylation and Mammalian Development. Cell 1999; 99:247-257.

102. Bestor T, Laudano A, Mattaliano R, Ingram V. Cloning and sequencing of a cDNA encoding DNA methyltransferase of mouse cells: The carboxyl-terminal domain of the mammalian enzymes is related to bacterial restriction methyltransferases. J Mol Biol 1988; 203:971-983.

103. Li E, Bestor TH, Jaenisch R. Targeted mutation of the DNA methyltransferase gene results in embryonic lethality. Cell 1992; 69:915-926.

104. Chiang PK, Gordon RK, Tal J, Zeng GC, Doctor BP, Pardhasaradhi K, McCann PP. S-Adenosylmethionine and methylation. The FASEB Journal 1996; 10:471-480.

105. Cantoni GL. THE NATURE OF THE ACTIVE METHYL DONOR FORMED ENZYMATICALLY FROM L-METHIONINE AND ADENOSINETRIPHOSPHATE1,2. Journal of the American Chemical Society 1952; 74:2942-2943.

106. Cheng X, Roberts RJ. AdoMet-dependent methylation, DNA methyltransferases and base flipping. Nucleic Acids Res 2001; 29:3784-3795.

107. Sharif J, Muto M, Takebayashi S-i, Suetake I, Iwamatsu A, Endo TA, Shinga J, Mizutani-Koseki Y, Toyoda T, Okamura K, Tajima S, Mitsuya K, et al. The SRA protein Np95 mediates epigenetic inheritance by recruiting Dnmt1 to methylated DNA. Nature 2007; 450:908-912.

108. Cirio MC, Ratnam S, Ding F, Reinhart B, Navara C, Chaillet JR. Preimplantation expression of the somatic form of Dnmt1 suggests a role in the inheritance of genomic imprints. BMC Dev Biol 2008; 8:9.

109. Bonfils C, Beaulieu N, Chan E, Cotton-Montpetit J, MacLeod AR. Characterization of the Human DNA Methyltransferase Splice Variant Dnmt1b. Journal of Biological Chemistry 2000; 275:10754-10760.

110. Mertineit C, Yoder JA, Taketo T, Laird DW, Trasler JM, Bestor TH. Sex-specific exons control DNA methyltransferase in mammalian germ cells. Development 1998; 125:889-897.

111. Okano M, Xie S, Li E. Cloning and characterization of a family of novel mammalian DNA (cytosine-5) methyltransferases. Nat Genet 1998; 19:219-220.

112. Kato Y, Kaneda M, Hata K, Kumaki K, Hisano M, Kohara Y, Okano M, Li E, Nozaki M, Sasaki H. Role of the Dnmt3 family in de novo methylation of

imprinted and repetitive sequences during male germ cell development in the mouse. Human Molecular Genetics 2007; 16:2272-2280.

113. Bourc'his D, Xu G-L, Lin C-S, Bollman B, Bestor TH. Dnmt3L and the Establishment of Maternal Genomic Imprints. Science 2001; 294:2536-2539.

114. Kaneda M, Hirasawa R, Chiba H, Okano M, Li E, Sasaki H. Genetic evidence for Dnmt3a-dependent imprinting during oocyte growth obtained by conditional knockout with Zp3-Cre and complete exclusion of Dnmt3b by chimera formation. Genes to Cells 2010; 15:169-179.

115. Jia D, Jurkowska RZ, Zhang X, Jeltsch A, Cheng X. Structure of Dnmt3a bound to Dnmt3L suggests a model for de novo DNA methylation. Nature 2007; 449:248-251.

116. Jurkowska RZ, Anspach N, Urbanke C, Jia D, Reinhardt R, Nellen W, Cheng X, Jeltsch A. Formation of nucleoprotein filaments by mammalian DNA methyltransferase Dnmt3a in complex with regulator Dnmt3L. Nucleic Acids Res 2008; 36:6656-6663.

117. Berger SL. The complex language of chromatin regulation during transcription. Nature 2007; 447:407-412.

118. Newell-Price J, Clark AJL, King P. DNA Methylation and Silencing of Gene Expression. Trends in Endocrinology & Metabolism 2000; 11:142-148.

119. Bird A. The essentials of DNA methylation. Cell 1992; 70:5-8.

120. Fujita N, Watanabe S, Ichimura T, Tsuruzoe S, Shinkai Y, Tachibana M, Chiba T, Nakao M. Methyl-CpG binding domain 1 (MBD1) interacts with the Suv39h1-HP1 heterochromatic complex for DNA methylation-based transcriptional repression. J Biol Chem 2003; 278:24132-24138.

121. Peters AHFM, O'Carroll D, Scherthan H, Mechtler K, Sauer S, Schöfer C, Weipoltshammer K, Pagani M, Lachner M, Kohlmaier A, Opravil S, Doyle M, et al. Loss of the Suv39h Histone Methyltransferases Impairs Mammalian Heterochromatin and Genome Stability. Cell 2001; 107:323-337.

122. Lachner M, O'Carroll D, Rea S, Mechtler K, Jenuwein T. Methylation of histone H3 lysine 9 creates a binding site for HP1 proteins. Nature 2001; 410:116-120.

123. Zhang Y, Ng H-H, Erdjument-Bromage H, Tempst P, Bird A, Reinberg D. Analysis of the NuRD subunits reveals a histone deacetylase core complex and a connection with DNA methylation. Genes & development 1999; 13:1924-1935.

124. Xue Y, Wong J, Moreno GT, Young MK, Côté J, Wang W. NURD, a Novel Complex with Both ATP-Dependent Chromatin-Remodeling and Histone Deacetylase Activities. Molecular Cell 1998; 2:851-861.

125. Tong JK, Hassig CA, Schnitzler GR, Kingston RE, Schreiber SL. Chromatin deacetylation by an ATP-dependent nucleosome remodelling complex. Nature 1998; 395:917-921.

126. Jones PL, Jan Veenstra GC, Wade PA, Vermaak D, Kass SU, Landsberger N, Strouboulis J, Wolffe AP. Methylated DNA and MeCP2 recruit histone deacetylase to repress transcription. Nat Genet 1998; 19:187-191.

127. Hendrich B, Bird A. Identification and Characterization of a Family of Mammalian Methyl-CpG Binding Proteins. Mol Cell Biol 1998; 18:6538-6547.

128. Hendrich B, Guy J, Ramsahoye B, Wilson VA, Bird A. Closely related proteins MBD2 and MBD3 play distinctive but interacting roles in mouse development. Genes & development 2001; 15:710-723.

129. Reese KJ, Lin S, Verona RI, Schultz RM, Bartolomei MS. Maintenance of paternal methylation and repression of the imprinted H19 gene requires MBD3. PLoS Genet 2007; 3:e137.

130. Brenet F, Moh M, Funk P, Feierstein E, Viale AJ, Socci ND, Scandura JM. DNA methylation of the first exon is tightly linked to transcriptional silencing. PLoS One 2011; 6:e14524.

131. Lyko F, Foret S, Kucharski R, Wolf S, Falckenhayn C, Maleszka R. The honey bee epigenomes: differential methylation of brain DNA in queens and workers. PLoS Biol 2010; 8:e1000506.

132. Maunakea AK, Nagarajan RP, Bilenky M, Ballinger TJ, D'Souza C, Fouse SD, Johnson BE, Hong C, Nielsen C, Zhao Y, Turecki G, Delaney A, et al. Conserved role of intragenic DNA methylation in regulating alternative promoters. Nature 2010; 466:253-257.

133. Yoder JA, Walsh CP, Bestor TH. Cytosine methylation and the ecology of intragenomic parasites. Trends in Genetics 1997; 13:335-340.

134. Walsh CP, Chaillet JR, Bestor TH. Transcription of IAP endogenous retroviruses is constrained by cytosine methylation. Nat Genet 1998; 20:116-117.

135. Santos F, Hendrich B, Reik W, Dean W. Dynamic Reprogramming of DNA Methylation in the Early Mouse Embryo. Developmental Biology 2002; 241:172-182.

136. Monk M, Boubelik M, Lehnert S. Temporal and regional changes in DNA methylation in the embryonic, extraembryonic and germ cell lineages during mouse embryo development. Development 1987; 99:371-382.

137. Monk M, Adams RL, Rinaldi A. Decrease in DNA methylase activity during preimplantation development in the mouse. Development 1991; 112:189-192.

138. Carlson LL, Page AW, Bestor TH. Properties and localization of DNA methyltransferase in preimplantation mouse embryos: implications for genomic imprinting. Genes & development 1992; 6:2536-2541.

139. Hajkova P, Jeffries SJ, Lee C, Miller N, Jackson SP, Surani MA. Genome-Wide Reprogramming in the Mouse Germ Line Entails the Base Excision Repair Pathway. Science 2010; 329:78-82.

140. Ginsburg M, Snow MH, McLaren A. Primordial germ cells in the mouse embryo during gastrulation. Development 1990; 110:521-528.

141. Anderson R, Copeland TK, Schöler H, Heasman J, Wylie C. The onset of germ cell migration in the mouse embryo. Mechanisms of Development 2000; 91:61-68.

142. Hajkova P, Erhardt S, Lane N, Haaf T, El-Maarri O, Reik W, Walter J, Surani MA. Epigenetic reprogramming in mouse primordial germ cells. Mechanisms of Development 2002; 117:15-23.

143. Gu TP, Guo F, Yang H, Wu HP, Xu GF, Liu W, Xie ZG, Shi L, He X, Jin SG, Iqbal K, Shi YG, et al. The role of Tet3 DNA dioxygenase in epigenetic reprogramming by oocytes. Nature 2011; 477:606-610.

144. Howell CY, Bestor TH, Ding F, Latham KE, Mertineit C, Trasler JM, Chaillet JR. Genomic Imprinting Disrupted by a Maternal Effect Mutation in the Dnmt1 Gene. Cell 2001; 104:829-838.

145. Kobayashi H, Sakurai T, Imai M, Takahashi N, Fukuda A, Yayoi O, Sato S, Nakabayashi K, Hata K, Sotomaru Y, Suzuki Y, Kono T. Contribution of intragenic DNA methylation in mouse gametic DNA methylomes to establish oocyte-specific heritable marks. PLoS Genet 2012; 8:e1002440.

146. Rai K, Huggins IJ, James SR, Karpf AR, Jones DA, Cairns BR. DNA Demethylation in Zebrafish Involves the Coupling of a Deaminase, a Glycosylase, and Gadd45. Cell 2008; 135:1201-1212.

147. Morgan HD, Dean W, Coker HA, Reik W, Petersen-Mahrt SK. Activation-induced Cytidine Deaminase Deaminates 5-Methylcytosine in DNA and Is Expressed in Pluripotent Tissues: IMPLICATIONS FOR EPIGENETIC REPROGRAMMING. Journal of Biological Chemistry 2004; 279:52353-52360.

148. Tahiliani M, Koh KP, Shen Y, Pastor WA, Bandukwala H, Brudno Y, Agarwal S, Iyer LM, Liu DR, Aravind L, Rao A. Conversion of 5-methylcytosine to 5-hydroxymethylcytosine in mammalian DNA by MLL partner TET1. Science 2009; 324:930-935.

149. Popp C, Dean W, Feng S, Cokus SJ, Andrews S, Pellegrini M, Jacobsen SE, Reik W. Genome-wide erasure of DNA methylation in mouse primordial germ cells is affected by AID deficiency. Nature 2010; 463:1101-1105.

150. Valinluck V, Sowers LC. Endogenous Cytosine Damage Products Alter the Site Selectivity of Human DNA Maintenance Methyltransferase DNMT1. Cancer Res 2007; 67:946-950.

151. Valinluck V, Tsai HH, Rogstad DK, Burdzy A, Bird A, Sowers LC. Oxidative damage to methyl-CpG sequences inhibits the binding of the methyl-CpG binding domain (MBD) of methyl-CpG binding protein 2 (MeCP2). Nucleic Acids Res 2004; 32:4100-4108.

152. Jin S-G, Kadam S, Pfeifer GP. Examination of the specificity of DNA methylation profiling techniques towards 5-methylcytosine and 5-hydroxymethylcytosine. Nucleic Acids Res 2010; 38:e125.

153. Boorstein RJ, Cummings A, Jr., Marenstein DR, Chan MK, Ma Y, Neubert TA, Brown SM, Teebor GW. Definitive identification of mammalian 5-hydroxymethyluracil DNA N-glycosylase activity as SMUG1. J Biol Chem 2001; 276:41991-41997.

154. Ito S, D'Alessio AC, Taranova OV, Hong K, Sowers LC, Zhang Y. Role of Tet proteins in 5mC to 5hmC conversion, ES-cell self-renewal and inner cell mass specification. Nature 2010; 466:1129-1133.

155. Nolte F, Hofmann WK. Myelodysplastic syndromes: molecular pathogenesis and genomic changes. Ann Hematol 2008; 87:777-795.

156. Tefferi A, Lim KH, Abdel-Wahab O, Lasho TL, Patel J, Patnaik MM, Hanson CA, Pardanani A, Gilliland DG, Levine RL. Detection of mutant TET2 in myeloid malignancies other than myeloproliferative neoplasms: CMML, MDS, MDS/MPN and AML. Leukemia 2009; 23:1343-1345.

157. Kosmider O, Gelsi-Boyer V, Cheok M, Grabar S, Della-Valle V, Picard F, Viguie F, Quesnel B, Beyne-Rauzy O, Solary E, Vey N, Hunault-Berger M, et al. TET2 mutation is an independent favorable prognostic factor in myelodysplastic syndromes (MDSs). Blood 2009; 114:3285-3291.

158. Smallwood SA, Tomizawa S, Krueger F, Ruf N, Carli N, Segonds-Pichon A, Sato S, Hata K, Andrews SR, Kelsey G. Dynamic CpG island methylation landscape in oocytes and preimplantation embryos. Nat Genet 2011; 43:811-814.

159. Oakes CC, La Salle S, Smiraglia DJ, Robaire B, Trasler JM. Developmental acquisition of genome-wide DNA methylation occurs prior to meiosis in male germ cells. Developmental Biology 2007; 307:368-379.

160. Hata K, Okano M, Lei H, Li E. Dnmt3L cooperates with the Dnmt3 family of de novo DNA methyltransferases to establish maternal imprints in mice. Development 2002; 129:1983-1993.

161. Seisenberger S, Andrews S, Krueger F, Arand J, Walter J, Santos F, Popp C, Thienpont B, Dean W, Reik W. The Dynamics of Genome-wide DNA Methylation Reprogramming in Mouse Primordial Germ Cells. Molecular Cell 2012; 48:849-862.

162. Obata Y, Kaneko-Ishino T, Koide T, Takai Y, Ueda T, Domeki I, Shiroishi T, Ishino F, Kono T. Disruption of primary imprinting during oocyte growth leads to the modified expression of imprinted genes during embryogenesis. Development 1998; 125:1553-1560.

163. Kaneda M, Okano M, Hata K, Sado T, Tsujimoto N, Li E, Sasaki H. Essential role for de novo DNA methyltransferase Dnmt3a in paternal and maternal imprinting. Nature 2004; 429:900-903.

164. Bourc'his D, Bestor TH. Meiotic catastrophe and retrotransposon reactivation in male germ cells lacking Dnmt3L. Nature 2004; 431:96-99.

165. Williamson CM, Blake A, Thomas S, Beechey CV, Hancock J, Cattanach BM, Peters J. World Wide Web Site - Mouse Imprinting Data and References. In, vol. 2013. Oxfordshire: MRC Harwell; 2013.

166. Morison IM, Paton CJ, Cleverley SD. The imprinted gene and parent-of-origin effect database. In, vol. 29(1), 2001 ed: Nucleic Acids Research; 2001: 275-276.

167. Luedi PP, Dietrich FS, Weidman JR, Bosko JM, Jirtle RL, Hartemink AJ. Computational and experimental identification of novel human imprinted genes. Genome Res 2007; 17:1723-1730.

168. McGrath J, Solter D. Completion of mouse embryogenesis requires both the maternal and paternal genomes. Cell 1984; 37:179-183.

169. Surani MAH, Barton SC, Norris ML. Development of reconstituted mouse eggs suggests imprinting of the genome during gametogenesis. Nature 1984; 308:548-550.

170. Surani MAH, Barton SC, Norris ML. Influence of parental chromosomes on spatial specificity in androgenetic [harr] parthenogenetic chimaeras in the mouse. Nature 1987; 326:395-397.

171. Cattanach BM, Kirk M. Differential activity of maternally and paternally derived chromosome regions in mice. Nature 1985; 315:496-498.

172. Lyon MF, Ward HC, Simpson GM. A genetic method for measuring non-disjunction in mice with Robertsonian translocations. Genet Res 1975; 26:283-295.

173. Searle AG, Beechey CV. Complementation studies with mouse translocations. Cytogenet Cell Genet 1978; 20:282-303.

174. Lyon MF, Glenister PH. Factors affecting the observed number of young resulting from adjacent-2 disjunction in mice carrying a translocation. Genet Res 1977; 29:83-92.

175. Johnson DR. Further observations on the haipin-tail (Thp) mutation in the mouse. Genet Res 1974; 24:207-213.

176. Barlow DP, Stoger R, Herrmann BG, Saito K, Schweifer N. The mouse insulin-like growth factor type-2 receptor is imprinted and closely linked to the Tme locus. Nature 1991; 349:84-87.

177. DeChiara TM, Robertson EJ, Efstratiadis A. Parental imprinting of the mouse insulin-like growth factor II gene. Cell 1991; 64:849-859.

178. Surani MA, Reik W, Allen ND. Transgenes as molecular probes for genomic imprinting. Trends Genet 1988; 4:59-62.

179. Bartolomei MS, Zemel S, Tilghman SM. Parental imprinting of the mouse H19 gene. Nature 1991; 351:153-155.

180. Ferguson-Smith AC, Cattanach BM, Barton SC, Beechey CV, Surani MA. Embryological and molecular investigations of parental imprinting on mouse chromosome 7. Nature 1991; 351:667-670.

181. Constancia M, Dean W, Lopes S, Moore T, Kelsey G, Reik W. Deletion of a silencer element in Igf2 results in loss of imprinting independent of H19. Nat Genet 2000; 26:203-206.

182. Froesch ER, xFc, rgi H, Ramseier EB, Bally P, Labhart A. Antibody-suppressible and nonsuppressible insulin-like activities in human serum and their physiologic significance. An insulin assay with adipose tissue of increased precision and specificity*. J Clin Invest 1963; 42:1816-1834.

183. Rinderknecht E, Humbel RE. Amino-terminal sequences of two polypeptides from human serum with nonsuppressible insulin-like and cell-growth-promoting activities: evidence for structural homology with insulin B chain. Proc Natl Acad Sci U S A 1976; 73:4379-4381.

184. Zapf J, Froesch ER. Insulin-like growth factors/somatomedins: structure, secretion, biological actions and physiological role. Horm Res 1986; 24:121-130.

185. Daughaday WH, Rotwein P. Insulin-Like Growth Factors I and II. Peptide, Messenger Ribonucleic Acid and Gene Structures, Serum, and Tissue Concentrations. Endocrine Reviews 1989; 10:68-91.

186. Adashi EY, Resnick CE, D'Ercole AJ, Svoboda ME, Wyk JJV. Insulin-Like Growth Factors as Intraovarian Regulators of Granulosa Cell Growth and Function. Endocrine Reviews 1985; 6:400-420.

187. Kamada S, Kubota T, Taguchi M, Ho WR, Sakamoto S, Aso T. Effects of insulin-like growth factor-II on proliferation and differentiation of ovarian granulosa cells. Horm Res 1992; 37:141-149.

188. Baxter RC. The insulin-like growth factors and their binding proteins. Comp Biochem Physiol B 1988; 91:229-235.

189. White MF. Regulating insulin signaling and β-cell function through IRS proteinsThis paper is one of a selection of papers published in this Special Issue, entitled Second Messengers and Phosphoproteins—12th International Conference. Canadian Journal of Physiology and Pharmacology 2006; 84:725-737.

190. Wilson EM, Hsieh MM, Rotwein P. Autocrine Growth Factor Signaling by Insulin-like Growth Factor-II Mediates MyoD-stimulated Myocyte Maturation. Journal of Biological Chemistry 2003; 278:41109-41113.

191. Wilson EM, Rotwein P. Control of MyoD Function during Initiation of Muscle Differentiation by an Autocrine Signaling Pathway Activated by Insulin-like Growth Factor-II. Journal of Biological Chemistry 2006; 281:29962-29971.

192. Minuto F, Palermo C, Arvigo M, Barreca AM. The IGF system and bone. J Endocrinol Invest 2005; 28:8-10.

193. Soares MB, Turken A, Ishii D, Mills L, Episkopou V, Cotter S, Zeitlin S, Efstratiadis A. Rat insulin-like growth factor II gene. A single gene with two promoters expressing a multitranscript family. J Mol Biol 1986; 192:737-752.

194. Sussenbach JS. The gene structure of the insulin-like growth factor family. Prog Growth Factor Res 1989; 1:33-48.

195. Ueno T, Takahashi K, Matsuguchi T, Endo H, Yamamoto M. A new leader exon identified in the rat insulin-like growth factor II gene. Biochem Biophys Res Commun 1987; 148:344-349.

196. Yaseen M, Wrenzycki C, Herrmann D, Carnwath J, Niemann H. Changes in the relative abundance of mRNA transcripts for insulin-like growth factor (IGF-I and IGF-II) ligands and their receptors (IGF-IR/IGF-IIR) in preimplantation bovine embryos derived from different in vitro systems. Reproduction 2001; 122:601-610.

197. Chao W, D'Amore PA. IGF2: Epigenetic regulation and role in development and disease. Cytokine & Growth Factor Reviews 2008; 19:111-120.

198. Hansen TV, Hammer NA, Nielsen J, Madsen M, Dalbaeck C, Wewer UM, Christiansen J, Nielsen FC. Dwarfism and impaired gut development in insulin-like growth factor II mRNA-binding protein 1-deficient mice. Mol Cell Biol 2004; 24:4448-4464.

199. Nielsen J, Christiansen J, Lykke-Andersen J, Johnsen AH, Wewer UM, Nielsen FC. A Family of Insulin-Like Growth Factor II mRNA-Binding Proteins Represses Translation in Late Development. Mol Cell Biol 1999; 19:1262-1270.

200. Burns JL, Hassan AB. Cell survival and proliferation are modified by insulin-like growth factor 2 between days 9 and 10 of mouse gestation. Development 2001; 128:3819-3830.

201. Nissley P, Lopaczynski W. Insulin-like growth factor receptors. Growth Factors 1991; 5:29-43.

202. LeRoith D, Werner H, Beitner-Johnson D, Roberts Jr CT. Molecular and Cellular Aspects of the Insulin-Like Growth Factor I Receptor. Endocrine Reviews 1995; 16:143-163.

203. Denley A, Cosgrove LJ, Booker GW, Wallace JC, Forbes BE. Molecular interactions of the IGF system. Cytokine & Growth Factor Reviews 2005; 16:421-439.

204. Stylianopoulou F, Herbert J, Soares MB, Efstratiadis A. Expression of the insulin-like growth factor II gene in the choroid plexus and the leptomeninges of the adult rat central nervous system. Proc Natl Acad Sci U S A 1988; 85:141-145.

205. Vu TH, Hoffman AR. Promoter-specific imprinting of the human insulin-like growth factor-II gene. Nature 1994; 371:714-717.

206. Lee JE, Pintar J, Efstratiadis A. Pattern of the insulin-like growth factor II gene expression during early mouse embryogenesis. Development (Cambridge, England) 1990; 110:151-159.

207. Stylianopoulou F, Efstratiadis A, Herbert J, Pintar J. Pattern of the insulin-like growth factor II gene expression during rat embryogenesis. Development 1988; 103:497-506.

208. Latham KE, Doherty AS, Scott CD, Schultz RM. Igf2r and Igf2 gene expression in androgenetic, gynogenetic, and parthenogenetic preimplantation mouse embryos: absence of regulation by genomic imprinting. Genes & development 1994; 8:290-299.

209. DeChiara TM, Efstratiadis A, Robertson EJ. A growth-deficiency phenotype in heterozygous mice carrying an insulin-like growth factor II gene disrupted by targeting. Nature 1990; 345:78-80.

210. Brunkow ME, Tilghman SM. Ectopic expression of the H19 gene in mice causes prenatal lethality. Genes Dev 1991; 5:1092-1101.

211. Pachnis V, Brannan CI, Tilghman SM. The structure and expression of a novel gene activated in early mouse embryogenesis. EMBO J 1988; 7:673-681.

212. Pachnis V, Belayew A, Tilghman SM. Locus unlinked to alpha-fetoprotein under the control of the murine raf and Rif genes. Proceedings of the National Academy of Sciences 1984; 81:5523-5527.

213. Davis RL, Weintraub H, Lassar AB. Expression of a single transfected cDNA converts fibroblasts to myoblasts. Cell 1987; 51:987-1000.

214. Poirier F, Chan CT, Timmons PM, Robertson EJ, Evans MJ, Rigby PW. The murine H19 gene is activated during embryonic stem cell differentiation in vitro and at the time of implantation in the developing embryo. Development 1991; 113:1105-1114.

215. Brannan CI, Dees EC, Ingram RS, Tilghman SM. The product of the H19 gene may function as an RNA. Mol Cell Biol 1990; 10:28-36.

216. Hao Y, Crenshaw T, Moulton T, Newcomb E, Tycko B. Tumour-suppressor activity of H19 RNA. Nature 1993; 365:764-767.

217. Yoshimizu T, Miroglio A, Ripoche M-A, Gabory A, Vernucci M, Riccio A, Colnot S, Godard C, Terris B, Jammes H, Dandolo L. The H19 locus acts in vivo as a tumor suppressor. Proceedings of the National Academy of Sciences of the United States of America 2008; 105:12417-12422.

218. Bartolomei MS, Webber AL, Brunkow ME, Tilghman SM. Epigenetic mechanisms underlying the imprinting of the mouse H19 gene. Genes Dev 1993; 7:1663-1673.

219. Zemel S, Bartolomei MS, Tilghman SM. Physical linkage of two mammalian imprinted genes, H19 and insulin-like growth factor 2. Nat Genet 1992; 2:61-65.

220. Leibovitch MP, Nguyen VC, Gross MS, Solhonne B, Leibovitch SA, Bernheim A. The human ASM (adult skeletal muscle) gene: expression and chromosomal assignment to 11p15. Biochem Biophys Res Commun 1991; 180:1241-1250.

221. Okazaki Y FM, Kasukawa T, Adachi J, Bono H, Kondo S, Nikaido I, Osato N, Saito R, Suzuki H, Yamanaka I, Kiyosawa H, Yagi K, Tomaru Y, Hasegawa Y, Nogami A, Schönbach C, Gojobori T, Baldarelli R, Hill DP, Bult C, Hume DA, Quackenbush J, Schriml LM, Kanapin A, Matsuda H, Batalov S, Beisel KW, Blake JA, Bradt D, Brusic V, Chothia C, Corbani LE, Cousins S, Dalla E, Dragani TA, Fletcher CF, Forrest A, Frazer KS, Gaasterland T, Gariboldi M, Gissi C, Godzik A, Gough J, Grimmond S, Gustincich S, Hirokawa N, Jackson IJ, Jarvis ED, Kanai A, Kawaji H, Kawasawa Y, Kedzierski RM, King BL, Konagaya A, Kurochkin IV, Lee Y, Lenhard B, Lyons PA, Maglott DR, Maltais L, Marchionni L, McKenzie L, Miki H, Nagashima T, Numata K, Okido T, Pavan WJ, Pertea G, Pesole G, Petrovsky N, Pillai R, Pontius JU, Qi D, Ramachandran S, Ravasi T, Reed JC, Reed DJ, Reid J, Ring BZ, Ringwald M, Sandelin A, Schneider C, Semple CA, Setou M, Shimada K, Sultana R, Takenaka Y, Taylor MS, Teasdale RD, Tomita M, Verardo R, Wagner L, Wahlestedt C, Wang Y, Watanabe Y, Wells C, Wilming LG, Wynshaw-Boris A, Yanagisawa M, Yang I, Yang L, Yuan Z, Zavolan M, Zhu Y, Zimmer A, Carninci P, Hayatsu N, Hirozane-Kishikawa T, Konno H, Nakamura M, Sakazume N, Sato K, Shiraki T, Waki K, Kawai J, Aizawa K, Arakawa T, Fukuda S, Hara A, Hashizume W, Imotani K, Ishii Y, Itoh M, Kagawa I, Miyazaki A, Sakai K, Sasaki D, Shibata K, Shinagawa A, Yasunishi A, Yoshino M, Waterston R, Lander ES, Rogers J, Birney E, Hayashizaki Y; FANTOM Consortium; RIKEN Genome Exploration Research Group Phase I & II Team. Analysis of the mouse transcriptome based on functional annotation of 60,770 full-length cDNAs. Nature 2002; 420:563-573.

222. Doherty AS, Mann MR, Tremblay KD, Bartolomei MS, Schultz RM. Differential effects of culture on imprinted H19 expression in the preimplantation mouse embryo. Biol Reprod 2000; 62:1526-1535.

223. Verona RI, Mann MR, Bartolomei MS. Genomic imprinting: intricacies of epigenetic regulation in clusters. Annu Rev Cell Dev Biol 2003; 19:237-259.

224. Paulsen M, El-Maarri O, Engemann S, Strödicke M, Franck O, Davies K, Reinhardt R, Reik W, Walter J. Sequence conservation and variability of

imprinting in the Beckwith–Wiedemann syndrome gene cluster in human and mouse. Human Molecular Genetics 2000; 9:1829-1841.

225. Bartolomei MS, Tilghman SM. Genomic imprinting in mammals. Annu Rev Genet 1997; 31:493-525.

226. Tremblay KD, Saam JR, Ingram RS, Tilghman SM, Bartolomei MS. A paternal-specific methylation imprint marks the alleles of the mouse H19 gene. Nat Genet 1995; 9:407-413.

227. Kim J-M, Ogura A. Changes in allele-specific association of histone modifications at the imprinting control regions during mouse preimplantation development. genesis 2009; 47:611-616.

228. Leighton PA, Saam JR, Ingram RS, Stewart CL, Tilghman SM. An enhancer deletion affects both H19 and Igf2 expression. Genes Dev 1995; 9:2079-2089.

229. Yoo-Warren H, Pachnis V, Ingram RS, Tilghman SM. Two regulatory domains flank the mouse H19 gene. Mol Cell Biol 1988; 8:4707-4715.

230. Kaffer CR, Grinberg A, Pfeifer K. Regulatory mechanisms at the mouse Igf2/H19 locus. Mol Cell Biol 2001; 21:8189-8196.

231. Davis TL, Trasler JM, Moss SB, Yang GJ, Bartolomei MS. Acquisition of theH19Methylation Imprint Occurs Differentially on the Parental Alleles during Spermatogenesis. Genomics 1999; 58:18-28.

232. Ueda T, Abe K, Miura A, Yuzuriha M, Zubair M, Noguchi M, Niwa K, Kawase Y, Kono T, Matsuda Y, Fujimoto H, Shibata H, et al. The paternal methylation imprint of the mouse H19 locus is acquired in the gonocyte stage during foetal testis development. Genes to Cells 2000; 5:649-659.

233. Davis TL, Yang GJ, McCarrey JR, Bartolomei MS. The H19 methylation imprint is erased and re-established differentially on the parental alleles during male germ cell development. Hum Mol Genet 2000; 9:2885-2894.

234. Ferguson-Smith AC, Sasaki H, Cattanach BM, Surani MA. Parental-origin-specific epigenetic modification of the mouse H19 gene. Nature 1993; 362:751-755.

235. Tremblay KD, Duran KL, Bartolomei MS. A 5' 2-kilobase-pair region of the imprinted mouse H19 gene exhibits exclusive paternal methylation throughout development. Mol Cell Biol 1997; 17:4322-4329.

236. Thorvaldsen JL, Mann MR, Nwoko O, Duran KL, Bartolomei MS. Analysis of sequence upstream of the endogenous H19 gene reveals elements both essential and dispensable for imprinting. Mol Cell Biol 2002; 22:2450-2462.

237. Bell AC, West AG, Felsenfeld G. The Protein CTCF Is Required for the Enhancer Blocking Activity of Vertebrate Insulators. Cell 1999; 98:387-396.

238. Engel N, Thorvaldsen JL, Bartolomei MS. CTCF binding sites promote transcription initiation and prevent DNA methylation on the maternal allele at the imprinted H19/Igf2 locus. Hum Mol Genet 2006; 15:2945-2954.

239. Nikolaev LG, Akopov SB, Didych DA, Sverdlov ED. Vertebrate Protein CTCF and its Multiple Roles in a Large-Scale Regulation of Genome Activity. Curr Genomics 2009; 10:294-302.

240. Bell AC, Felsenfeld G. Methylation of a CTCF-dependent boundary controls imprinted expression of the Igf2 gene. Nature 2000; 405:482-485.

241. Engel N, Raval AK, Thorvaldsen JL, Bartolomei SM. Three-dimensional conformation at the H19/Igf2 locus supports a model of enhancer tracking. Human Molecular Genetics 2008; 17:3021-3029.

242. Kurukuti S, Tiwari VK, Tavoosidana G, Pugacheva E, Murrell A, Zhao Z, Lobanenkov V, Reik W, Ohlsson R. CTCF binding at the H19 imprinting control region mediates maternally inherited higher-order chromatin conformation to restrict enhancer access to Igf2. Proc Natl Acad Sci U S A 2006; 103:10684-10689.

243. Leighton PA, Ingram RS, Eggenschwiler J, Efstratiadis A, Tilghman SM. Disruption of imprinting caused by deletion of the H19 gene region in mice. Nature 1995; 375:34-39.

244. Ainscough JF, John RM, Barton SC, Surani MA. A skeletal muscle-specific mouse Igf2 repressor lies 40 kb downstream of the gene. Development 2000; 127:3923-3930.

245. Eden S, Constancia M, Hashimshony T, Dean W, Goldstein B, Johnson AC, Keshet I, Reik W, Cedar H. An upstream repressor element plays a role in Igf2 imprinting. EMBO J 2001; 20:3518-3525.

246. Reik W, Constancia M, Dean W, Davies K, Bowden L, Murrell A, Feil R, Walter J, Kelsey G. Igf2 imprinting in development and disease. Int J Dev Biol 2000; 44:145-150.

247. Mattick JS. Non-coding RNAs: the architects of eukaryotic complexity. EMBO Rep 2001; 2:986-991.

248. Fitzpatrick GV, Soloway PD, Higgins MJ. Regional loss of imprinting and growth deficiency in mice with a targeted deletion of KvDMR1. Nat Genet 2002; 32:426-431.

249. Penny GD, Kay GF, Sheardown SA, Rastan S, Brockdorff N. Requirement for Xist in X chromosome inactivation. Nature 1996; 379:131-137.

250. Pal-Bhadra M, Bhadra U, Birchler JA. Cosuppression of Nonhomologous Transgenes in Drosophila Involves Mutually Related Endogenous Sequences. Cell 1999; 99:35-46.

251. Hamilton AJ, Baulcombe DC. A species of small antisense RNA in posttranscriptional gene silencing in plants. Science 1999; 286:950-952.

252. Elbashir SM, Lendeckel W, Tuschl T. RNA interference is mediated by 21- and 22-nucleotide RNAs. Genes Dev 2001; 15:188-200.

253. Hamilton A, Voinnet O, Chappell L, Baulcombe D. Two classes of short interfering RNA in RNA silencing. EMBO J 2002; 21:4671-4679.

254. Lee RC, Feinbaum RL, Ambros V. The C. elegans heterochronic gene lin-4 encodes small RNAs with antisense complementarity to lin-14. Cell 1993; 75:843-854.

255. Ambros V, Lee RC, Lavanway A, Williams PT, Jewell D. MicroRNAs and Other Tiny Endogenous RNAs in C. elegans. Current Biology 2003; 13:807-818.

256. Saito K, Nishida KM, Mori T, Kawamura Y, Miyoshi K, Nagami T, Siomi H, Siomi MC. Specific association of Piwi with rasiRNAs derived from retrotransposon and heterochromatic regions in the Drosophila genome. Genes Dev 2006; 20:2214-2222.

257. Grivna ST, Beyret E, Wang Z, Lin H. A novel class of small RNAs in mouse spermatogenic cells. Genes Dev 2006; 20:1709-1714.

258. Koerner MV, Pauler FM, Huang R, Barlow DP. The function of non-coding RNAs in genomic imprinting. Development (Cambridge, England) 2009; 136:1771-1783.

259. Ideraabdullah FY, Vigneau S, Bartolomei MS. Genomic imprinting mechanisms in mammals. Mutation Research/Fundamental and Molecular Mechanisms of Mutagenesis 2008; 647:77-85.

260. Mancini-Dinardo D, Steele SJ, Levorse JM, Ingram RS, Tilghman SM. Elongation of the Kcnq1ot1 transcript is required for genomic imprinting of neighboring genes. Genes Dev 2006; 20:1268-1282.

261. Lee MP, DeBaun MR, Mitsuya K, Galonek HL, Brandenburg S, Oshimura M, Feinberg AP. Loss of imprinting of a paternally expressed transcript, with antisense orientation to KVLQT1, occurs frequently in Beckwith-Wiedemann syndrome and is independent of insulin-like growth factor II imprinting. Proc Natl Acad Sci U S A 1999; 96:5203-5208.

262. Terranova R, Yokobayashi S, Stadler MB, Otte AP, van Lohuizen M, Orkin SH, Peters AHFM. Polycomb Group Proteins Ezh2 and Rnf2 Direct Genomic

Contraction and Imprinted Repression in Early Mouse Embryos. Developmental Cell 2008; 15:668-679.

263. Pandey RR, Mondal T, Mohammad F, Enroth S, Redrup L, Komorowski J, Nagano T, Mancini-Dinardo D, Kanduri C, Biologiska s, Institutionen för cell- och m, Uppsala u, et al. Kcnq1ot1 antisense noncoding RNA mediates lineage-specific transcriptional silencing through chromatin-level regulation. Molecular Cell 2008; 32:232-246.

264. Muller J. Transcriptional silencing by the Polycomb protein in Drosophila embryos. EMBO J 1995; 14:1209-1220.

265. Simon J. Locking in stable states of gene expression: transcriptional control during Drosophila development. Curr Opin Cell Biol 1995; 7:376-385.

266. Margueron R, Reinberg D. The Polycomb complex PRC2 and its mark in life. Nature 2011; 469:343-349.

267. Lin YW, Chen HM, Fang JY. Gene silencing by the Polycomb group proteins and associations with cancer. Cancer Invest 2011; 29:187-195.

268. Lewis A, Green K, Dawson C, Redrup L, Huynh KD, Lee JT, Hemberger M, Reik W. Epigenetic dynamics of the Kcnq1 imprinted domain in the early embryo. Development 2006; 133:4203-4210.

269. Lewis A, Mitsuya K, Umlauf D, Smith P, Dean W, Walter J, Higgins M, Feil R, Reik W. Imprinting on distal chromosome 7 in the placenta involves repressive histone methylation independent of DNA methylation. Nat Genet 2004; 36:1291-1295.

270. Umlauf D, Goto Y, Cao R, Cerqueira F, Wagschal A, Zhang Y, Feil R. Imprinting along the Kcnq1 domain on mouse chromosome 7 involves repressive histone methylation and recruitment of Polycomb group complexes. Nat Genet 2004; 36:1296-1300.

271. Mikkelsen TS, Ku M, Jaffe DB, Issac B, Lieberman E, Giannoukos G, Alvarez P, Brockman W, Kim TK, Koche RP, Lee W, Mendenhall E, et al. Genome-wide

maps of chromatin state in pluripotent and lineage-committed cells. Nature 2007; 448:553-560.

272. Yatsuki H, Joh K, Higashimoto K, Soejima H, Arai Y, Wang Y, Hatada I, Obata Y, Morisaki H, Zhang Z, Nakagawachi T, Satoh Y, et al. Domain regulation of imprinting cluster in Kip2/Lit1 subdomain on mouse chromosome 7F4/F5: large-scale DNA methylation analysis reveals that DMR-Lit1 is a putative imprinting control region. Genome Res 2002; 12:1860-1870.

273. Ueda T, Yamazaki K, Suzuki R, Fujimoto H, Sasaki H, Sakaki Y, Higashinakagawa T. Parental methylation patterns of a transgenic locus in adult somatic tissues are imprinted during gametogenesis. Development 1992; 116:831-839.

274. Lucifero D, Mann MRW, Bartolomei MS, Trasler JM. Gene-specific timing and epigenetic memory in oocyte imprinting. Human Molecular Genetics 2004; 13:839-849.

275. Chotalia M, Smallwood SA, Ruf N, Dawson C, Lucifero D, Frontera M, James K, Dean W, Kelsey G. Transcription is required for establishment of germline methylation marks at imprinted genes. Genes & development 2009; 23:105-117.

276. Kobayashi H, Suda C, Abe T, Kohara Y, Ikemura T, Sasaki H. Bisulfite sequencing and dinucleotide content analysis of 15 imprinted mouse differentially methylated regions (DMRs): paternally methylated DMRs contain less CpGs than maternally methylated DMRs. Cytogenetic and Genome Research 2006; 113:130-137.

277. Tomizawa S-i, Kobayashi H, Watanabe T, Andrews S, Hata K, Kelsey G, Sasaki H. Dynamic stage-specific changes in imprinted differentially methylated regions during early mammalian development and prevalence of non-CpG methylation in oocytes. Development 2011; 138:811-820.

278. Woodfine K, Huddleston JE, Murrell A. Quantitative analysis of DNA methylation at all human imprinted regions reveals preservation of epigenetic stability in adult somatic tissue. Epigenetics Chromatin 2011; 4:1.

279. Kobayashi H, Yamada K, Morita S, Hiura H, Fukuda A, Kagami M, Ogata T, Hata K, Sotomaru Y, Kono T. Identification of the mouse paternally expressed

imprinted gene Zdbf2 on chromosome 1 and its imprinted human homolog ZDBF2 on chromosome 2. Genomics 2009; 93:461-472.

280. Hiura H, Obata Y, Komiyama J, Shirai M, Kono T. Oocyte growth-dependent progression of maternal imprinting in mice. Genes to Cells 2006; 11:353-361.

281. Xu G-L, Bestor TH, Bourc'his D, Hsieh C-L, Tommerup N, Bugge M, Hulten M, Qu X, Russo JJ, Viegas-Pequignot E. Chromosome instability and immunodeficiency syndrome caused by mutations in a DNA methyltransferase gene. Nature 1999; 402:187-191.

282. Ooi SKT, Qiu C, Bernstein E, Li K, Jia D, Yang Z, Erdjument-Bromage H, Tempst P, Lin S-P, Allis CD, Cheng X, Bestor TH. DNMT3L connects unmethylated lysine 4 of histone H3 to de novo methylation of DNA. Nature 2007; 448:714-717.

283. Ciccone DN, Su H, Hevi S, Gay F, Lei H, Bajko J, Xu G, Li E, Chen T. KDM1B is a histone H3K4 demethylase required to establish maternal genomic imprints. Nature 2009; 461:415-418.

284. Dennis K, Fan T, Geiman T, Yan Q, Muegge K. Lsh, a member of the SNF2 family, is required for genome-wide methylation. Genes & development 2001; 15:2940-2944.

285. Fan T, Hagan JP, Kozlov SV, Stewart CL, Muegge K. Lsh controls silencing of the imprinted Cdkn1c gene. Development 2005; 132:635-644.

286. Mager J, Montgomery ND, de Villena FP-M, Magnuson T. Genome imprinting regulated by the mouse Polycomb group protein Eed. Nat Genet 2003; 33:502-507.

287. Monk D, Wagschal A, Arnaud P, Muller PS, Parker-Katiraee L, Bourc'his D, Scherer SW, Feil R, Stanier P, Moore GE. Comparative analysis of human chromosome 7q21 and mouse proximal chromosome 6 reveals a placental-specific imprinted gene, TFPI2/Tfpi2, which requires EHMT2 and EED for allelic-silencing. Genome Res 2008; 18:1270-1281.

288. Xin Z, Tachibana M, Guggiari M, Heard E, Shinkai Y, Wagstaff J. Role of Histone Methyltransferase G9a in CpG Methylation of the Prader-Willi Syndrome Imprinting Center. Journal of Biological Chemistry 2003; 278:14996-15000.

289. Olek A, Walter J. The pre-implantation ontogeny of the H19 methylation imprint. Nat Genet 1997; 17:275-276.

290. Nakamura T, Arai Y, Umehara H, Masuhara M, Kimura T, Taniguchi H, Sekimoto T, Ikawa M, Yoneda Y, Okabe M, Tanaka S, Shiota K, et al. PGC7/Stella protects against DNA demethylation in early embryogenesis. Nat Cell Biol 2007; 9:64-71.

291. Nakamura T, Liu Y-J, Nakashima H, Umehara H, Inoue K, Matoba S, Tachibana M, Ogura A, Shinkai Y, Nakano T. PGC7 binds histone H3K9me2 to protect against conversion of 5mC to 5hmC in early embryos. Nature 2012; 486:415-419.

292. Hirasawa R, Chiba H, Kaneda M, Tajima S, Li E, Jaenisch R, Sasaki H. Maternal and zygotic Dnmt1 are necessary and sufficient for the maintenance of DNA methylation imprints during preimplantation development. Genes & development 2008; 22:1607-1616.

293. Li X, Ito M, Zhou F, Youngson N, Zuo X, Leder P, Ferguson-Smith AC. A Maternal-Zygotic Effect Gene, Zfp57, Maintains Both Maternal and Paternal Imprints. Developmental Cell 2008; 15:547-557.

294. Ayyanathan K, Lechner MS, Bell P, Maul GG, Schultz DC, Yamada Y, Tanaka K, Torigoe K, Rauscher FJ. Regulated recruitment of HP1 to a euchromatic gene induces mitotically heritable, epigenetic gene silencing: a mammalian cell culture model of gene variegation. Genes & development 2003; 17:1855-1869.

295. Lehnertz B, Ueda Y, Derijck AAHA, Braunschweig U, Perez-Burgos L, Kubicek S, Chen T, Li E, Jenuwein T, Peters AHFM. Suv39h-Mediated Histone H3 Lysine 9 Methylation Directs DNA Methylation to Major Satellite Repeats at Pericentric Heterochromatin. Current Biology 2003; 13:1192-1200.

296. Green K, Lewis A, Dawson C, Dean W, Reinhart B, Chaillet JR, Reik W. A developmental window of opportunity for imprinted gene silencing mediated by DNA methylation and the Kcnq1ot1 noncoding RNA. Mamm Genome 2007; 18:32-42.

297. Li E, Beard C, Jaenisch R. Role for DNA methylation in genomic imprinting. Nature 1993; 366:362-365.

298. Caspary T, Cleary MA, Baker CC, Guan X-J, Tilghman SM. Multiple Mechanisms Regulate Imprinting of the Mouse Distal Chromosome 7 Gene Cluster. Mol Cell Biol 1998; 18:3466-3474.

299. Sasaki H, Ferguson-Smith AC, Shum AS, Barton SC, Surani MA. Temporal and spatial regulation of H19 imprinting in normal and uniparental mouse embryos. Development 1995; 121:4195-4202.

300. Moore T, Constancia M, Zubair M, Bailleul B, Feil R, Sasaki H, Reik W. Multiple imprinted sense and antisense transcripts, differential methylation and tandem repeats in a putative imprinting control region upstream of mouse Igf2. Proceedings of the National Academy of Sciences 1997; 94:12509-12514.

301. Lopes S, Lewis A, Hajkova P, Dean W, Oswald J, Forne T, Murrell A, Constancia M, Bartolomei M, Walter J, Reik W. Epigenetic modifications in an imprinting cluster are controlled by a hierarchy of DMRs suggesting long-range chromatin interactions. Hum Mol Genet 2003; 12:295-305.

302. John RM, Hodges M, Little P, Barton SC, Surani MA. A human p57(KIP2) transgene is not activated by passage through the maternal mouse germline. Hum Mol Genet 1999; 8:2211-2219.

303. Bhogal B, Arnaudo A, Dymkowski A, Best A, Davis TL. Methylation at mouse Cdkn1c is acquired during postimplantation development and functions to maintain imprinted expression. Genomics 2004; 84:961-970.

304. Sasaki H, Allen ND, Surani MA. DNA methylation and genomic imprinting in mammals. EXS 1993; 64:469-486.

305. Feil R, Walter J, Allen ND, Reik W. Developmental control of allelic methylation in the imprinted mouse Igf2 and H19 genes. Development 1994; 120:2933-2943.

306. John RM, Lefebvre L. Developmental regulation of somatic imprints. Differentiation 2011; 81:270-280.

307. Brandeis M, Kafri T, Ariel M, Chaillet JR, McCarrey J, Razin A, Cedar H. The ontogeny of allele-specific methylation associated with imprinted genes in the mouse. EMBO J 1993; 12:3669-3677.

308. Chen M, Wang J, Dickerson KE, Kelleher J, Xie T, Gupta D, Lai EW, Pacak K, Gavrilova O, Weinstein LS. Central Nervous System Imprinting of the G Protein Gsα and Its Role in Metabolic Regulation. Cell Metabolism 2009; 9:548-555.

309. Li L-L, Keverne EB, Aparicio SA, Ishino F, Barton SC, Surani MA. Regulation of Maternal Behavior and Offspring Growth by Paternally Expressed Peg3. Science 1999; 284:330-334.

310. Lefebvre L, Viville S, Barton SC, Ishino F, Keverne EB, Surani MA. Abnormal maternal behaviour and growth retardation associated with loss of the imprinted gene Mest. Nat Genet 1998; 20:163-169.

311. Surani MA, Kothary R, Allen ND, Singh PB, Fundele R, Ferguson-Smith AC, Barton SC. Genome imprinting and development in the mouse. Dev Suppl 1990:89-98.

312. Surani MAH, Barton SC. Development of Gynogenetic Eggs in the Mouse: Implications for Parthenogenetic Embryos. Science 1983; 222:1034-1036.

313. Kono T, Obata Y, Yoshimzu T, Nakahara T, Carroll J. Epigenetic modifications during oocyte growth correlates with extended parthenogenetic development in the mouse. Nat Genet 1996; 13:91-94.

314. Kono T, Obata Y, Wu Q, Niwa K, Ono Y, Yamamoto Y, Park ES, Seo J-S, Ogawa H. Birth of parthenogenetic mice that can develop to adulthood. Nature 2004; 428:860-864.

315. Lin S-P, Youngson N, Takada S, Seitz H, Reik W, Paulsen M, Cavaille J, Ferguson-Smith AC. Asymmetric regulation of imprinting on the maternal and paternal chromosomes at the Dlk1-Gtl2 imprinted cluster on mouse chromosome 12. Nat Genet 2003; 35:97-102.

316. Schmidt JV, Matteson PG, Jones BK, Guan X-J, Tilghman SM. The Dlk1 and Gtl2 genes are linked and reciprocally imprinted. Genes & development 2000; 14:1997-2002.

317. Kawahara M, Wu Q, Takahashi N, Morita S, Yamada K, Ito M, Ferguson-Smith AC, Kono T. High-frequency generation of viable mice from engineered bi-maternal embryos. Nat Biotech 2007; 25:1045-1050.

318. Kawahara M, Obata Y, Sotomaru Y, Shimozawa N, Bao S, Tsukadaira T, Fukuda A, Kono T. Protocol for the production of viable bimaternal mouse embryos. Nat. Protocols 2008; 3:197-209.

319. Horsthemke B, Wagstaff J. Mechanisms of imprinting of the Prader–Willi/Angelman region. American Journal of Medical Genetics Part A 2008; 146A:2041-2052.

320. Weksberg R, Shuman C, Smith AC. Beckwith–Wiedemann syndrome. American Journal of Medical Genetics Part C: Seminars in Medical Genetics 2005; 137C:12-23.

321. Williams CA, Zori RT, Hendrickson J, Stalker H, Marum T, Whidden E, Driscoll DJ. Angelman syndrome. Curr Probl Pediatr 1995; 25:216-231.

322. Kishino T, Lalande M, Wagstaff J. UBE3A/E6-AP mutations cause Angelman syndrome. Nat Genet 1997; 15:70-73.

323. Nicholls RD, Knepper JL. Genome organization, function, and imprinting in Prader-Willi and Angelman syndromes. Annu Rev Genomics Hum Genet 2001; 2:153-175.

324. Goldstone AP. Prader-Willi syndrome: advances in genetics, pathophysiology and treatment. Trends in Endocrinology & Metabolism 2004; 15:12-20.

325. DeBaun MR, Niemitz EL, McNeil DE, Brandenburg SA, Lee MP, Feinberg AP. Epigenetic Alterations of H19 and LIT1 Distinguish Patients with Beckwith-Wiedemann Syndrome with Cancer and Birth Defects. The American Journal of Human Genetics 2002; 70:604-611.

326. Maher ER, Brueton LA, Bowdin SC, Luharia A, Cooper W, Cole TR, Macdonald F, Sampson JR, Barratt CL, Reik W, Hawkins MM. Beckwith-Wiedemann syndrome and assisted reproduction technology (ART). J Med Genet 2003; 40:62-64.

327. DeBaun MR, Niemitz EL, Feinberg AP. Association of in vitro fertilization with Beckwith-Wiedemann syndrome and epigenetic alterations of LIT1 and H19. Am J Hum Genet 2003; 72:156-160.

328. Smilinich NJ, Day CD, Fitzpatrick GV, Caldwell GM, Lossie AC, Cooper PR, Smallwood AC, Joyce JA, Schofield PN, Reik W, Nicholls RD, Weksberg R, et al. A maternally methylated CpG island in KvLQT1 is associated with an antisense paternal transcript and loss of imprinting in Beckwith-Wiedemann syndrome. Proc Natl Acad Sci U S A 1999; 96:8064-8069.

329. Mitsuya K, Meguro M, Lee MP, Katoh M, Schulz TC, Kugoh H, Yoshida MA, Niikawa N, Feinberg AP, Oshimura M. LIT1, an imprinted antisense RNA in the human KvLQT1 locus identified by screening for differentially expressed transcripts using monochromosomal hybrids. Hum Mol Genet 1999; 8:1209-1217.

330. De Souza AT, Hankins GR, Washington MK, Orton TC, Jirtle RL. M6P/IGF2R gene is mutated in human hepatocellular carcinomas with loss of heterozygosity. Nat Genet 1995; 11:447-449.

331. Oka Y, Waterland RA, Killian JK, Nolan CM, Jang HS, Tohara K, Sakaguchi S, Yao T, Iwashita A, Yata Y, Takahara T, Sato S, et al. M6P/IGF2R tumor suppressor gene mutated in hepatocellular carcinomas in Japan. Hepatology 2002; 35:1153-1163.

332. Jamieson TA, Brizel DM, Killian JK, Oka Y, Jang HS, Fu X, Clough RW, Vollmer RT, Anscher MS, Jirtle RL. M6P/IGF2R loss of heterozygosity in head and neck cancer associated with poor patient prognosis. BMC Cancer 2003; 3:4.

333. Centers for Disease Control and Prevention, American Society for Reproductive Medicine, Society for Assisted Reproductive Technology. 2010 Assisted Reproductive Technology National Summary Report. Atlanta: U.S. Department of Health and Human Services; 2012. In; 2012.

334. ESHRE. ART Fact Sheet. In, vol. 2013; 2013.

335. Anderson JE, Farr SL, Jamieson DJ, Warner L, Macaluso M. Infertility services reported by men in the United States: national survey data. Fertility and Sterility 2009; 91:2466-2470.

336. SART. National Data Summary: Clinic Summary Report. In, vol. 2013; 2011.

337. Dondorp W, de Wert G. Innovative reproductive technologies: risks and responsibilities. Human Reproduction 2011; 26:1604-1608.

338. SART. A Patient's Guide to Assisted Reproductive Technology, General Information, ART: Step-by-Step Guide. In, vol. 2013; 2011.

339. Mann MRW, Lee SS, Doherty AS, Verona RI, Nolen LD, Schultz RM, Bartolomei MS. Selective loss of imprinting in the placenta following preimplantation development in culture. Development 2004; 131:3727-3735.

340. Rinaudo P, Schultz RM. Effects of embryo culture on global pattern of gene expression in preimplantation mouse embryos. Reproduction 2004; 128:301-311.

341. Rivera RM, Stein P, Weaver JR, Mager J, Schultz RM, Bartolomei MS. Manipulations of mouse embryos prior to implantation result in aberrant expression of imprinted genes on day 9.5 of development. Hum Mol Genet 2008; 17:1-14.

342. Huffman SR, Rivera RM. Superovulation induces alterations in the epigenome of zygotes and results in differences in gene expression at the blastocyst stage in mice. In: University of Missouri - Columbia; 2013.

343. Almamun M. Size-dependent acquisition of global DNA methylation in oocytes is altered by hormonal stimulation. Ann Arbor: University of Missouri - Columbia; 2011.

344. Fortier AL, Lopes FL, Darricarrère N, Martel J, Trasler JM. Superovulation alters the expression of imprinted genes in the midgestation mouse placenta. Human Molecular Genetics 2008; 17:1653-1665.

345. Van der Auwera I, D'Hooghe T. Superovulation of female mice delays embryonic and fetal development. Human Reproduction 2001; 16:1237-1243.

346. Ertzeid G, Storeng R. Adverse effects of gonadotrophin treatment on pre- and postimplantation development in mice. Journal of Reproduction and Fertility 1992; 96:649-655.

347. Ertzeid G, Storeng R. The impact of ovarian stimulation on implantation and fetal development in mice. Human Reproduction 2001; 16:221-225.

348. Halliday J, Oke K, Breheny S, Algar E, D JA. Beckwith-Wiedemann syndrome and IVF: a case-control study. Am J Hum Genet 2004; 75:526-528.

349. Gicquel C, Gaston V, Mandelbaum J, Siffroi JP, Flahault A, Le Bouc Y. In vitro fertilization may increase the risk of Beckwith-Wiedemann syndrome related to the abnormal imprinting of the KCN1OT gene. Am J Hum Genet 2003; 72:1338-1341.

350. Lim D, Bowdin SC, Tee L, Kirby GA, Blair E, Fryer A, Lam W, Oley C, Cole T, Brueton LA, Reik W, Macdonald F, et al. Clinical and molecular genetic features of Beckwith–Wiedemann syndrome associated with assisted reproductive technologies. Human Reproduction 2009; 24:741-747.

351. Gavriil P, Jauniaux E, Leroy F. Pathologic examination of placentas from singleton and twin pregnancies obtained after in vitro fertilization and embryo transfer. Pediatr Pathol 1993; 13:453-462.

352. Delle Piane L, Lin W, Liu X, Donjacour A, Minasi P, Revelli A, Maltepe E, Rinaudo PF. Effect of the method of conception and embryo transfer procedure on mid-gestation placenta and fetal development in an IVF mouse model. Hum Reprod 2010; 25:2039-2046.

353. Market Velker BA, Denomme MM, Mann MR. Loss of genomic imprinting in mouse embryos with fast rates of preimplantation development in culture. Biol Reprod 2012; 86:143, 141-116.

354. Negrón-Pérez VM, Echevarría FD, Huffman SR, Rivera RM. Determination of Allelic Expression of H19 in Pre- and Peri-Implantation Mouse Embryos1. Biol Reprod 2013; 88:Article 97, 91-11.

355. Gabory A, Jammes H, Dandolo L. The H19 locus: Role of an imprinted non-coding RNA in growth and development. BioEssays 2010; 32:473-480.

356. Mann MR, Chung YG, Nolen LD, Verona RI, Latham KE, Bartolomei MS. Disruption of imprinted gene methylation and expression in cloned preimplantation stage mouse embryos. Biol Reprod 2003; 69:902-914.

357. Chiesa N, De Crescenzo A, Mishra K, Perone L, Carella M, Palumbo O, Mussa A, Sparago A, Cerrato F, Russo S, Lapi E, Cubellis MV, et al. The KCNQ1OT1 imprinting control region and non-coding RNA: new properties derived from the study of Beckwith-Wiedemann syndrome and Silver-Russell syndrome cases. Human Molecular Genetics 2012; 21:10-25.

358. Nagy A, Gertsenstein M, Vintersten K, Behringer R. Manipulating the Mouse Embryo, A laboratory manual, third edition. Cold Spring Harbor Laboratory Press 2003.

359. Huffman SR, Almamun M, Rivera RM. Isolation of RNA and DNA from single preimplantation embryos and a small number of Mammalian oocytes for imprinting studies. Methods Mol Biol 2012; 925:201-209.

360. Rasband WS, ImageJ, Bethesda MD. U. S. National Institutes of Health. 1997-2012.

361. Brazda V, Laister RC, Jagelska EB, Arrowsmith C. Cruciform structures are a common DNA feature important for regulating biological processes. BMC Mol Biol 2011; 12:33.

362. Alexiadis V, Waldmann T, Andersen J, Mann M, Knippers R, Gruss C. The protein encoded by the proto-oncogene DEK changes the topology of chromatin and reduces the efficiency of DNA replication in a chromatin-specific manner. Genes Dev 2000; 14:1308-1312.

363. Waldmann T, Scholten I, Kappes F, Hu HG, Knippers R. The DEK protein--an abundant and ubiquitous constituent of mammalian chromatin. Gene 2004; 343:1-9.

364. Yoshikawa T, Piao Y, Zhong J, Matoba R, Carter MG, Wang Y, Goldberg I, Ko MSH. High-throughput screen for genes predominantly expressed in the ICM of mouse blastocysts by whole mount in situ hybridization. Gene expression patterns : GEP 2006; 6:213-224.

365. Klaffky E, Williams R, Yao CC, Ziober B, Kramer R, Sutherland A. Trophoblast-specific expression and function of the integrin alpha 7 subunit in the peri-implantation mouse embryo. Developmental Biology 2001; 239:161-175.

366. Ripoche MA, Kress C, Poirier F, Dandolo L. Deletion of the H19 transcription unit reveals the existence of a putative imprinting control element. Genes & development 1997; 11:1596-1604.

367. Gabory A, Ripoche MA, Le Digarcher A, Watrin F, Ziyyat A, Forne T, Jammes H, Ainscough JF, Surani MA, Journot L, Dandolo L. H19 acts as a trans regulator of the imprinted gene network controlling growth in mice. Development 2009; 136:3413-3421.

368. Runge S, Nielsen FC, Nielsen J, Lykke-Andersen J, Wewer UM, Christiansen J. H19 RNA binds four molecules of insulin-like growth factor II mRNA-binding protein. The Journal of biological chemistry 2000; 275:29562-29569.

369. Senner CE, Hemberger M. Regulation of early trophoblast differentiation - lessons from the mouse. Placenta 2010; 31:944-950.

370. Gardner RL, Davies TJ. Lack of coupling between onset of giant transformation and genome endoreduplication in the mural trophectoderm of the mouse blastocyst. J Exp Zool 1993; 265:54-60.

371. Margalit Y, Yarus S, Shapira E, Gruenbaum Y, Fainsod A. Isolation and characterization of target sequences of the chicken CdxA homeobox gene. Nucleic Acids Res 1993; 21:4915-4922.

372. Rath B, Pandey RS, Debata PR, Maruyama N, Supakar PC. Molecular characterization of senescence marker protein-30 gene promoter: identification of repressor elements and functional nuclear factor binding sites. BMC Mol Biol 2008; 9:43.

373. Berteaux N, Aptel N, Cathala G, Genton C, Coll J, Daccache A, Spruyt N, Hondermarck H, Dugimont T, Curgy JJ, Forne T, Adriaenssens E. A novel H19 antisense RNA overexpressed in breast cancer contributes to paternal IGF2 expression. Mol Cell Biol 2008; 28:6731-6745.

374. Adam GI, Cui H, Miller SJ, Flam F, Ohlsson R. Allele-specific in situ hybridization (ASISH) analysis: a novel technique which resolves differential allelic usage of H19 within the same cell lineage during human placental development. Development (Cambridge, England) 1996; 122:839-847.

375. Librach CL, Werb Z, Fitzgerald ML, Chiu K, Corwin NM, Esteves RA, Grobelny D, Galardy R, Damsky CH, Fisher SJ. 92-kD type IV collagenase mediates invasion of human cytotrophoblasts. J Cell Biol 1991; 113:437-449.

376. Cross JC, Anson-Cartwright L, Scott IC. Transcription factors underlying the development and endocrine functions of the placenta. Recent Prog Horm Res 2002; 57:221-234.

377. Jouvenot Y, Poirier F, Jami J, Paldi A. Biallelic transcription of Igf2 and H19 in individual cells suggests a post-transcriptional contribution to genomic imprinting. Curr Biol 1999; 9:1199-1202.

378. Varrault A, Gueydan C, Delalbre A, Bellmann A, Houssami S, Aknin C, Severac D, Chotard L, Kahli M, Le Digarcher A, Pavlidis P, Journot L. Zac1 Regulates an Imprinted Gene Network Critically Involved in the Control of Embryonic Growth. Developmental Cell 2006; 11:711-722.

379. Sutherland AE, Calarco PG, Damsky CH. Developmental regulation of integrin expression at the time of implantation in the mouse embryo. Development 1993; 119:1175-1186.

380. Griffin J, Emery BR, Huang I, Peterson CM, Carrell DT. Comparative analysis of follicle morphology and oocyte diameter in four mammalian species (mouse, hamster, pig, and human). J Exp Clin Assist Reprod 2006; 3:2.

381. Lander ES, Linton LM, Birren B, Nusbaum C, Zody MC, Baldwin J, Devon K, Dewar K, Doyle M, FitzHugh W, Funke R, Gage D, et al. Initial sequencing and analysis of the human genome. Nature 2001; 409:860-921.

382. Kuff EL, Lueders KK. The intracisternal A-particle gene family: structure and functional aspects. Adv Cancer Res 1988; 51:183-276.

383. Lowy DR, Rowe WP, Teich N, Hartley JW. Murine leukemia virus: high-frequency activation in vitro by 5-iododeoxyuridine and 5-bromodeoxyuridine. Science 1971; 174:155-156.

384. Kaplan HS. On the natural history of the murine leukemias: presidential address. Cancer Res 1967; 27:1325-1340.

APPENDIX 1

Immunofluorescent localization of integrin alpha 7 in peri-implantation mouse embryos

Primary trophoblast giant cells express laminin-binding integrins to regulate uterine invasion. Alpha 7 integrin (Itga7) is a subtype of laminin-receptors previously detected in preimplantation and early post-implantation [365, 379]. We used Itga7 as a marker for the qRT-PCR analysis on the ICM- and PTGC-containing sections and to further look at the specificity of Itga7 to the PTGC we followed an immunofluorescence protocol to localize Itga7 in peri-implantation blastocysts.

For the immunofluorescent procedure, the embryos were flushed from the uterus at 109h post-ovulation with MEM+PVP at 37 °C, washed in 400 µl 1xPBS at room temperature (RT), fixed in 2% formaldehyde for 40 min at RT by adding 100 µl 10% formaldehyde into the well to reduce concentration, and washed through 2 drops of 1xPBS. Embryos were then permeabilized in 0.1% Triton X-100 in 1xPBS for 40 min at RT, and non-specific binding was blocked by incubating for 30 min at RT in 5%NGS, 0.1%Triton X-100 in 1xPBS. These were incubated in primary antibody solution for 40 min at RT (1:200 rabbit anti-Itga7 and 1:200 mouse anti-Oct4 in 1%NGS, 0.1%Triton X-100, 1xPBS), washed in 400 µl of 1%NGS, 0.1%Triton X-100 in 1xPBS, incubated in secondary antibody solution for 40 min at RT (1:800 goat anti-rabbit , 1:500 goat anti-mouse, & 1:80 DAPI (200 µg/mL stock) in 1%NGS, 0.1%Triton X-100 in 1xPBS), washed in 400 µl of 1%NGS, 0.1%Triton X-100 in 1xPBS and mounted in a 10 µl drop

of VectaShield. Images were acquired with a Nikon Eclipse 800 microscope with Cool Snap camera and MetaMorph software.

We did not observe specific expression for the PTGC containing section. We found Itga7 to be highly expressed in the cytoplasm of both polar and mural trophectoderm (**Figure A1.1**). We attempted to follow the same procedure without permeabilizing the embryo and found no difference in expression in the different cell types (not shown). As expected, Oct4 (**Figure A1.1D**) was only expressed in the ICM allowing us to distinguish and identify corresponding embryonic cell types. Negative controls were embryos that went through the immunofluorescence procedure but without antibodies in the incubation step. Negative controls were incubated in1%NGS, 0.1%Triton X-100, 1xPBS solution without antibodies (*i.e.* rabbit anti-Itga7, mouse anti-Oct4, goat anti-rabbit or goat anti-mouse). Negative samples showed no background fluorescence (not shown).

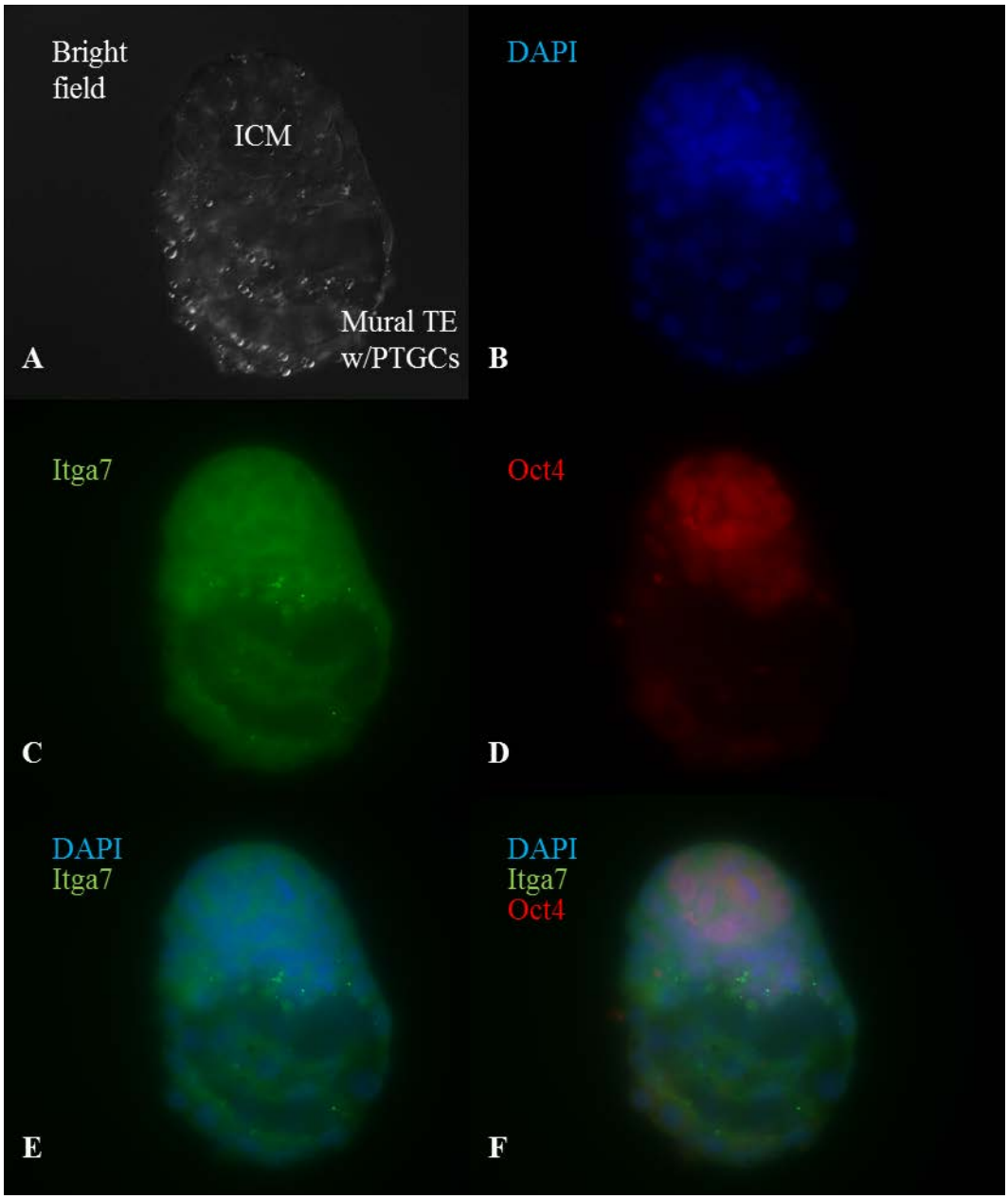

Figure A1.1. Immunofluorescent localization of Itga7 in day ~5.5E mouse blastocyst

Figure A1.1. Immunofluorescent localization of Itga7 in day ~5.5E mouse blastocyst. Peri-implantation blastocysts were collected from the uterus from unstimulated females at 109h (day ~5.5E) post presumed ovulation. Blastocysts were then treated for immunolocalization of Itga7 and Oct4. **A**. Mouse blastocyst as it looks under bright field. **B**. DAPI nuclear staining (blue). **C.** Itga7 immunolocalization (green). **D**. Oct4 immunolocalization (red). **E**. Merge of DAPI and Itga7. **F**. Merge of DAPI, Itga7 and Oct4. Original magnification x600. ICM = inner cell mass. Mural TE w/ PTGC = mural trophectoderm with primary trophoblast giant cells. No specific fluorescence was observed in the embryos in the negative control.

Appendix 2

Immunohistochemical localization of 5-methylcytosine in FSH receptor beta knockout mice

This work was performed to follow up a previous study designed to determine if FSH has a regulatory function in the acquisition of DNA methylation in the oocyte.

Immunohistochemical localization of 5-methylcytosine (5meC) in mouse ovaries

Previous observations in our laboratory suggested that the acquisition of DNA methylation was an FSH driven event. The first observation was that injection of eCG caused a decrease in DNA methylation in the oocyte [343]. A follow up compared levels of global DNA methylation in young (8 weeks) and aged (66-68 weeks – high endogenous FSH) females showed that there were higher levels of 5meC detected in old females [Huffman *et al.*, unpublished].

After personal communication with Dr. T. Rajendra Kumar from The University of Kansas Medical Center and literature searches, we learned that even though there are higher levels of FSH in older females when compared to young females, the isoform of FSH in the old females is different and does not bind to the receptor in granulosa cells therefore depriving the growing follicle of FSH stimulation. Then, in collaboration with Dr. Kumar, we began to study the acquisition of DNA methylation in FSH-beta receptor knockout females ($FSH^{K/O}$) of 3-weeks (3wk), 9-weeks (9wk) and 10-month (10mo) old females. $FSH^{K/O}$ females are equally deprived of FSH as an old female as the FSH

cannot bind regardless of the levels present. We hypothesized that the acquisition of DNA methylation in the oocyte is an FSH driven event and if so, we will observe higher levels of 5meC present in 3wk and 9wk $FSH^{K/O}$ females.

To study this, we collected ovaries from control and $FSH^{K/O}$ females at 3wk, 9wk and 10mo of age. Ovaries were fixed, sectioned and immunohistochemically stained against 5meC as previously described [343].Images of immunohistochemical staining are currently being analyzed. **Figure A2.1** shows an example of sections for each group.

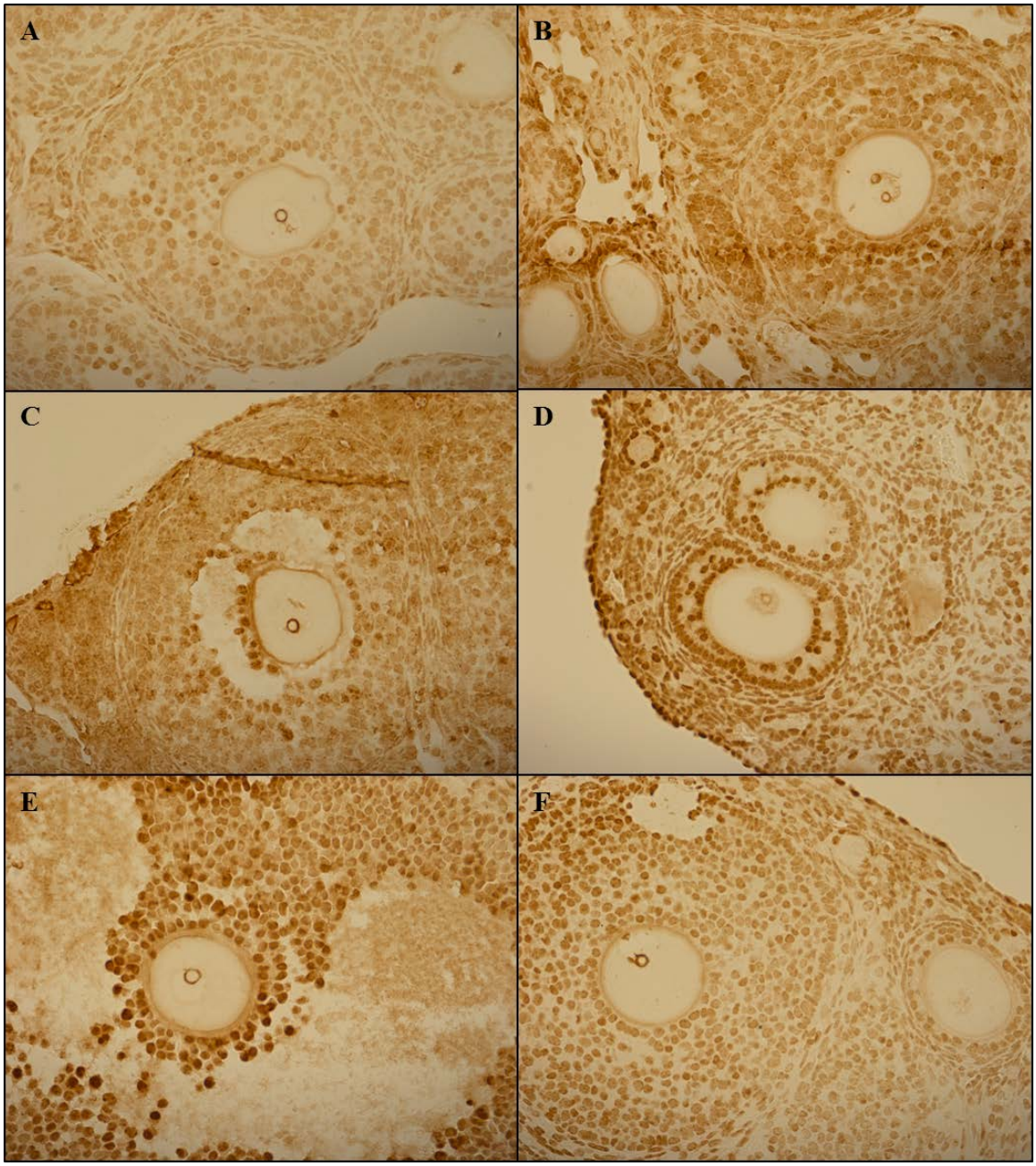

Figure A2.1. 5-methylcytosine immunohistochemical localization in mouse ovarian sections

Figure A2.1. 5-methylcytosine immunohistochemical localization in mouse ovarian sections. Shown are representative pictures of growing oocytes in ovaries from control **(A, C, E)** females and FSH beta-subunit receptor knockout **(B, D, F)**. Global DNA methylation was determined at different ages, **A** and **B**. three weeks old; **C** and **D**. nine weeks old; **E** and **F**. ten months old. No specific staining was observed in the ovarian sections in the negative control (data not shown).

Appendix 3

Effect of superovulation on Iap and Mlv1 expression

Previous work in our laboratory has demonstrated a decrease in DNA methylation after administering exogenous gonadotropins for superovulation (*i.e.* eCG and hCG) [343]. In that study, ovarian sections were immunohistochemically stained and analyzed to detect amount of 5meC. Each section was analyzed to find growing oocytes and compare levels of DNA methylation in oocytes of different size. Results showed that 40-50 µm oocytes from superovulated females reached a plateau in DNA methylation levels while oocytes from naturally ovulated females showed a constant increase in DNA methylation as they increased in size. Also, another experiment showed an effect on gene expression in blastocysts from superovulated females (Huffman *et al.* [342]; unpublished). Finally, we have noticed that at collection, oocytes from superovulated females are of various sizes ranging from 60-80 µm while a naturally ovulated oocyte measure approximately 80µm [380]. This suggests that smaller oocytes from superovulated females have different developmental potential.

Parasitic sequences or transposable elements are present in all eukaryotic genomes affecting the regulation of genes with promoter regions close to these or by retrotransposition [381]. Regulation of parasitic sequences can be controlled by DNA methylation [133]. Based on this and previous observations, we suggest that repetitive elements are upregulated as a result of the decrease in DNA methylation caused by

superovulation and that smaller oocytes will show higher levels of expression of two such elements: Iap and Mlv1.

To test this and the effect of superovulation in growing oocytes, we naturally ovulated (NO) and superovulated (SO) randomly selected females and collected ovulated oocytes (*i.e.* eggs) in pools of 30 (**Figure A3.1A**). Eggs were collected from four groups of females: after NO (control), after SO (C0; 20h post-hCG), one estrous cycle after SO (C1; 116-140h post-hCG), and two estrous cycles after SO (C2; 212-236h post-hCG). The injection scheme consisted of 5IU eCG when females were in diestrus followed by 5IU hCG 44h later. Females then were paired with vasectomized males and ovulation was determined by the presence of copulatory plug the morning after mating. RNA was extracted following manufacturer's instruction for Stratagene Absolutely RNA kit (Agilent Technologies) followed by reverse transcriptase reaction to make cDNA. To normalize RNA content, exogenous ZmNIP3-1 RNA (1ng/µl) was added before each extraction. The ZmNIP3-1 *in vitro* transcribed RNA was kindly donated by Dr. Amanda Durbak a post-doctoral fellow in Dr. McSteen's laboratory in Biological Sciences at MU. Finally, the expression of two endogenous retroviruses, *Iap* (intracisternal A particle [134, 382]) and *Mlv1* (murine leukemia virus 1 [383, 384]), was analyzed using qRT-PCR. Taqman probes were designed to detect *Iap*, *Mlv1*, *H19*/*Igf2* ICR and *ZmNIP3-1*; *H19*/*Igf2* ICR probes were used as control for genomic DNA contamination. **Figure A3.1B and 3.1C** show our preliminary results from qRT-PCR after normalizing with*ZmNIP3*. It is important to note that we did not detect any genomic DNA contamination.

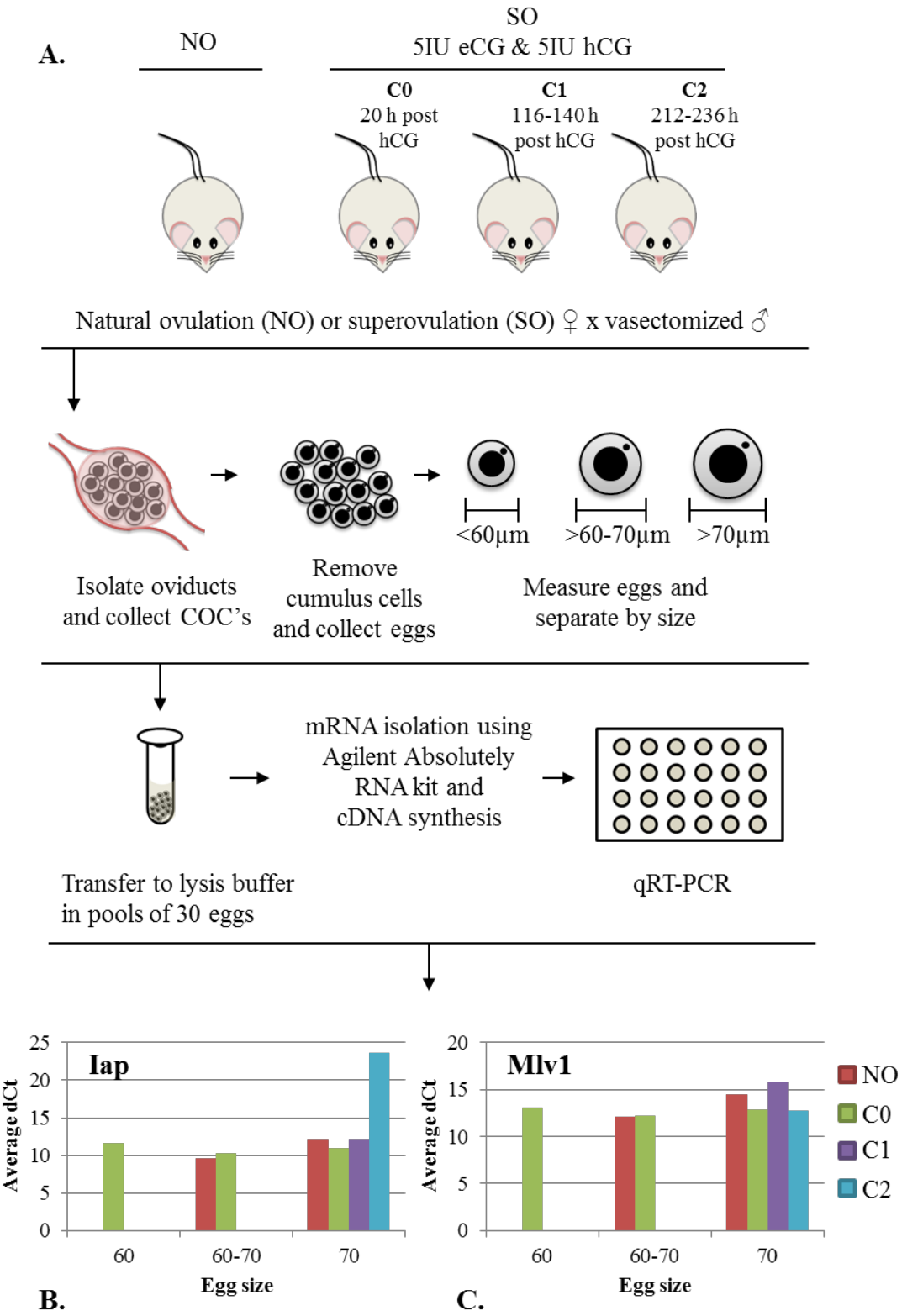

Figure A3.1. Repetitive elements analysis in mouse eggs

Figure A3.1. Repetitive element analysis in mouse eggs. A. Natural ovulation (NO) and superovulation (SO) scheme for ovulated oocytes (eggs) collection. Females in the SO group were injected with 5IU of equine chorionic gonadotropin (eCG) during diestrus, followed by 5IU of human chorionic gonadotropin (hCG) 44 hours (h) later. C0 (cycle 0) females were immediately paired with vasectomized males and cumulus-oocyte complex (COC) were collected 20 h post-hCG. C1 (cycle 1) females were mated one estrous cycle (96 h) post hCG and COC were collected 20-44 h later (116-140 h post hCG). C2 (cycle 2) females were mated two estrous cycles (192h) post hCG and COC were collected 20 – 44 h later (212-236 h post hCG). NO females received no injections and were mated during estrous with vasectomized males. COCs were collected after noticing a copulatory plug indicating ovulation had occurred. Cumulus cells were removed by incubating COCs in 500 µg/ml of hyaluronidase in MEM + PVP for 1-2 min, and rinsed in fresh MEM + PVP. Eggs were measured with the use of an eyepiece micrometer. Measurements included the zona pellucida and separated by size in three groups; <60 µm, >60-70 µm and >70 µm. Eggs were collected in pools of 30 and transferred to lysis buffer for mRNA extraction and subsequent cDNA conversion. qRT-PCR was used to determine the amount of Iap (**B**) and Mlv1(**C)** mRNA present in each pool. **B** and **C** show average dCt after normalizing to *ZmNIP3*. Red bar = NO; green bar = C0; purple bar = C1; blue bar = C2. Total number of eggs analyzed = n; NO>60-70 µm: n = 30; NO >70 µm: n = 90; C0<60 µm: n = 116; C0>60-70 µm: n = 120; C0 >70 µm: n = 120; C1>70 µm: n = 30; C2>70 µm: n = 60. Eggs of size <60 µm and >60-70 µm were not collected in NO, C1 and C2 females as naturally ovulated oocytes are >70 µm.

VITA

Verónica M. Negrón Pérez was born October 14, 1988 in San Juan, Puerto Rico. She started her college education in Agricultural Sciences at the University of Puerto Rico – Mayagüez where she completed a Bachelor of Sciences in Animal Science in June 2011. Throughout her undergraduate degree she participated in swine and dairy reproduction research at The Ohio State University (2010) and at the University of Puerto Rico – Mayagüez (2010-2011) where she developed her interest in reproductive physiology. In August 2011, Verónica began to work on her Master of Science degree in developmental epigenetics under the supervision of Dr. Rocío M. Rivera in the Division of Animal Sciences at the University of Missouri. Upon completing her M.S., she will move to Florida to continue her graduate studies. She will be working on her Doctor of Philosophy degree in the Animal Molecular and Cellular Biology Program at the University of Florida under the supervision of Dr. Peter J. Hansen.